Tunable Antennas to Address the LTE Bandwidth Challenge on Small Mobile Terminals: One World, One Radio.

Barrio, Samantha Caporal Del

Publication date:
2013

Document Version
Early version, also known as pre-print

Tunable Antennas to Address the LTE Bandwidth Challenge on Small Mobile Terminals: One World, One Radio.

Ph.D. Dissertation

Samantha Caporal Del Barrio

Aalborg University
Faculty of Engineering and Science
Department of Electronic Systems
Fredrik Bajers Vej 7B
DK-9220 Aalborg

Abstract

This thesis concerns frequency-reconfigurable antennas with the aim of addressing the challenge of band proliferation for small mobile terminals. This challenge arose with the worldwide standardization of Long Term Evolution (LTE). Designing a worldwide LTE phone (i.e. a world-phone) with conventional techniques reaches the limit of component integration, given the very tight platforms of typical smart-phones. A shift in architecture is required in order to cover the bandwidth needed for worldwide LTE roaming. This thesis investigates a co-design of the antennas and the front-end of mobile phones, aiming at limiting the component count and dramatically reducing the complexity of the required hardware. This novel architecture can provide worldwide LTE roaming capabilities to next generations of mobile phones.

The first part investigates the trade-offs of narrow-band tunable antennas, with respect to achievable tuning range, tuning resolution and efficiency. It also investigates the limitations of these antennas, from an efficiency perspective. The second part compares the effect of the user for conventional antennas and narrow-band antennas. The last part investigates the antenna isolation on a typical mobile terminal, and a mock-up of the complete world-phone architecture is assembled. The two major outcomes are the understanding of the loss mechanism for small frequency-reconfigurable antennas and the accomplishment of a proof-of-concept of a world-phone.

Resumé

Denne afhandling omhandler frekvens-rekonfigurerbare antenner med det mål at adressere udfordringen omkring udvidelsen af båndbredde i Long-Term-Evolution (LTE) på små mobile terminaler. Denne udfordring er et resultat af den verdensomspændende standardisering af LTE. En telefon med verdensomspændende roaming kapabilitet (en verdenstelefon) kræver mere front-end hardware end en typisk smartphone kan rumme, hvis et konventionelt design anvendes. Et arkitekturskifte er nødvendigt for at dække båndbredden af et verdensomspændende LTE. Denne afhandling undersøger et fælles design af antennerne og mobiltelefonens front-end, med det mål at begrænse antallet af komponenter og at reducere kompleksiteten af det nødvendige hardware dramatisk. Denne nye arkitektur kan sikre verdensomspændende LTE roaming kapabilitet til næste generationer af mobiltelefoner.
Den første del omhandler afvejningen mellem opnåelig justeringsspæn, justeringsfinhed og effektivitet hos justerbare smalbåndsantenner. Første del omhandler også begrænsningerne ved disse antenner med hensyn til effektivitet. I anden del sammenlignes brugerens indflydelse på henholdsvis konventionelle antenner og smalbåndsantenner. I sidste del undersøges antennens isolering på en typisk mobil terminal og en prototype af den færdige arkitektur til en verdenstelefon samles. De to vigtigste resultater er forståelsen for tabsmekanismerne i små frekvens-rekonfigurerbare antenner og et proof of concept af en verdenstelefon.

Contents

Thesis Details

Thesis Title:	Tunable Antennas to Address the LTE Bandwidth Challenge on Small Mobile Terminals: One World, One Radio.
Ph.D. Student:	Samantha Caporal Del Barrio
Supervisors:	Prof. Gert F. Pedersen, Aalborg University
	Assist. Prof. Mauro Pelosi, Aalborg University

The main body of this thesis consists of the following papers.

[A] Del Barrio, S.C. ; Pelosi, M. ; Pedersen, G.F. and Morris, A., "Challenges for Frequency-Reconfigurable Antennas in Small Terminals," *76th Vehicular Technology Conference (VTC Fall), 2012 IEEE*, pp. 1–5, Sept., 2012.

[B] Del Barrio, S.C. ; Pelosi, M. and Pedersen, G.F., "On the efficiency of frequency reconfigurable high-Q antennas for 4G standards," *Electronics Letters*, vol. 48, no. 16, pp. 982–983, Aug., 2012.

[C] Del Barrio, S.C. ; Pedersen, G.F., "On the Efficiency of Capacitively Loaded Frequency Reconfigurable Antennas," *International Journal of Distributed Sensor Networks (IJDSN)*, Special Issue on Smart and Reconfigurable Antenna Applications in Wireless Sensor Networks, Article ID 232909, June, 2013.

[D] Del Barrio, S.C. ; Bahramzy, P. ; Svendsen, S. ; Jagielski, O. and Pedersen, G.F., "Loss Limitations of Frequency Reconfigurable Antennas," *Submitted to Transaction on Antennas and Propagation*, Aug., 30th, 2013.

[E] Del Barrio, S.C. ; Pelosi, M. ; Franek, O. and Pedersen, G.F., "The Effect of the User's Body on High-Q and Low-Q Planar Inverted F Antennas for LTE Frequencies," *75th Vehicular Technology Conference (VTC Spring), 2012 IEEE 75th*, pp. 1–4, May, 2012.

[F] Del Barrio, S.C. ; Pelosi, M. ; Franek, O. and Pedersen, G.F., "Coupling element antenna with slot tuning for handheld devices at LTE frequencies," *6th European Conference on Antennas and Propagation (EuCAP)*, pp. 3587–3590, March, 2012.

[G] Del Barrio, S.C. and Pedersen, G.F., "Antenna design exploiting duplex isolation for 4G communication on handsets," *Electronics Letters, Volume 49, Issue 19*, pp. 1197 – 1198, Sept., 2013.

[H] Del Barrio, S.C. ; Tatomirescu A. ; Pedersen, G.F. and Morris, A., "Novel architecture for worldphones," *Submitted to Antennas and Wireless Propagation Letters*, Special Cluster on Terminal Antenna Systems for 4G and Beyond, Oct. 8^{th}, 2013.

In addition to the main papers, the following publications have also been made during the Ph.D. project. Their full content is not included in the next chapter, as they are side tracks to the main focus of this thesis. They address other fundamental challenges of small antennas for mobile terminals, such as circuit modeling, correlation and MIMO.

[1] Del Barrio, S.C. ; Pelosi, M. ; Franek, O. ; Pedersen, G.F., "Equivalent Circuit Model of a High Q Tunable PIFA," *74^{th} Vehicular Technology Conference (VTC Fall), 2011 IEEE*, pp. 1–4, 2011.

[2] Del Barrio, S.C. ; Pelosi, M. ; Franek, O. ; Pedersen, G.F., "Tuning Range Optimization of a Planar Inverted F Antenna for the LTE Low Frequency Bands," *74^{th} Vehicular Technology Conference (VTC Fall), 2011 IEEE*, pp. 1–5, 2011.

[3] Del Barrio, S.C. ; Pedersen, G.F., "Correlation Evaluation on Small LTE Handsets," *76^{th} Vehicular Technology Conference (VTC Fall), 2012 IEEE*, pp. 1–4, 2012.

[4] Del Barrio, S.C. ; Pelosi, M. ; Franek, O. ; Pedersen, G.F., "On the currents magnitude of a tunable Planar-Inverted-F Antenna for low-band frequencies," *6^{th} European Conference on Antennas and Propagation (EuCAP)*, pp. 3173–3176, 2012.

[5] Del Barrio, S.C. ; Yanakiev, B. ; Pedersen, G.F., "Portable MIMO-LTE antennas for different hand-held device sizes," *Loughborough Antennas and Propagation Conference (LAPC)*, pp. 1–4, 2012.

[6] Del Barrio, S.C. ; Pedersen, G.F., "High-Q antennas: Simulator limitations," *7^{th} European Conference on Antennas and Propagation (EuCAP)*, pp. 1567–1571, 2013.

This thesis has been submitted for assessment in partial fulfillment of the PhD degree. The thesis is based on the submitted or published scientific papers which are listed above. Parts of the papers are used directly or indirectly in the extended summary of the thesis. As part of the assessment, co-author statements have been made available to the assessment committee and are also available at the Faculty. The thesis is not in its present form acceptable for open publication but only in limited and closed circulation as copyright may not be ensured.

Preface

This thesis is submitted as partial fulfillment of the requirements for the degree of Doctor of Philosophy at Aalborg University, Denmark. The main part of the thesis is a collection of papers published in or submitted to peer-reviewed conferences and journals. It is the results of three years of research in the Section of Antennas, Propagation and radio Networking (APNet), at the Department of Electronic Systems, Aalborg University, in the period October, 15^{th} 2010 - October, 8^{th} 2013.

The contributions to this thesis were done under the supervision of Assist. Prof. Mauro Pelosi and of Prof. Gert F. Pedersen, to whom I would like to express my sincere gratitude for sharing their expertise and enthusiasm. The work has been done within the Smart Antenna Front End (SAFE) project, funded by The Danish National Advanced Technology Foundation, during which a close collaboration with Intel Mobile Communication, Intel Antenna Business and WiSpry Inc. has been initiated. Through this collaboration, the high quality knowledge of Simon Svendsen, Ole Jagielski and Art Morris has been a great inspiration and lead to many of the presented results. I would also like to thank the Laboratory team of APNet: Kim Olesen, Kristian Bank, Ben Krøyer and Peter Jensen for their help with the measurement preparations. Finally, the support and encouragement of my family and friends has everyday been a strong motivation.

Samantha Caporal Del Barrio
Aalborg University, October 8, 2013

Part I

Introduction

Introduction

1 Background of the Thesis

Nowadays, a large number of services provided by mobile phones relies on their antennas, e.g. telephony, browsing, high speed applications (gaming or streaming), localization, live-video, and so forth. The user's experience of his mobile phone depends on the performance of the bi-directional radio link between the handset and the base station. The base station is typically equipped with a high gain antenna, however the handset is constrained to a low-profile antenna, providing restricted performances. This thesis focuses on the mobile antenna.

1.1 The Race for Bandwidth

From GSM to 4G, users have experienced the enhancement of the capabilities of their mobile phones. The trend initiated with dramatically reducing their size. Once mobile devices could not be shrunk anymore, the development shifted its focus towards improving functionality. First the access to Internet, and then the ever increasing data rates, allowing high-definition streaming and sharing of heavy files over the air, and more. What has technologically happened to enable these new functionalities is described in this section.
In Global System for Mobile communications (GSM) systems the base stations are serving the users by dedicating time-slots and frequencies to them, with a maximum bandwidth of 200 kHz. In 2001, the introduction of the General Packet Radio Service (GPRS) in public GSM networks allowed access to the Internet over the air. The GSM/GPRS network is specified as a second generation (2G) network. The narrowband nature of the carrier bandwidth remained the limiting factor of 2G. To overcome the limitations of 2G, Code Division Multiple Access (CDMA) was developed for the third generation (3G) systems and bandwidths were increased to 5 MHz. CDMA allows a base station to communicate with multiple users at the same time and on the same carrier frequency.
The 3G networks were developed while the second generation GSM/GPRS was still

evolving. In 2005, the availability of color and high resolution displays, the development of user-friendly browsers and email clients with WAP 2.0, and the use of the packet-based networks built the bridge allowing mobile Internet to enter the mass market. In 2006, 3G Universal Mobile Telecommunications System (UMTS) networks implemented High Speed Data Packet Access (HSDPA), which improved data scheduling. Data rates up to 1 and 3 Mbps were reached and the GSM Association stated in a press release of August 2006, that network operator registrations reached 1000 new users per minute [1]. Due to the rising number of users and multimedia content, bandwidth requirements dramatically increased in the following years. As 2G did earlier, 3G also reached its design limitations. Bandwidths wider than the initially designed 5MHz could not be supported by CDMA, due to multipath fading. To meet the demand, the Long Term Evolution (LTE) technology was developed as the fourth generation (4G) of mobile communication, enabling data rates of 100 Mbps, and up to 1 Gbps [2], depending on the mobility of the user. 4G uses a new air interface, Orthogonal Frequency Division Multiplexing (OFDM), operating in flexible bandwidths from 1.4 MHz up to 20 MHz [3]. 4G also brought a major enhancement, which is the use of Multiple Input Multiple Output (MIMO) technology. MIMO enables base stations to transmit several data streams over the same carrier simultaneously. MIMO increases the data rate linearly with the number of antennas, under good signal conditions. Further enhancements of LTE are already specified, under LTE-Advanced technology. To enhance data speed, Carrier Aggregation has been defined, combining the capacity of several independent carriers. As a result a maximum bandwidth of 100 MHz can be achieved, combining 5 individual carriers of 20 MHz each.

1.2 A Worldwide Phone

In Europe, GSM was first only specified in the 900 MHz band. The total bandwidth of 25 MHz in Downlink (DL) and in Uplink (UL) was split into 125 channels (including a guard space) of 200 kHz each [4]. Soon it became obvious that the number of channels was not sufficient to support the growing demand. The 1800 MHz band was then assigned, to enhance the bandwidth with 375 additional channels. The GSM standard rapidly spread around the world, enabling roaming possibilities. However, in some countries frequency allocation is different. For example, in North America the European bands of GSM were already allocated, and GSM was adopted in a new set of bands, the 850 MHz band and the 1900 MHz band. In order for Europeans to roam in North America, and vice versa, they need a phone equipped with a quad-band antenna. For UMTS purposes, a new band has been added at 2100 MHz in Europe and Asia, and a band at 1700 MHz has been added in North America. The new LTE networks are also deployed in different frequency bands, depending on the geographical location. Over the years, the list of bands where LTE is deployed is likely to grow. Some of the main bands to cover nowadays are summarized in Table 1 with their DL and UL frequencies. All the

4G bands standardized by the 3^{rd} Generation Partnership Project (3GPP) are defined in [2]. In order for the users to have an LTE worldwide phone, i.e. able to roam data and speech in any country, a tremendous amount of bands needs to be supported. So far, there are 28 bands supporting Frequency Division Duplexing (FDD), and 12 bands supporting Time Division Duplexing (TDD). This very large number of bands to cover across a wide frequency spread is a major challenge for handset antenna designers.

Band	Name	DL [MHz]	UL [MHz]	Band	Name	DL [MHz]	UL [MHz]
1	IMT 2100	[2110-2170]	[1920-1980]	5	US 850	[869-894]	[824-849]
2	PCS 1900	[1930-1990]	[1850-1910]	8	GSM 900	[925-960]	[880-915]
3	DCS 1800	[2110-2170]	[1710-1785]	12	US 700a Lower	[729-746]	[699-716]
4	AWS	[2110-2155]	[1710-1155]	13	US 700b Lower	[734-746]	[704-716]
7	2.6 GHz	[2610-2690]	[2500-2570]	17	US 700 Upper	[746-756]	[777-787]
9	1700 MHz	[1845-1870]	[1750-1785]	18	Japan 800 Lower	[860-875]	[815-830]
11	Japan 1500	[1476-1496]	[1428-1448]	20	Europe 800	[791-821]	[832-862]

Table 1: 4G Frequency bands

1.3 The Compactness Challenge

The recent years have testified of a significant size reduction of the phones. In the past three decades, their volume has decreased from 6700 cm^3 to less than 100 cm^3 [5]. The electronics inside the mobile phone have also followed a similar trend, and the same demand is now put on the antennas. Consequently one of the major research areas in handset antennas has been efficient miniaturization. Nowadays, antennas are integrated inside the handset, and have become invisible to the user. However, antennas are governed by fundamental laws that inversely relate their efficiency to their bandwidth and size [6]. In other words, enhancement of the antenna bandwidth and toughening of the volume constraints will result in a degradation of the antenna efficiency. Antenna designers work with this trade-off and optimize it, depending on the application. Additionally, antennas must exhibit good performances in close proximity of bulky metallic components such as battery, camera, vibrator, mini-usb connector and so forth. Finally, more than one antenna must fit into an already tight volume, for MIMO operation of handsets.

1.4 MIMO Antennas

The two main challenges of MIMO for antenna designs are decoupling and decorrelation. Indeed, in order to have MIMO operation on a mobile phone, several antennas are needed. In order to have a benefit from MIMO, these antennas must see different signals. However, on small platforms, these antennas will be closely placed, operating at the same frequency and sharing the same ground plane. Moreover, at low frequencies

(below 1 GHz) the ground plane is also the main radiator. In order to isolate these antennas, a number of techniques have been investigated over the years, including neutralization lines [7, 8], decoupling networks [9–13], parasitic elements [14, 15], defected ground plane structures [16–19], polarization diversity and excitation of different modes of the common ground plane [20, 21]. The latter will be further discussed in Section 1.6.
MIMO antenna design itself is not addressed in this thesis, however decoupling techniques are relevant, as multiple antennas will be needed for the proposed architecture.

1.5 The User Effect

Beyond the challenges of designing a compact wide-band antenna, come the disturbances added by the user, which affect the antenna properties. The user's effect on the antenna is two-fold: antenna detuning and absorption of some of the radiated power. Therefore, the consequences of the user's hand and head are mismatch loss and absorption loss. The interactions between the user and the antenna depend strongly on the antenna type, the user's characteristics (size, grip, tissue, etc.) and the frequency. Typically, user's head and hand can cause a loss varying from 4 dB to 10 dB, directly on the radio link [22]. A large variation of the user effect is reported, depending on antenna type and user. However, in all cases, the major part of the loss is due to absorption. Absorption loss increases with frequency, and detuning increases with tightening of the grip. The effect of the user has been studied for many years [22–33] and specific tests finally entered the standard of the Wireless Association (CTIA) and are available for testing of phone prototypes [34, 35]. This standardization has been reached after public awareness of the antenna performance deterioration was raised, with the release of the iPhone 4 and its *death-grip* issue.
The interaction between the antenna and the user is bi-directional, and the antenna also has an effect on the user. Some energy is absorbed by the human body when exposed to a Radio Frequency (RF) electromagnetic field, thus one can measure the Specific Absorption Rate (SAR), which is the amount of power absorbed per mass of tissue. SAR investigations have compared antenna types and their effect on the head absorption, namely [36–38]. SAR issues are not addressed in this thesis.

1.6 Antenna Designs to Address 4G Requirements

In order to address the bandwidth issue unveiled by the standardization of 4G, two main streams in small antenna design started to develop: enhancing the antenna bandwidth or embedding tunability. The first one aims at increasing the antenna bandwidth with a passive design, mainly coupling to the ground plane, whereas the second one uses active components to dynamically change the resonance frequency of a narrow-band self-resonating antenna. In the first case, the main challenge is to achieve antenna decoupling, when two or more antennas are considered, as strong currents are carried

on the board. In the latter case, the antenna has an instantaneously narrow bandwidth but can effectively cover a wide range of frequencies.The state-of-the art of these two techniques is described below.

Compact and Multiband Antennas

Because of the many different applications to support (worldwide coverage, WiFi, GPS, Bluetooth, and so forth), nowadays handsets require wideband antennas or multiple antennas. In both cases more volume needs to be dedicated to the antenna on the handsets. Because of the limited volume available for the antenna and the likelihood of an ever increasing number of bands to cover, the wideband antenna approach does not seem feasible for a long term solution. Moreover an antenna able to cover all the required frequencies at once is unnecessary as one rarely needs to operate in all bands simultaneously. However these antennas present some advantages from a system perspective, e.g. a unique feeding line on the board, or ease of to implementation of carrier aggregation. They have been widely investigated over the past years and an overview is given in this section.

The Chu-Harrington limit relates the antenna achievable bandwidth to its volume [6] - in this definition the volume corresponds to the smallest sphere enclosing the antenna. Wideband antenna designers have for main goal to optimize this relation and get the closest possible to the limit. For this purpose the volume needs to be best utilized, however in mobile phones this is rarely affordable. Obtaining antenna bandwidth is most challenging at low frequencies (below 1 GHz) as the antenna is electrically small. The board is typically about $\lambda/4$ long at low frequencies, thus the main radiator is actually the whole board. The antenna rather acts as a Capacitive Coupling Element (CCE) adequately exciting the board. This way of looking at the antenna was defined and described in [39], exhibiting the low-profile potential of CCE. CCE designs, as opposed to self-resonant designs like [40], [41], [42], [43] and [44], were then extensively investigated to get the maximum bandwidth out of the board. In [45], the authors obtain significant volume-to-bandwidth ratio improvements, halving it at 900 MHz with the use of a CCE instead of a self-resonant antenna. A comprehensive equivalent circuit model of the relation between a CCE and a ground plane is given in [46]. However, CCE designs require a matching circuitry, which will affect their efficiency. The authors in [47] used the CCE concept to cover the bands 5 and 8 in the low-band with a given matching circuit, and the region from 1.6 GHz to 2.2 GHz in the high-band with another circuitry. The use of complex matching inevitably degrades the radiation efficiency, which was about 40 % at 900 MHz. Same efficiency was obtained with the design in [48]. The design proposed in [49] used a reconfigurable matching network on a single CCE and achieved 55 % efficiency at 900 MHz. In [50] the 700 MHz band was addressed, with an efficiency of only 20 %. At the same frequency [51] reached a 62 % efficient design with a fixed matching network. The above-mentioned examples show the kind of efficiency that has been achieved on handsets in the low-bands. However antenna design comparison

is a delicate task as antenna volumes need to be compared as well, and antenna volume is very difficult to estimate. The Quality factor (Q) of an antenna relates stored energy and dissipated energy, and it is inversely proportional to the bandwidth. The smaller the antenna, electrically, the higher the minimum achievable Q and the narrower the achievable bandwidth.
The drawback of CCE appears, when one considers multiple of them on the same board. Indeed if several antennas are needed, as in the case of MIMO, these antennas need to be isolated in order to radiate into the far-field. This is a difficult task to achieve, when each of them utilizes the full board to resonate. The design in [52] achieved -10 dB isolation, but at a quite high frequency of operation, namely 1600 MHz. In order to isolate antennas at the low-bands, antenna designers have primarily used the characteristic modes theory. The theory was first developed in [53] and refined in [54], both in 1971. A lot of attention is being given to it in the recent years, as the interest to the interaction CCE-ground plane has grown. Characteristic modes not only give a real insight into the radiation mechanism of any metallic structure, but they also provide very attractive orthogonality properties. Different modes can be simultaneously excited on the ground plane, in order to obtain orthogonal radiation patterns. Recent studies exploiting this theory for contemporary antenna design challenges include [55], [56], [57], [58], [20], [21] and [59]. An isolation above 20 dB at 900 MHz has been achieved with an efficiency above 65 % [20]. The commercial 3D electromagnetic software FEKO proposes the option of calculating characteristic modes, bringing this theory to a wide audience.

Compact and Narrow-band Antennas

A promising way to cut down in the volume occupied by the antenna is the use of a single narrow-band antenna that can be reconfigured to provide a wide palette of frequencies of operation. Such an antenna is called frequency reconfigurable antenna. The idea of a reconfigurable antenna was mentioned for the first time in a U.S. patent in 1983 [60], where pattern and polarization reconfigurability were also included. A large overview of reconfigurability possibilities for antennas is given in [61]. This thesis focuses on frequency-reconfigurability in the 4G operating bands for mobile phone platforms.
Frequency reconfigurable antennas can be obtained in a number of ways, such as modifying the resonance length, re-routing the current paths on the antenna element or connecting different elements together. These mechanisms are accomplished with the use of active components like switches or variable loads.
In [62] the authors proposed an antenna capable of switching between the US cellular band and the European GSM bands, with a switch between two transmission lines. A similar design is also proposed in [63]. Reconfigurable slot antennas were proposed in [64], where the resonating length could be controlled by different combinations of switches. Another slot antenna design was proposed for continuous tuning between 1.2 GHz and 1.65 GHz [65], using a varactor diode for improved ohmic resistance. Similar results were found in [66] and another slot design was proposed in [67]. Slot antennas

present a convenient design for component insertion across the slot. A varactor was also used in [68], which proposes a patch antenna for phone implementation. A similar implementation was also proposed by the same authors for cognitive radio in [69]. Recently, development of RF Micro-Electro-Mechanical Systems (MEMS) provides low power consumption, high linearity and high Q parts. RF MEMS are nowadays very attractive for antenna tuning implementation. Among the first publications with MEMS tunable capacitors for antenna tuning, the authors in [70] and [71] used them in the 15 GHz band. In the mobile communication bands, [72] used MEMS Switches to cover one octave, and MEMS variable capacitors were used in [73] to cover multiple bands between 700 MHz and 2700 MHz and in [74] to cover PCS and IMT bands. Variable capacitor systems have also been investigated for the Digital Terrestrial Broadcasting (DTB) bands and the low Ultra High Rrequency (UHF) bands, as in [75], [76], [77] and in [78]. This work is relevant if one considers the future bands to be added to the 4G spectrum, towards 600 MHz and lower.
This thesis addresses the case where loading of the antenna is performed with a variable capacitor in order to modify its resonance frequency.

1.7 Front-end and Antenna Architecture to Address 4G Requirements

The specifications for 4G do not only bring new challenges on the antenna design, but also on the RF Front-End (FE) architecture of the mobile phone. The FE is mainly responsible for the filtering and amplification of the signals. The RF FE is part of the overall receiver-transmitter (transceiver) system. Its role is to interface the antennas to the transceiver. It groups all the components between the antenna and the digital baseband system. The FE is responsible for processing the modulated signals received at the antenna into signals suitable for input into the baseband Analog-to-Digital Converter (ADC), and vice versa. The main components of the mobile FE are filters, Power Amplifiers (PA) and Low Noise Amplifiers (LNA). Mixers and synthesizers are part of the transceiver. When receiving, the main specifications are sensitivity and selectivity, whereas the linearity is the main concern when transmitting. The RF FE is a crucial part of the communication system as it sets the limits on the Bit Error Rate (BER).
When the number of communication bands started to expand, the complexity of the RF FE increased accordingly. RF engineers are nowadays looking at a step from a 5-band architecture to support 3G, to a 40-band architecture for worldwide 4G. The very tough requirements for TX/RX isolation have made highly selective filters unavoidable, leading to parallelization of the receiving and transmitting paths. For each band to operate in, the FE needs a dedicated RF chain. Therefore, the high number of bands will inevitably lead to component duplication, thus larger volume occupied on the board, higher power consumption and increased cost of the FE.

Conventional Architecture

Following the user's demand for more data rates, more frequency bands are allocated to mobile communications. The more bands to address in a mobile phone, the more discrete components are needed. The main component needed for 3G and 4G systems is the duplex filter, as they rely on Frequency Division Duplex (FDD) for data transmission and reception. However with the tendency for bigger screens, better processors, higher connectivity and battery life, there is no room left to expand the space dedicated to the FE anymore.
An example of 2G FE is shown in Fig. 1. The 3G FE is more complex than a 2G architecture, and one can see in the example of Fig. 2 the Surface Acoustic Waves (SAW) filters, as well as the addition of the duplex filters. The duplexers are needed to reject TX interferences from the RX path. The SAW filters are typically used for their high selectivity, suppressing out-of-band interferences, by a sharp transition from pass-band to stop-band. For example a typical 2G/3G FE that covers 7 bands, quad-band for GSM and tri-band for UMTS, can need up to 5 PA, 3 LNA, 3 duplex filters, 10 SAW filters, and a multiple-throw switch, as described in [79]. The FE complexity of a 3G phone affects its cost and battery life compared to a 2G phone. For example the cost of a WCDMA phone is triple than the cost of a GSM phone, and its talk-time is half the one of a GSM phone, as reported in [79]. This phenomenon is due to the higher component count of the FE of the 3G phone, mainly due to the duplexers. The FE for a 4G phone operating worldwide will have to cover, not 5 or 7 bands like in 3G, but about 40 bands. If the same architecture model (one RF chain with dedicated components per band) is applied, the RF component count of a 4G phone would explode. This very high complexity of the FE design would lead to component duplication and inefficient use of the board space. Traditionally designers resort to stacked architectures and banks of components. Manufacturers came up with several ways of combining the components, as a solution for downsizing, however it does not reduce the component count.

Proposed Architecture

Phones for a worldwide LTE operation need a shift in architecture in order to eliminate component duplication and redundancies. The requirements on the mobile phones market are to drive down cost, Printed Circuit Board (PCB) area and power consumption. This sub-section presents a novel architecture, that will enable multi-band multi-mode operation, while reducing complexity. This architecture has been patented in [82, 83] and its concept has been discussed in [84]. A radio block of the proposed architecture is shown in Fig. 3. The main feature of the proposed architecture is to separate the Transmitting (TX) path and the Receiving (RX) path into two independent RF chains and into two distinct antennas. In that way, duplex filters can be eliminated, playing a major role in the component duplication. Suppressing components from the FE will ensure a gain in space and in current consumption. The rejection of the transmitted

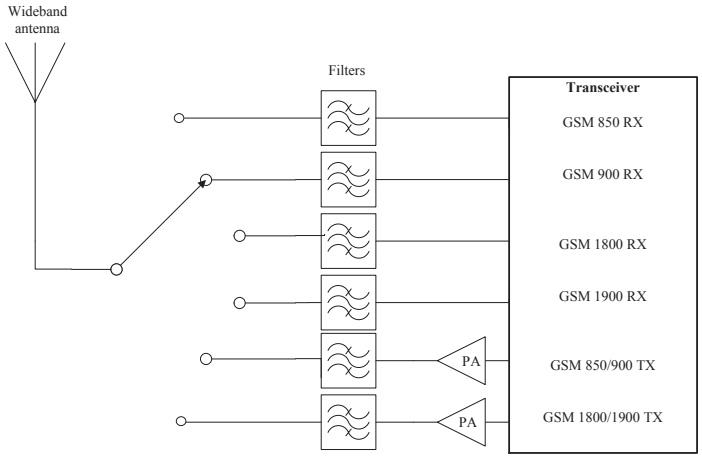

Fig. 1: GSM front-end architecture [80].

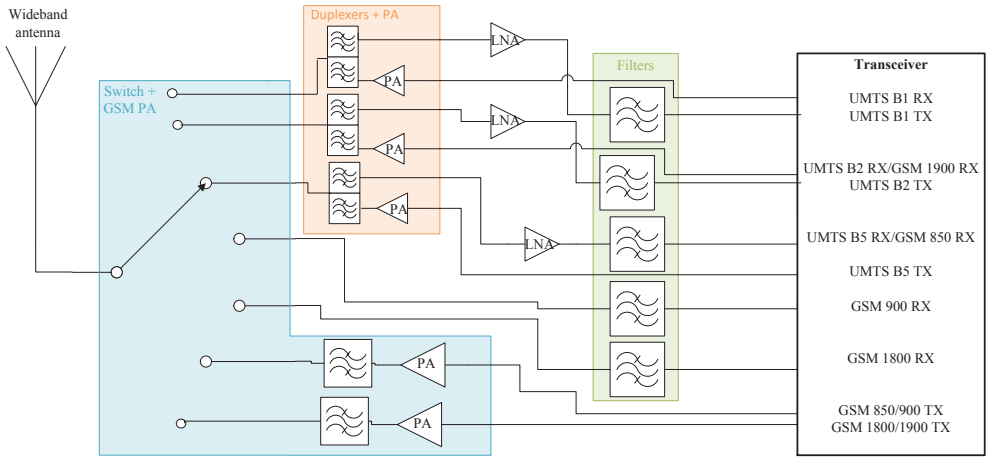

Fig. 2: Typical 3G front-end architecture [81].

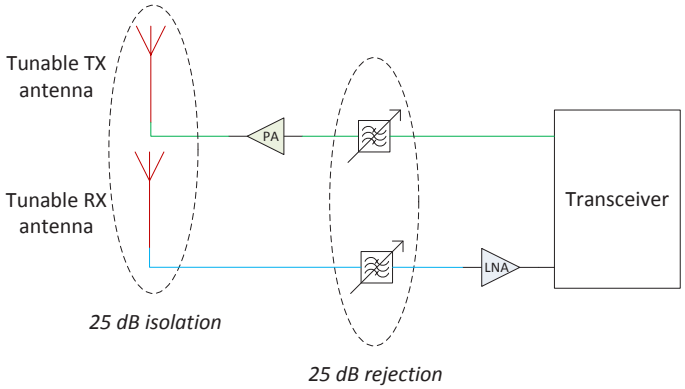

Fig. 3: Proposed architecture [Paper H].

signals into the receiving path must then be ensured by the antennas and the filters. A typical duplex filter provides 50 dB rejection between the RX and the TX [85]. In the proposed architecture, 25 dB of rejection can be obtained from the tunable filters. Therefore, a duplex isolation of 25 dB needs to be provided by the antennas. Both TX and RX antennas are narrow-band in order to cover only one channel and to provide the required isolation. Additionally both the antennas and the filters are tunable, in order to cover the whole 4G frequency spectrum. With the proposed architecture, the board space is efficiently utilized and the power consumption reduced.
The papers presented in the thesis are made in the scope of this new architecture, enabling world-phones. They are dealing with narrow-band antenna challenges, tunability using MEMS tunable capacitors and duplex isolation on mobile phone platforms.

2 Aims of the Work

In the introduction, a novel architecture to address the need for bandwidth of modern wireless phones has been proposed. In order to make this architecture feasible, the antennas need to be designed according to the specific requirements of this architecture. These design requirements will be investigated in the following work.
The focus of this thesis is three-fold: the challenges of small and narrow-band frequency-reconfigurable antennas, the impact of the user on narrow-band antennas, and the challenges of high antenna isolation on a small platform. Therefore the thesis will be divided into three parts, addressing each of these issues, in the scope of the previously detailed architecture. This architecture re-arranges the front-end of the mobile phone and the requirements on the antennas, in order to open the possibility for worldwide phones.

2.1 Frequency Tuning

Frequency tuning is a promising technique to enhance the bandwidth of an electrically small antenna. However, to optimize antenna tuning, one needs to understand the new trade-offs of co-designing the antenna and the tuner. Moreover, efficiency is a major objective of antenna designs and the leading axis of research is understanding the loss mechanism of small and narrow-band antennas when they are tuned to different operating frequencies. Achievable efficiency is a limiting factor of frequency-reconfigurable antennas, thus quantifying and optimizing this loss is fundamental.

2.2 User's Impact

This thesis investigates a new type of antennas for mobile phones, namely narrow-band antennas. While the effects of the user's hand and head are well established for typical handset antennas, they are not clear for narrow-band antennas. Detuning and absorption loss are compared between a conventional antenna and a narrow-band one, on a small hand-held platform. Understanding the specific interaction between a user and an antenna exhibiting a high quality factor is the aim of this section.

2.3 Antenna Isolation

Achieving antenna isolation is a real challenge on small platforms, especially at low-bands (below 1 GHz). The main limitations to high isolation are the electrically small distance separating the antennas, and the common ground plane, which also is the main radiator at low frequencies. In the scope of the proposed architecture, an isolation above 25 dB is needed between duplex antennas, resulting from the elimination of the duplexers. The operating frequencies of the TX and RX antennas are separated by 30 MHz or more. The goal of this section has been understanding how to design duplex antennas, exhibiting such isolation.

3 Thesis Contributions

This thesis presents a novel architecture addressing the LTE bandwidth challenge for mobile phones, which is detailed in Paper H. This concept has been previously patented in [82, 83]. The aim of the architecture is to reduce the occupied space on the PCB, the power consumption and the antenna dimensions. Duplex antennas are used for that purpose, i.e. separate TX and RX antennas. These antennas must be narrow-band, compact and frequency-reconfigurable. Such a design is proposed in Paper F for a small mobile terminal. It addresses the low-bands of LTE, as they are the toughest for small platforms. This design is improved for a duplex antenna application in Paper G, exhibiting 25 dB isolation in band 12. Finally, the duplex antenna design is enhanced to cover both high-bands and low-bands of the LTE spectrum, in Paper H.

A prerequisite for this architecture is to be able to use the antennas as radiators, as well as filters. Thus the antennas must be narrow-band. Narrow-band and tunable antennas have the advantage of being compact and cover an effectively wide bandwidth. However, a high field concentration might lead to efficiency challenges. Paper A examines the challenges of the design of a narrow-band antenna and depicts the trade-offs that such a design unveils, e.g. tuner location and achievable tuning range. This paper also reports a significant degradation of the measured total efficiency of the tunable antenna. This issue is examined more closely in Paper B, with a single-band antenna and a fixed capacitor. The tuning loss due to the series resistance of the fixed capacitor can be estimated, but does not match the total measured loss. Paper C proposes to distribute the tuning in order to reduce the loss due to the tuner. Finally, Paper D performs a thorough investigation of the source of loss of narrow-band tunable antennas, and concludes with the existence of conductive loss for such antennas. Achievable efficiency is the limiting factor of these antenna types.

The results of Paper D and Paper G are complementary. The tracks leading to each of these papers have been pursued in parallel. Paper A, B and C have contributed to the results found in Paper D. Similarly, Paper F and G have contributed to the design presented in Paper H. On a side track, Paper E has initiated an investigation of the user effect on narrow-band antennas. All the papers collected in this thesis have as goal to contribute to the architecture presented in Paper H. They have addressed specific challenges, that contribute to the overall architecture design. Paper H presents the idea behind, and the reason for investigating the particular aspects of narrow-band antennas or duplex isolation.

4 Summary of Papers

4.1 Antenna tuning

Paper A

Challenges for Frequency-Reconfigurable Antennas in Small Terminals
76^{th} Vehicular Technology Conference, pp. 1–5, Sept., 2012, IEEE

Motivation
A number of tuning techniques for small antennas have been published in the literature. This paper aims at giving an overview and comparing the advantages and disadvantages of each tuning technique. In the project's framework (detailed in 1.7), continuous tuning of narrow-band antennas is required, its feasibility and performance are investigated with a typical antenna for mobiles phones. The investigation is run at the low-bands of the LTE spectrum, in order to show a tough scenario for small terminals.

Paper
The paper starts with presenting a state-of-the-art of the tuning techniques published in the literature. MEMS tunable capacitors present a higher Q than other techniques, which is essential for tuning of a high-Q antenna. The high voltage handling and high linearity makes this tuning technique feasible for mobile phones applications. The paper continues with explaining the trade-offs specific to narrow-band antennas and continuous tuning, and gives some design guidelines for such an antenna. Finally, an example of a Planar-Inverted-F Antenna (PIFA) is built to test the concept.

Main results
MEMS tunable capacitors are the most suitable tuning technique for the architecture proposed in this thesis. At the design stage of a capacitively loaded antenna, the location of the tuner, achievable tuning range, tuning resolution and voltage handling are the main trade-offs. Moreover the location of the tuner and its insertion loss will determine the antenna efficiency. As the antenna is tuned further away from its initial resonance frequency, its Q value increases and its efficiency dramatically decreases. The main reason of the efficiency degradation is the Equivalent Series Resistance (ESR) of the tuner. However the measured efficiency of a high-Q tunable antenna resulted to be lower than expected, inferring that the ESR of the tuner is not the only source of loss for narrow-band tunable antennas. Achieving high efficiency will be the main challenge of narrow-band tunable antennas.

Paper B

On the efficiency of frequency reconfigurable high-Q antennas for 4G standards

Electronics Letters, Vol. 48, Issue 16, pp. 982–983, Aug., 2012, IET

Motivation

As shown in paper A, the measured efficiency of a high-Q tunable antenna is significantly degraded, as the antenna is tuned further away from its original resonance frequency. In order to demonstrate the particularity of high-Q antennas in a tunable architecture, paper B compares measured efficiencies of a low-Q and a high-Q antenna, both at their initial resonance frequency and at a tuned frequency.

Paper

In order to focus the investigation, the antenna design is made following these guidelines:

- single-band antenna design
- pure copper for the ground and the PIFA
- high-Q fixed capacitor
- minimum use of tin

The height of the PIFA over the ground plane is the main design parameter to determine the antenna Q value, thus in order to compare a low-Q and a high-Q antenna, two versions of the mock-up are manufactured with two different antenna heights (2mm and 10 mm above the ground).

Main results

The high-Q antenna exhibits higher numerical field values than a low-Q antenna, resulting in higher currents flowing to its tuning capacitor. Therefore the impact of the tuner is more significant in the case of a high-Q antennas, than a low-Q antenna. As the antenna is tuned further away from its original resonance frequency, the antenna Q increases, so do the currents and the loss due to the ESR of the tuning capacitor. Narrow-band tunable antennas are prone to be lossier than conventional designs.

Paper C

On the Efficiency of Capacitively Loaded Frequency Reconfigurable Antennas
International Journal of Distributed Sensor Networks (IJDSN), Special Issue on Smart and Reconfigurable Antenna Applications in Wireless Sensor Networks, Article ID 232909, June, 2013

Motivation
Paper B showed that the currents delivered to the capacitor are an issue, in the case of high-Q antennas for tuning. Paper C aims at proposing a way to reduce the impact of the ESR due to the tuner, or fixed capacitor.

Paper
In order to minimize the ESR loss, this paper proposes to use a distributed tuning mechanism. A detailed example is given for the case of two tuning points on the antenna. In that way the surface of high current concentration is larger (depending on the relative distance of both tuning points) and the current flowing to each of the capacitors is reduced. This paper uses fixed capacitors for a proof of concept, but the principle can be applied to a single tuner, with two independent banks. The main focus is put on the ESR loss, in order to isolate this impact, high care of the mock-up is taken: using pure copper, minimizing or suppressing the tin for sensitive locations, as for example at the short and at the tuning points, which are high current density locations.

Main results
The loss could be reduced by 1 dB at 700 MHz with a distributed tuning mechanism. The main strength of this approach is that the loss reduction becomes more significant as the antenna is tuned further away from its original resonance, i.e. as the ESR loss increases. This solution does not increase the complexity of the design, as it is feasible with a single tuner, as long as the two tuning points are in reasonable distance to each other. As in paper A, this papers highlights the existence of an additional source of loss.

Paper D

Loss Limitations of Frequency Reconfigurable Antennas
Submitted to Transaction on Antennas and Propagation, Aug., 2013

Motivation
Paper A and B showed that the ESR of the tuning capacitor is a major factor in the tuning loss. Paper A and C inferred that the ESR loss is not the only source of loss in the case of tuning for high-Q antennas. Paper D intends to understand and characterize

the loss mechanism of high-Q antennas.

Paper
The paper compares three different high-Q antenna designs. The first one is a mobile phone antenna design, where the antenna is made according the requirements of the proposed architecture (detailed in 1.7), i.e. two different antennas for the TX and the RX operation and duplex isolation of -25 dB. The second one is a simple radiator above a large ground plane. That design can vary its Q, by varying the width of the radiator. Several measurements are made at 700 MHz to compare efficiencies for different Q values. The third design is a loop antenna, where the diameter of the loop changes its resonance frequency. Several loops of different sizes are built and measurement are made at 700 MHz, using a tuning fixed capacitor. Moreover different materials are used to compare the effect of the metal conductivity.

Main results
Measurements show that even with the best material - from a conductivity point of view - available nowadays i.e. silver, the efficiency of a high-Q tunable antenna is limited by its conductive loss. This loss is intrinsic to the antenna material and increase with the tuning range. In the case copper for example, the antenna was tuned from 2.69 GHz to 700 MHz, which is the LTE spectrum so far, and the conductive loss raised to 7 dB. Analytical results confirm the measurements.

4.2 User's Impact

Paper E

The Effect of the User's Body on High-Q and Low-Q Planar Inverted F Antennas for LTE Frequencies
75^{th} Vehicular Technology Conference, pp. 1–4, May, 2012 IEEE

Motivation
The user's body has a major impact on the properties of a mobile phone antenna. The impact of the hand and head of the user have been investigated for different grip types and on different antenna types. However these antennas are typical GSM antennas, i.e. antennas exhibit a low-Q value. The user's impact on high-Q antennas still needs to be investigated.

Paper
This paper addresses the impact of the user on a narrow-band antenna and compares it with a typical antenna design. The hand of the user and especially the index finger being the main disturbance to the antenna radiation properties, the distance antenna-finger is kept constant for both high-Q and low-Q designs. Results are based on FDTD

simulations.

Main results
On the one hand, the detuning effect of the user is significantly reduced with the high-Q antenna compared to the low-Q antenna. On the other hand the absorption loss is significantly larger for the high-Q antenna than for the low-Q antenna. Summing up both effects, the user seems to have similar impact on both antenna types.

4.3 Antenna Isolation

Paper F

Coupling element antenna with slot tuning for handheld devices at LTE frequencies
6^{th} European Conference on Antennas and Propagation (EuCAP), pp. 3587–3590, March, 2012 IEEE

Motivation
Antenna designs that can cover frequencies as low as 700 MHz are generally very bulky. With the high integration required in mobile phones, designing compact antennas is a prerequisite.

Paper
This paper proposes the design of a very compact antenna, on a 100 × 40 mm phone form factor, composed of a coupler and a slotted ground plane. This design is meant to be continuously tuned and uses capacitive loading with steps of 1/8 pF. The slot provides easy insertion of a tunable capacitor, which will enable the antenna to cover all the frequencies from 960 MHz to 700 MHz. The location of the tuning capacitor will impact the tuning resolution and the loss, thus a trade-off is chosen. The impact of the user's hand is also briefly investigated with simulations.

Main results
Design of a very compact narrow-band antenna was achieved. Continuous tuning of the antenna, in the low-bands of the LTE spectrum, was implemented. Efficiency measurements and analytical loss decomposition proved that the major cause of efficiency deterioration comes from the resistance of the capacitor.

Paper G

Antenna design exploiting duplex isolation for 4G communication on handsets
Electronics Letters, Vol. 49, Issue 19, pp 1197–1198, Sept., 2013 IET

Motivation
In order for the architecture detailed in 1.7 to be realized, duplex tunable and compact antennas are needed. The low-band frequencies being the toughest on small terminals, they are addressed first.

Paper
A duplex antenna is designed, inspired from the design proposed in paper F. The design is very compact and an understanding of the isolation is made through surface current analysis. Data on the antenna quality factor is also given for understanding possible conductive loss (form paper D). The mock-up is built with pure copper and fixed capacitors, as a proof of concept of the design.

Main results
The duplex antennas are isolated below 25 dB throughout their tuning range. Tuning can go as low as 700 MHz and efficiency is above -4.5 dB at 700 MHz, where 2 dB are due to the insertion loss of the capacitors.

Paper H

Novel architecture for world-phones
Submitted to Antennas and Wireless Propagation Letters, Special Cluster on Terminal Antenna Systems for 4G and Beyond, Oct. 8th 2013, IEEE

Motivation
The band proliferation due to the standardization of 4G communications impacted not only antennas but also the front-end architecture of mobile phones. This paper proposes a novel design that will address the LTE bandwidth challenges by a shift in front-end architecture and in antenna design. With the knowledge from antenna tunability (paper A, B , C and D) and antenna isolation (paper F and G), this paper describes a novel architecture for world-phones.

Paper
The paper proposes a novel architecture that limits component duplication in the front-end, which also implies saving board space and battery life. The architecture presented requires narrow-band antennas with a high isolation. A design inspired from paper F and paper G is used, and covers the low-band as well as the high bands of the LTE spectrum.

Main results
This paper is made with the knowledge built form the previous papers, on narrow-band antennas, tunable antennas and isolation investigation. It shows a dual-band duplex antenna together with a 2-path front-end architecture. Isolation between the antennas

reaches 25 dB and tunability covers from 600 MHz to 2.17 GHz. The efficiency is limited by the tuner insertion loss and drops from -3 dB to -4 dB at the high bands, similar performance is observed in the GSM band.

5 Discussion

The work presented in this thesis has been made in connection with the feasibility of the front-end architecture described in the introduction. This architecture would drive down the cost, PCB board space and power consumption. In order to build such an architecture, narrow-band and tunable antennas are needed. They are also required to exhibit a duplex isolation higher than 25 dB and a high efficiency. The isolation requirements descend from the suppression of the duplex filters, originally providing 50 dB rejection [85] from the transmitted signal into the receiver path. The tunable filters used in the proposed architecture are able to provide 25 dB of rejection, thus the antennas must provide 25 dB of isolation. The first design challenge that has been tackled was the design of tunable high-Q antennas and their achievable efficiency. Following this the user impact on such antennas has been investigated through simulations, and finally the isolation on small terminals was addressed.

5.1 Frequency Tuning

The aspects of frequency tuning discussed in this work are continuous tuning with high resolution on high-Q antennas. The main issue throughout the work on high-Q tunable antennas has been their efficiency. Antenna efficiency is a delicate task to investigate. In order to be simulated with time-domain techniques, it requires a very large amount of computational time, specially for high-Q structures. In order to be measured, it requires a high accuracy of the anechoic chamber and, more importantly, mechanically stable mock-ups. The details of the structure and its stability are crucial to repeatability of these measurements. The investigation of the loop designs with a fixed capacitor in paper D has the advantages of being very simple to manufacture, of minimizing the use of tin, and of using the forces of the metal itself to ensure stability. These designs were small enough to exhibit an amount of loss much larger than the chamber accuracy, providing quantifiable results. As a counter-example, when the same investigation is run on a patch antenna, stability of the height of the patch is an issue for high-Q structures and the loss of 120 mm-long ground plane at 700 MHz is within 1 dB, thus difficult to characterize accurately and investigate. The loss mechanism of such antennas has been thoroughly investigated and it is two-fold: part of the loss is due to the tuning capacitor and part of the loss is due to conductivity. The loss due to the fixed capacitor is intrinsic to the component and it can be reduced by carefully choosing its placement or distribute the tuning, as seen in paper C. The loss due to the metal is the limiting factor of tunable antenna designs. Experiments were run with the best conductors available nowadays, ultimately when the structure is electrically very small (about $\lambda/30$ in the presented investigation) the loss is significant (approaching 10 dB in the presented investigation). Conductive loss is the limiting factor to the high integration of antennas, e.g. to how small one can make it at a given frequency. This has major consequences on low-band

performance of small terminals.
Throughout this investigation, the difficulty of comparing antenna designs was encountered. In order to make a fair comparison, one must change only one parameter at the time, however with antenna designs, where it is all about trade-offs (size, efficiency, bandwidth and frequency), this way of comparing designs is not easily applicable. For example, in order to rank designs, one must be able to make two different antennas, that occupy the same volume, exhibit the same bandwidth, but have different radiation efficiencies at a given frequency. Not to mention that estimating the volume of a mobile phone antenna is challenging in itself, due to the ground plane resonance. Comparing antennas to optimize radiation efficiency is a challenging task, participating to the complexity of designing tunable high-Q antennas. Nonetheless, the antenna quality factor is a quantity that includes the main design parameters (volume, bandwidth and frequency). The efficiency ranking can also be made according to the difference between the unloaded and the loaded quality factor. Therefore, to have a complete overview of the design and its characteristics, one must look at both unloaded and loaded quality factors, as well as their ratio. Paper D proposes and uses this metric.

5.2 User's Impact

Narrow-band tunable antennas exhibit higher numerical field values than conventional antennas, whereby the interaction with a user may be different, and must be investigated. The two effects that the user has on antennas are detuning and absorption. Depending on the antenna type and on its location, the hand grip has different impacts with respect to mismatch and absorption losses. It has been reported in [86] that the hand has the largest effect on the antenna detuning, specially the index finger for top-located patch antennas. For that reason, when paper E compared the hand and head effect on two different top-located patch antennas, the distance from the antenna to the index finger was kept constant. It has been observed that the antenna exhibiting the higher quality factor does not suffer from detuning, as opposed to the antenna exhibiting the lower quality factor. However, the absorption loss is significantly higher on the antenna exhibiting the higher quality factor. When summing up both hand losses, mismatch and absorption, and considering the impact of the user's head as well, the total loss is comparable on the patch with the higher and the lower quality factors. This investigation only considers a patch antenna, three different quality factors and two grip types. In order to build strong conclusions on the effect of the hand and the head on antennas exhibiting a high quality factor, as narrow-band tunable antennas, a larger number of hand grips and index positions must be investigated, and applied to a large number of antenna types. However, this initial investigation in paper E, infers that higher quality factor antennas are more robust against detuning.
As narrow-band antennas exhibit higher numerical field values, the impact of these antennas on the user must also be investigated. As it has been seen, absorption loss on

a narrow-band antenna is higher than on a conventional antenna. Therefore, higher heating of the tissue must be expected. The measure of the energy absorbed by the human body, specific absorption rate, is a mandatory requirement. Narrow-band antennas must be designed to comply to the specifications, in order to be allowed on the market. These specifications are also a limiting factor to how high the quality factor of an antenna can be, and how small it can be designed. Fortunately, the absorption does not only depend on design parameters of the antenna element, but also on the ground plane dimensions and the antenna positioning. Therefore, antenna engineers have additional degrees of freedom, to allow them to design small and tunable antennas, that can also have a low specific absorption rate.

5.3 Duplex Isolation

Typically the isolation is considered for antennas operating at the same resonance frequency. In the case of the architecture proposed in this thesis, the isolation is needed between transmitting and receiving frequencies, i.e. duplex isolation. High duplex isolation from the antennas, combined with high filter rejection, will allow to suppress the duplexers from the front-end design. Achieving high isolation for frequencies below the resonance of the ground plane (typically 1 GHz) is a major challenge, because the actual ground is the main resonator for these frequencies. In papers G and H, an isolation of 25 dB was achieved at low-band frequencies. The two main contributions to achieving high isolation are are the duplex distance and the high quality factor of the antennas. Indeed the smallest duplex distance defined in the LTE standard is 30 MHz, and the high quality factor of the antennas confines the fields around the antenna structure, preventing from high leakage through the ground plane.
Isolated narrow-band antennas do not use the entire ground plane to radiate. In that sense the dimensions of the ground plane do not affect their radiation properties, thus they have the potential of being ground-plane independent. The design proposed in paper G is compact and easy to add to the side of a ground. Extending the length of the ground will only help the isolation, whereas extending its width will have a minimal impact, as the fields are confined on one side of the board. Investigating the portability of narrow-band antennas can be very promising, in order to achieve a universal design for rectangular boards.
Ground planes can resonate in different modes, which depend on their shape. The theory of characteristic modes has been developed in order to predict these modes. Its main strength is to predict orthogonal modes, thus giving high isolation between antennas. The excitation of certain modes of a given ground plane shape depends on the location of the antenna element and its shape. In the design proposed in paper H, the low-band radiators are placed orthogonally in order to minimize antenna coupling. No investigation of the characteristic modes has been done, as the orthogonal position can be found intuitively. However, using the characteristic modes theory will provide a better insight

into the chassis behavior and should be investigated in order to optimize performance.

6 Conclusion

This thesis describes a novel front-end architecture for future mobile phone communications. The feasibility of such an architecture as achieved with fitted antennas, that are narrow-band, tunable, isolated and efficient. The two main antenna challenges for the proposed architecture were to understand the loss mechanism of narrow-band tunable antennas and its implications, and to achieve high isolation at frequencies as low as 700 MHz, or even 600 MHz according to the future US auction. It has been found that beyond insertion loss due to the tuner, there is also a loss due to the metal conductivity. This loss grows as the size of the antenna shrinks, and can be a limiting factor to antenna integration. However, this loss is only significant for electrically very small structures. It has also be found that a duplex isolation of 25 dB can be reached for the low and the high bands of the LTE frequency spectrum. This level of isolation combined with tunable filters also exhibiting a good level of rejection allows for removing the duplex filters from the front-end designs of mobile phones. New challenges like carrier aggregation also have a feasible implementation with the proposed architecture, using dual-low-band resonators. The proposed architecture has a strong potential given today's market expectations. Removing the duplex filter, main actor of the component duplication, has been proven feasible using narrow-band antennas and tunability. Its potential is tremendous in today's mobile phone market, where all phone manufacturers aim at driving down the cost, shrinking the size and increasing the battery life. The proposed architecture can be a shift in the way future mobile phones front-end and antennas will be conceived.

References

[1] G. A. (GSMA), "Web Press Release: 1000 New Mobile Phone Users per Minute," 2006. [Online]. Available: http://mobilesociety.typepad.com/mobile_life/2006/08/1000_new_mobile.html

[2] 3GPP TS 36.101, "LTE; Evolved Universal Terrestrial Radio Access (E-UTRA); User Equipment (UE) radio transmission and reception," p. V11.3.0 Realease 11, 2013.

[3] M. Rumney, *LTE and the Evolution to 4G Wireless: Design and Measurement Challenges*, 2nd ed. John Wiley & Sons, Ltd, 2013.

[4] M. Sauter, *From GSM to LTE: An Introduction to Mobile Networks and Mobile Broadband*. John Wiley & Sons, Ltd, 2011.

[5] Z. N. Chen and M. Y. W. Chia, *Broadband Planar Antennas: Design and Applications*. John Wiley & Sons, Ltd, 2006.

[6] R. F. Harrington, "Effect of Antenna Size on Gain, Bandwidth, and Efficiency," *Journal of Research of the National Bureau of Standards- D. Radio Propagation*, vol. 64D, no. 1, pp. 1–12, 1960. [Online]. Available: http://archive.org/details/jresv64Dn1p1

[7] A. Chebihi, C. Luxey, A. Diallo, P. Le Thuc, and R. Staraj, "A novel isolation technique for closely spaced pifas for umts mobile phones," *Antennas and Wireless Propagation Letters, IEEE*, vol. 7, pp. 665–668, 2008.

[8] A. Diallo, C. Luxey, P. Le Thuc, R. Staraj, and G. Kossiavas, "Enhanced two-antenna structures for universal mobile telecommunications system diversity terminals," *Microwaves, Antennas Propagation, IET*, vol. 2, no. 1, pp. 93–101, 2008.

[9] J. Andersen and H. Rasmussen, "Decoupling and descattering networks for antennas," *Antennas and Propagation, IEEE Transactions on*, vol. 24, no. 6, pp. 841–846, 1976.

[10] C. Volmer, J. Weber, R. Stephan, K. Blau, and M. Hein, "An eigen-analysis of compact antenna arrays and its application to port decoupling," *Antennas and Propagation, IEEE Transactions on*, vol. 56, no. 2, pp. 360–370, 2008.

[11] B. K. Lau, J. r. B. Andersen, L. Fellow, G. Kristensson, S. Member, and A. F. Molisch, "Impact of Matching Network on Bandwidth of Compact Antenna Arrays," *IEEE Transactions on Antennas and Propagation*, vol. 54, no. 11, pp. 3225–3238, 2006.

[12] S.-C. Chen, Y.-S. Wang, and S.-J. Chung, "A decoupling technique for increasing the port isolation between two strongly coupled antennas," *Antennas and Propagation, IEEE Transactions on*, vol. 56, no. 12, pp. 3650–3658, 2008.

[13] R.-A. Bhatti, S. Yi, and S.-O. Park, "Compact antenna array with port decoupling for lte-standardized mobile phones," *Antennas and Wireless Propagation Letters, IEEE*, vol. 8, pp. 1430–1433, 2009.

[14] A. Mak, C. Rowell, and R. Murch, "Isolation enhancement between two closely packed antennas," *Antennas and Propagation, IEEE Transactions on*, vol. 56, no. 11, pp. 3411–3419, 2008.

[15] A. Abe, N. Michishita, Y. Yamada, J. Muramatsu, T. Watanabe, and K. Sato, "Mutual coupling reduction between two dipole antennas with parasitic elements composed of composite right-/left-handed transmission lines," in *Antenna Technology, 2009. iWAT 2009. IEEE International Workshop on*, 2009, pp. 1–4.

[16] F.-G. Zhu, J. D. Xu, and Q. Xu, "Reduction of mutual coupling between closely-packed antenna elements using defected ground structure," *Electronics Letters*, vol. 45, no. 12, pp. 601–602, 2009.

[17] C.-Y. Chiu, C.-H. Cheng, R. Murch, and C. Rowell, "Reduction of mutual coupling between closely-packed antenna elements," *Antennas and Propagation, IEEE Transactions on*, vol. 55, no. 6, pp. 1732–1738, 2007.

[18] Y. Gao, X. Chen, Z. Ying, and C. Parini, "Design and performance investigation of a dual-element pifa array at 2.5 ghz for mimo terminal," *Antennas and Propagation, IEEE Transactions on*, vol. 55, no. 12, pp. 3433–3441, 2007.

[19] Y. Chung, S.-S. Jeon, D. Ahn, J.-I. Choi, and T. Itoh, "High isolation dual-polarized patch antenna using integrated defected ground structure," *Microwave and Wireless Components Letters, IEEE*, vol. 14, no. 1, pp. 4–6, 2004.

[20] H. Li, S. Member, B. K. Lau, S. Member, and Z. Ying, "Decoupling of Multiple Antennas in Terminals With Chassis Excitation Using Polarization Diversity , Angle Diversity and Current Control," *IEEE Transactions on Antennas and Propagation*, vol. 60, no. 12, pp. 5947–5957, 2012.

[21] H. Li, Y. Tan, B. K. Lau, Z. Ying, and S. He, "Characteristic Mode Based Tradeoff Analysis of Antenna-Chassis Interactions for Multiple Antenna Terminals," *IEEE Transactions on Antennas and Propagation*, vol. 60, no. 2, pp. 490–502, Feb. 2012.

[22] G. F. l. Pedersen, *Thesis: Antennas for Small Mobile Terminals*. APNet, Aalborg University, 2003.

[23] M. Pelosi, *PhD Thesis: User's Influence Mitigation for Small Terminal Antenna Systems*. APNet, Aalborg University, 2009.

[24] M. Pelosi, O. Franek, M. Knudsen, G. Pedersen, and J. Andersen, "Antenna proximity effects for talk and data modes in mobile phones," *Antennas and Propagation Magazine, IEEE*, vol. 52, no. 3, pp. 15–27, 2010.

[25] M. Pelosi, G. Pedersen, and M. Knudsen, "A novel paradigm for high isolation in multiple antenna systems with user's influence," in *Antennas and Propagation (EuCAP), 2010 Proceedings of the Fourth European Conference on*, 2010, pp. 1–5.

[26] J. Ilvonen, O. Kivekas, J. Holopainen, R. Valkonen, K. Rasilainen, and P. Vainikainen, "Mobile terminal antenna performance with the user's hand: Effect of antenna dimensioning and location," *Antennas and Wireless Propagation Letters, IEEE*, vol. 10, pp. 772–775, 2011.

[27] A. Tatomirescu, M. Pelosi, O. Franek, and G. Pedersen, "The user's body effects on decoupling networks for compact mimo handsets," in *Antennas and Propagation (EUCAP), 2012 6th European Conference on*, 2012, pp. 1102–1104.

[28] M. Pelosi, O. Franek, M. Knudsen, and G. Pedersen, "Hand phantoms for browsing stance in mobile phones," in *Antennas and Propagation Society International Symposium, 2009. APSURSI '09. IEEE*, 2009, pp. 1–4.

[29] M. Pelosi, O. Franek, G. Pedersen, and M. Knudsen, "User's impact on pifa antennas in mobile phones," in *Vehicular Technology Conference, 2009. VTC Spring 2009. IEEE 69th*, 2009, pp. 1–5.

[30] C.-H. Li, E. Ofli, N. Chavannes, and N. Kuster, "Effects of hand phantom on mobile phone antenna performance," *Antennas and Propagation, IEEE Transactions on*, vol. 57, no. 9, pp. 2763–2770, 2009.

[31] S. Del Barrio, M. Pelosi, O. Franek, and G. Pedersen, "The effect of the user's body on high-q and low-q planar inverted f antennas for lte frequencies," in *Vehicular Technology Conference (VTC Spring), 2012 IEEE 75th*, 2012, pp. 1–4.

[32] M. Pelosi, O. Franek, M. Knudsen, M. Christensen, and G. Pedersen, "A grip study for talk and data modes in mobile phones," *Antennas and Propagation, IEEE Transactions on*, vol. 57, no. 4, pp. 856–865, 2009.

[33] M. Pelosi, O. Franek, M. Knudsen, and G. Pedersen, "User's proximity effects in mobile phones," in *Antennas and Propagation, 2009. EuCAP 2009. 3rd European Conference on*, 2009, pp. 1022–1024.

[34] IndexSar, "CTIA Phantom Hand Family," 2010. [Online]. Available: http://www.indexsar.com/ctia-phantomhands.html

[35] Speag, "SHO Hand Phantoms." [Online]. Available: http://www.speag.com/products/em-phantom/hand/

[36] G. Pedersen and J. Andersen, "Integrated antennas for hand-held telephones with low absorption," in *Vehicular Technology Conference, 1994 IEEE 44th*, 1994, pp. 1537–1541 vol.3.

[37] P. Eratuuli, P. Haapala, P. Aikio, and P. Vainikainen, "Measurements of internal handset antennas and diversity configurations with a phantom head," in *Antennas and Propagation Society International Symposium, 1998. IEEE*, vol. 1, 1998, pp. 126–129 vol.1.

[38] R. Vaughan and N. Scott, "Evaluation of antenna configurations for reduced power absorption in the head," *Vehicular Technology, IEEE Transactions on*, vol. 48, no. 5, pp. 1371–1380, 1999.

[39] P. Vainikainen, J. Ollikainen, O. Kivekäs, and I. Kelander, "Resonator-Based Analysis of the Combination of Mobile Handset Antenna and Chassis," *IEEE Transactions on Antennas and Propagation*, vol. 50, no. 10, pp. 1433–1444, 2002.

[40] Y.-x. Guo, M. Y. W. Chia, and Z. N. Chen, "Miniature Built-In Quad-Band Antennas for Mobile Handsets," *IEEE Antennas and Wireless Propagation Letters*, vol. 2, no. 10, pp. 30–32, 2003.

[41] P. Ciais, R. Staraj, G. Kossiavas, and C. Luxey, "Compact internal multiband antenna for mobile phone and WLAN standards," *Electronics Letters*, vol. 40, no. 15, pp. 3–4, 2004.

[42] F. N. Calvo, Z. Ying, and A. K. Skrivervik, "Design and optimization of a penta-band terminal antenna," in *Applied Electromagnetics and Communications, 2005. ICECom 2005. 18th International Conference on*, 2005, pp. 1–4.

[43] K. R. Boyle and P. J. Massey, "Nine-band Antenna System for Mobile Phones," *Electronics Letters*, vol. 42, no. 5, pp. 5–6, 2006.

[44] H. Rhyu, J. Byun, F. Harackiewicz, M.-J. Park, K. Jung, D. Kim, N. Kim, T. Kim, and B. Lee, "Multi-band hybrid antenna for ultra-thin mobile phone applications," *Electronics Letters*, vol. 45, no. 15, p. 773, 2009.

[45] J. Villanen, J. Ollikainen, and P. Vainikainen, "Coupling Element Based Mobile Terminal Antenna Structures," *IEEE Transactions on Antennas and Propagation*, vol. 54, no. 7, pp. 2142–2153, 2006.

[46] J. Holopainen, R. Valkonen, O. Kivekäs, J. Ilvonen, and P. Vainikainen, "Broadband Equivalent Circuit Model for Capacitive Coupling Element – Based Mobile Terminal Antenna," *IEEE Antennas and Wireless Propagation Letters*, vol. 9, pp. 716–719, 2010.

[47] A. Andújar, S. Member, J. Anguera, S. Member, and C. Puente, "Ground Plane Boosters as a Compact Antenna Technology for Wireless Handheld Devices," *Antennas and Propagation, IEEE Transactions on*, vol. 59, no. 5, pp. 1668–1677, 2011.

[48] I. Strip, S.-b. Wwan, Y.-l. Ban, C.-l. Liu, J. L.-w. Li, and R. Li, "Small-Size Wideband Monopole With Distributed Mobile Phone," *IEEE Antennas and Wireless Propagation Letters*, vol. 12, pp. 7–10, 2013.

[49] D. Manteuffel and M. Arnold, "Considerations for Reconfigurable Multi-Standard Antennas for Mobile Terminals total efficiency :," in *Antenna Technology: Small Antennas and Novel Metamaterials, 2008. iWAT 2008. International Workshop on*, 2008, pp. 231–234.

[50] A. Cihangir, F. Sonnerat, F. Ferrero, R. Pilard, F. Gianesello, D. Gloria, P. Brachat, G. Jacquemod, and C. Luxey, "Neutralisation technique applied to two coupling element antennas to cover low LTE and GSM communication standards," *Electronics Letters*, vol. 49, no. 13, pp. 5–6, 2013.

[51] J. Ilvonen, P. Vainikainen, R. Valkonen, and C. Icheln, "Inherently non-resonant multiband mobile terminal antenna," *Electronics Letters*, vol. 49, no. 1, pp. 11–13, Jan. 2013.

[52] A. A. H. Azremi, J. Toivanen, T. Laitinen, P. Vainikainen, X. Chen, N. Jamaly, P. O. Box, and F. Aalto, "On Diversity Performance of Two-Element Coupling Element Based Antenna Structure for Mobile Terminal," in *Antennas and Propagation (EuCAP), 2010 Proceedings of the Fourth European Conference on*, 2010.

[53] R. J. Garbacz and R. H. Turpin, "A Generalized Expansion for Radiated and Scattered Fields," *IEEE Transactions on Antennas and Propagation*, vol. 19, no. 3, pp. 348–358, 1971.

[54] R. F. Harrington and R. Mautz, Joseph, "Theory of Characteristic Modes for Conducting Bodies," *IEEE Transactions on Antennas and Propagation*, vol. 19, no. 5, pp. 622–628, 1971.

[55] M. Cabedo-fabres, E. Antonino-daviu, A. Valero-nogueira, M. F. Bataller, U. P. D. Valencia, and D. D. Comunicaciones, "The Theory of Characteristic Modes Revisited : A Contribution to the Design of Antennas for Modern Applications," *Antennas and Propagation Magazine, IEEE*, vol. 49, no. 5, pp. 52–68, 2007.

[56] R. Martens, E. Safin, and D. Manteuffel, "On the Relation between the Element Correlation of Antennas on Small Terminals and the Characteristic Modes of the Chassis," in *Antennas and Propagation Conference (LAPC), 2010 Loughborough*, no. November, 2010, pp. 457–460.

[57] W. L. Schroeder, C. T. Famdie, and K. Solbach, "Utilisation and Tuning of the Chassis Modes of a Handheld Terminal for the Design of Multiband Radiation Characteristics," in *Wideband and Multi-band Antennas and Arrays*, no. 5, 2005, pp. 117–121.

[58] R. Martens, E. Safin, and D. Manteuffel, "Selective Excitation of Characteristic Modes on Small Terminals," in *European Conference on Antennas and Propagation (EuCAP)*, 2011, pp. 2492–2496.

[59] M. Sonkki, "Wideband and Multi-element Antennas for Mobile Applications," Ph.D. dissertation, Universitatis Ouluensis, 2013.

[60] D. H. Schaubert, F. G. Farrar, S. T. Hayes, and A. R. Sindoris, "Frequency-agile, polarization diverse microstrip antennas and frequency scanned arrays," pp. US Patent H01Q001/38, 4 367 474, 1983.

[61] J. T. Bernhard, *Reconfigurable Antennas*. Morgan & Claypool, Jan. 2007, vol. 2, no. 1.

[62] O. Kivekäs, J. Ollikainen, and P. Vainikainen, "Frequency-tunable Internal Antenna for Mobile Phones," in *12th International Symposium on Antennas (JINA)*, vol. 2, no. November, 2002, pp. 53–56.

[63] R. Valkonen, J. Holopainen, C. Icheln, and P. Vainikainen, "Broadband tuning of mobile terminal antennas," in *IET Seminar Digests*. Iet, 2007, pp. 182–182.

[64] D. Peroulis, K. Sarabandi, and L. Katehi, "Design of reconfigurable slot antennas," *IEEE Transactions on Antennas and Propagation*, vol. 53, no. 2, pp. 645–654, Feb. 2005.

[65] N. Behdad and K. Sarabandi, "A Varactor-Tuned Dual-Band Slot Antenna," *IEEE Transactions on Antennas and Propagation*, vol. 54, no. 2, pp. 401–408, 2006.

[66] V.-a. Nguyen, R.-a. Bhatti, and S.-o. Park, "A Simple PIFA-Based Tunable Internal Antenna for Personal Communication Handsets," *IEEE Antennas and Wireless Propagation Letters*, vol. 7, pp. 130–133, 2008.

[67] H. Li, J. Xiong, Y. Yu, and S. He, "A Simple Compact Reconfigurable Slot Antenna With a Very Wide Tuning Range," *IEEE Transactions on Antennas and Propagation*, vol. 58, no. 11, pp. 3725–3728, 2010.

[68] S.-k. Oh, H.-s. Yoon, and S.-o. Park, "A PIFA-Type Varactor-Tunable Slim Antenna With a PIL Patch Feed for Multiband Applications," *Antennas and Wireless Propagation Letters*, vol. 6, no. 11, pp. 103–105, 2007.

[69] S.-h. Oh, H. Song, J. T. Aberle, B. Bakkaloglu, and C. Chakrabarti, "Automatic Antenna-tuning Unit for Software-defined and Cognitive Radio," *Wireless Communications and Mobile computing*, 2007.

[70] R. N. Simons, D. Chun, and L. P. B. Katehi, "Microelectromechanical Systems (MEMS) Actuators for Antenna Reconfigurability," in *Microwave Symposium Digest, 2001 IEEE MTT-S International*, 2001, pp. 215–218.

[71] E. Erdil, K. Topalli, M. Unlu, O. A. Civi, and T. Akin, "Frequency Tunable Microstrip Patch Antenna Using RF MEMS Technology," *IEEE Transactions on Antennas and Propagation*, vol. 55, no. 4, pp. 1193–1196, 2007.

[72] K. R. Boyle and P. G. Steeneken, "A Five-Band Reconfigurable PIFA for Mobile Phones," *IEEE Transactions on Antennas and Propagation*, vol. 55, no. 11, pp. 3300–3309, Nov. 2007.

[73] Q. Gu and J. R. D. Luis, "RF MEMS Tunable Capacitor Applications in Mobile Phones," in *Solid-State and Integrated Circuit Technology (ICSICT), 2010 10th IEEE International Conference on*, 2010, pp. 1–4.

[74] J. R. De Luis, A. Morris, Q. Gu, and F. de Flaviis, "Tunable Duplexing Antenna System for Wireless Transceivers," *IEEE Transactions on Antennas and Propagation*, vol. 60, no. 11, pp. 5484–5487, Nov. 2012.

[75] A. Suyama and H. Arai, "Meander Line Antenna Built in Folder-Type Mobile," in *International Symposium on Antennas and Propagation (ISAP)*, 2007, pp. 294–297.

[76] L. Huang and P. Russer, "Electrically Tunable Antenna Design Procedure for Mobile Applications," *IEEE Transactions on Microwave Theory and Techniques*, vol. 56, no. 12, pp. 2789–2797, Dec. 2008.

[77] Y. Tsutsumi, M. Nishio, S. Obayashi, H. Shoki, T. Ikehashi, H. Yamazaki, E. Ogawa, T. Saito, T. Ohguro, and T. Morooka, "Low Profile Double Resonance Frequency Tunable Antenna Using RF MEMS Variable Capacitor for Digital Terrestrial Broadcasting Reception," in *IEEE Asian Solid-State Circuits Conference*, 2009, pp. 125–128.

[78] M. Nishigaki, T. Nagano, T. Miyazaki, T. Kawakubo, K. Itaya, M. Nishio, and S. Sekine, "Piezoelectric MEMS Variable Capacitor for a UHF Band Tunable Built- in Antenna," in *Microwave Symposium IEEE/MTT-S International*, 2007, pp. 2079–2082.

[79] B. D. Pilgrim, "White paper: Simplifying RF front-end design in multiband handsets," pp. 30–33, 2008.

[80] S. K. Das, *Mobile Handset Design*. John Wiley & Sons, Ltd, 2010.

[81] D. Vye, "The Economics of Handset RF Front-end Integration," pp. 1–13, 2010. [Online]. Available: www.microwavejournal.com/articles/print/9983-the-economics-of-handset-rf-front-end-integration

[82] M. B. Knudsen, P. Bundgaard, J.-E. Mueller, G. F. Pedersen, and M. Pelosi, "Impedance Tuning of Transmitting and Receiving Antennas," 2012.

[83] M. B. Knudsen, B. Adler, P. Bundgaard, J.-E. Mueller, G. F. Pedersen, and M. Pelosi, "Wireless Communication Device Antenna with Tuning Elements," 2013.

[84] M. Pelosi, M. B. Knudsen, and G. F. l. Pedersen, "Decoupled Radiators," *IEEE Transactions on Antennas and Propagation*, vol. 60, no. 2, pp. 503–515, 2012.

[85] H. Darabi, A. Mirzaei, and M. Mikhemar, "Highly Integrated and Tunable RF Front Ends for Reconfigurable Multiband Transceivers: A Tutorial," *IEEE Transactions on Circuits and Systems*, vol. 58, no. 9, pp. 2038–2050, Sep. 2011. [Online]. Available: http://ieeexplore.ieee.org/lpdocs/epic03/wrapper.htm?arnumber=6003801

[86] M. Pelosi, O. Franek, M. B. Knudsen, M. Christensen, and G. F. l. Pedersen, "A Grip Study for Talk and Data Modes in Mobile Phones," *IEEE Transactions on Antennas and Propagation*, vol. 57, no. 4, pp. 856–865, 2009.

Part II

Papers

Paper A

Challenges for Frequency-Reconfigurable Antennas in Small Terminals

Caporal Del Barrio, S.[1] ; Pelosi, M.[1] ; Pedersen, G.F.[1] and Morris, A.[2]
[1]Section of Antennas, Propagation and Radio Networking (APNet), Department of Electronic Systems, Faculty of Engineering and Science, Aalborg University, DK-9220, Aalborg, Denmark, {scdb, mp, gfp}@es.aau.dk
[2]Wispry Inc, Irvine, USA art.morris@wispry.com

The paper has been published in the
76th Vehicular Technology Conference (VTC Fall) 3-6 Sept., 2012,
Quebec City, QC, pp. 1–5.

The layout has been revised.

Abstract

This paper gives an overview of the techniques published over the past years to address continuous frequency tuning. It presents the challenges that have been encountered and relates to each other the parameters that influence the losses of the resulting antenna structure. A mock-up is made with a PIFA and a packaged RF-MEMS tunable capacitor to measure its efficiency as the resonance is tuned towards the LTE-700 band.

1 Introduction

For the 4^{th} Generation (4G) of mobile communications the Long Term Evolution (LTE) standard requires the mobile terminals to operate in a significant amount of bands and a very wide range of frequencies. This is to say the handsets should be able to cover 24 different bands and all the frequencies from 700 MHz up to 2.7 GHz, which corresponds to the bands 12 and 7 [1]. Multi-band antennas have been largely used in the mobile phone industry in order to cover more than one band simultaneously. Their relatively easy-to-integrate structure and their low cost made them very attractive for antenna engineers. Nevertheless the ever increasing number of bands to cover, lower frequencies being part of the spectrum and the trend for smaller platforms reaches the limits of multi-band antennas integration. Additionally the implementation of Multiple-Input Multiple-Output (MIMO) systems will increase the number of antennas required on the platform. For the small handsets the main constraint is the space available.
As an alternative to multi-band antennas Frequency-Reconfigurable Antennas (FRA) - also called tunable antennas - have been investigated in order to provide maximum connectivity. FRA offer the possibility to dynamically change the resonance frequency of the antenna through electrical means. The space consumption is greatly reduced for FRA as one single resonant element can be used to cover all the bands. Furthermore this element is designed for its highest targeted band of operation which results in small size elements [2]. In addition to smaller elements, size reduction in the RF chain can be achieved by passing some of the filter requirements on a narrow-band antenna design.
This paper, besides giving an overview of the tuning methods published in the recent years, presents the challenges that can be met during design and fabrication processes of an FRA, from an efficiency point of view. This paper is structured in six sections. The common techniques for antenna tuning are introduced in Section II. Successively Section III describes the trade-offs to consider at a design stage of an FRA. This is followed in Section IV by challenges of the integration of the tuner within the FRA structure. A prototype antenna is built and measured with packaged MEMS capacitors in Section V. Conclusions end the paper in Section VI.

2 Tuning Techniques for Antennas in Small Terminals

Typical applications of FRA can be divided into two categories, the antennas that aim at switching between distinct frequency bands, or the antennas that aim at providing continuous tuning within - or between - operating bands and standards. The latter ones are of most interest as they will provide the maximum connectivity required for 4G. Additionally, their coverage requirement can be reduced to the bandwidth of a channel, as opposed to a full band. And the system design will benefit from a narrow-band antenna design, as it can have a filtering function which will relax the requirements on the filters themselves and provide a great size and cost reduction in the RF chain.
Continuous tuning - also called fine-tuning - is commonly achieved using tunable substrates or tunable components. On the one hand, the tunable substrates have the ability to vary their relative permittivity or permeability, which modifies the effective electrical length of the antenna, hence its operating frequency. Some examples are given in [3]- [4]. The main drawbacks of this technique are the fairly high electrical conductivity created - as high loss tangent of the substrate can severely degrade the efficiency of the antenna - and the limitations in achieving uniform films for planar structures. On the other hand, the tunable components are easier to physically integrate in the small antennas structure and are the focus of this paper. They are built based on electrically controlled reactances (usually capacitances) that can take a linear range of values in order to achieve smooth variations in the overall reactance of the antenna, and the resonance frequency.
Different techniques for continuous tuning using tunable components found in the literature will be summarized and compared in the following section. One of them will be chosen for the FRA presented in this paper.

2.1 Literature Examples

The components used for continuous tuning can be divided into three groups: the varactors, the PIN diodes or Field Effect Transistor (FET) and the RF Micro-Electro-Mechanical (MEMS). Examples of the integration of such components in Electrically Small Antennas (ESA) are presented.

Varactors

Varactors - also known as variable capacitor diodes or varicaps - can vary the resonance frequency of an antenna by providing different capacitance values in function of the bias applied across the diode. For instance, in [5] a variable capacitor is placed between a Planar Inverted-F Antenna (PIFA) and its Ground Plane (GP) at a fixed distance from the feed. With a range of capacitances between 3 and 20 pF, the inherently narrow-band

radiator can reach an effective bandwidth of 10 % around 900 MHz. A similar example on a patch antenna is shown in [6] with a tuning range up to 15% around 2.2 GHz, or on a dual-band slot antenna in [7] and [8] where the tuning range is above 1.2 GHz and efficiencies vary from 92% to 58 %.

PIN diodes and FET

Tuning components based on semiconductor switches are mainly PIN diodes and reactive FET. The main use of PIN diodes is switching between bands though, and fine-tuning within the band is further achieved with a varactor, as in [9] for frequencies between 2 and 5 GHz. Continuous tuning with only PIN diodes requires many of them for widely FRA, leading to an increased complexity of the structure and low switching efficiency. The use of FET in [10] provides a 10% tuning range around 10GHz. In [11] tuning over the GSM-900 band is shown, at the expense of 24% reduction in the efficiency. Indeed the high insertion loss [12] is the main drawback of this method.

RF-MEMS

More recent tuning techniques include RF-MEMS capacitors on patch antennas, as in [13] that shows tuning between 15 GHz and 16 GHz and in [14] that shows the integration of the RF-MEMS in a slot within the patch structure and tuning in the 1.5 GHz band. The main advantage of MEMS switches over semiconductor switches is their higher efficiency, which can be a result of galvanic contact in the on-sate for some components, or a result of a constant equivalent resistance in purely capacitive MEMS - as the one chosen for the prototype presented in the following sections.

2.2 Proposed Design

The selected tuning technique for the proposed design is RF-MEMS capacitors. The frequencies of interest will be below 1GHz as they are the most challenging for small platforms, as a result of resonance frequencies below the GP resonance. A dual-band low-profile patch antenna will be prototyped and an RF-MEMS tunable capacitor will be integrated in its structure in order to tune its low band from GSM-900 to LTE-700.

3 Design Trade-offs

Investigation of the tuning range, tuning resolution and the consequences on the bandwidth (BW), Quality factor (Q) and efficiency will be shown in this section.

3.1 Too High Quality factor (Q)

It is well know that the GP has a major function in the radiation mechanism of ESA. For typical mobile phone form factors, the resonance frequency of the GP is about 1 GHz. The Q of the radiating structure is the lowest when the antenna is designed to have the same resonance frequency as the GP [15]. As the resonance frequency of the antenna element is tuned further away from the GP resonance, the Q of the structure increases dramatically. This phenomenon leads to an inversely proportional reduction of the bandwidth [16], [17]. The main issues arising with a very high Q are:
- the bandwidth may be too narrow to cover one channel,
- tuning becomes coarser,
- the radiation efficiency may be below the acceptable threshold.
Consequently covering the low frequencies extending the tuning range is a major challenge.

3.2 Narrow Bandwidths

Depending on the Q of the original antenna design - without the tuner - and on the tuning range, the Q of the FRA at its lowest frequency will be very high. This phenomenon results in narrow bandwidths for frequencies as low as 700 MHz (band 12 of LTE standard). FRA only need to cover one channel, which varies in LTE from 1.4 MHz to 20 MHz [1].

3.3 Fine-tuning

To comply with the 4G standards using FRA antennas, not only the tuning range must be very wide but also every single band and channel between 700 MHz and 2.7 GHz must be covered with an acceptable level. Using varicaps for instance, the tuning step that can be reached with one capacitance stage is dependent on the amount of current that goes through the varicap. There is a first trade-off between the position of the varicap and the tuning step [18]. When the location of the tuning component is fixed, a step in increasing its reactance means a shift in frequency. This shift is constant over the tuning range but the bandwidth is not since the antenna Q increases. Fine-tuning is not possible anymore when the bandwidth gets too narrow to cover the immediate next channel. There is a second trade-off between the position of the varicap and the feasability of the design as currents and voltages at a given position can be very high and need to be handled by the varicap [19], losses should also be minimized.

3.4 Poor Matching

The antenna designers must aim for a structure covering every single frequency of the 4G radio spectrum with a Voltage Standing Wave Ratio (VSWR) at least equal to 3.

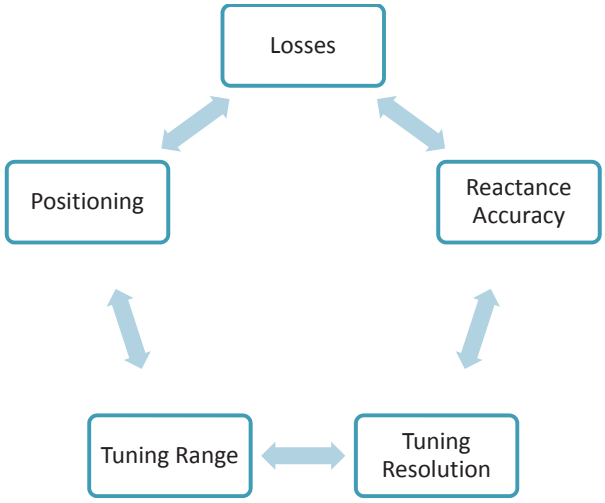

Fig. A.1: Design trade-offs.

However the antenna impedance is not constant throughout the tuning stages. A lossless simulation of an FRA will show a degrading matching as the operationg frequency it tuned far away from the original resonance frequency. This phenomenon can be observed in the Section 5. The mismatch efficiency being a part of the total efficiency of the antenna system, it is partly responsible of the performance deterioration of FRA. This parameter is an additional constraint to reaching a wide tuning range. Tuning matching networks can be added, at the expense of losses in the total efficiency.
The challenges that need to be dealt with while tuning towards LTE-700 frequencies are the Q increase, the BW degradation, the coarser tuning resolution and the matching to the 50 Ω feed line degradation. Optimization with the tuning component location and the antenna geometry can lead to a successful design.

4 Integration of the tuner

Implementations of packaged MEMS switches in FRA antennas are carried out in [20] and [21] where practical aspects involved are explained. Assembling the FRA showed that additional modifications needed to be done to the packaged components in order to reduce a severe impedance mismatch. Further adjustments had to be done to the antenna in order to include bias networks and utilize the RF ground plane as a shared DC power plane. The necessary post-design-modifications of both elements suggest that the MEMS and the antennas should be conceived throughout a joint fabrication process.

Tuning components are commonly placed between the radiating element and the ground plane, or within the radiating element itself. These locations usually result in significant losses since they are at high RF voltages and currents locations [22]. When selecting a tuning component to modify the resonance frequency of an antenna, particular attention should be paid to the additional losses it introduces, as it will degrade the total efficiency. Therefore the selection of the component should be done based on its Q value, which is function of its Equivalent Series Resistance (ESR). The insertion loss is used to rank the components. However it is given by the manufacturers in a 50 Ω environment, which is not the case when they are placed in the antenna structure. In [12] the insertion loss of a switch was measured 4 times higher than the one given by the manufacturers at the same frequency. This significant difference was due to the 10 Ω environment in which the switch was placed, close to the antenna feed point. In fact the power loss of the switch increases as the load resistance diverges from 50 Ω. In [23] the location of the integrated MEMS component lead to losses of 13 dB, even at high frequencies: 2 GHz. In an other example [24], the total efficiency of the MEMS reconfigurable antenna is below 50 % in the GSM-900 band and in the GSM-1800 band. Ways to artificially create an environment as close as possible to 50 Ω, in order to reduce the losses of the tuning component are presented in [12]. Shunt reactances between the antenna element and the tuner can be inserted without large additional losses, in order to modify the load resistance. MEMS are expected to meet the requirements on the component performances.

5 A prototype antenna

5.1 Antenna Design

The proposed antenna is a dual-band PIFA operating at the GSM bands. The prototype aims at fine-tuning the low-band resonance from the GSM-900 band to the band 14 of the LTE frequency spectrum with an RF-MEMS variable capacitor. These bands have been chosen because the low frequencies in small terminals are the most challenging. This is mainly for the required size at resonance compared to the available space, and because of a resonance significantly below the GP resonance. In the tuner [25] a range of capacitances varying between 0.125 pF (C1) and 1.875 pF (C2) - with 0.125 pF steps - is used. The location of the tuner on the antenna is chosen in order to optimize the tuning resolution with the capacitance steps. The tuner provides high performance and is implemented in contemporary phones, as Samsung Omnia [26]. It has a Q of 200 at 1 GHZ, a maximum signal voltage of 35 Volts and a self-resonance frequency at 5 GHz. The mocked-up antenna can be seen in Fig. A.2 and is detailed in [18]. The tuner and the antenna share a common GP.

The antenna was first simulated in a Finite-Difference Time-Domain (FDTD) software. The initial resonance frequency of the antenna is 960 MHz and its simulated Q is

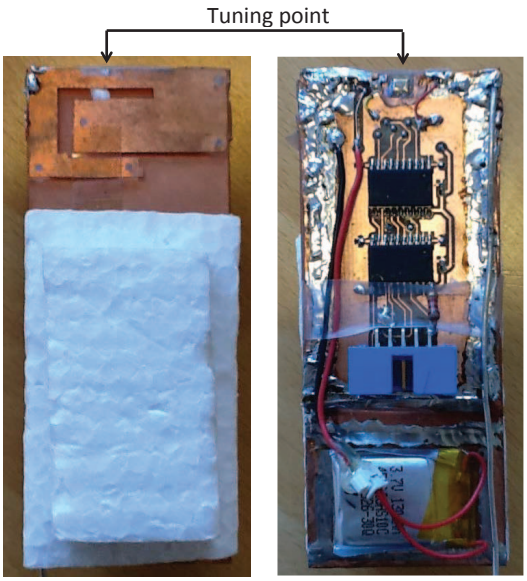

Fig. A.2: Prototyped antenna.

56 with a BW of 20 MHz. Adding the tuner to the mock-up, it was observed that the connection to the tuner - in its off-stage - shifts the resonance frequency to 890 MHz. Then, increasing the capacitance value of the tuner decreases the resonance frequency of the overall system. The system can be tuned until 790 MHz, where the simulated Q is 198 and its associated BW is 4 MHz. The magnitude of the reflection coefficient for the maximum and the minimum operating frequencies of the tuning range are plotted in Fig. A.3. The continuous tuning achieved by the prototyped antenna is shown in Fig. A.4. Good matching is shown in the measurements throughout the whole tuning range. Unlike the loss-less FDTD simulation, the measured antenna self-matches itself at the resonant frequency. This phenomenon is certainly due to the losses in the mock-up, which can also be seen in the very low reflection threshold (below -5 dB).

The Table A.1 summarizes the evolution of the Q and the BW throughout the tuning range. These values are compared to the simulated values and depicted in Fig. A.5. The measured resonance frequencies match with the values from the simulation tool. It can be observed that the measured Q is lower than the simulated Q, and correspondingly the measured BW is larger than the simulated one. The difference in Q and BW are explained by the losses of the real mock-up. Indeed the FDTD simulation is done with Perfect Electric Conductor (PEC) elements for the antenna and the GP, and ideal capacitors for the tuner. In both simulation and measurements, the Q is dramatically increased - up to 141 in the measurements and the BW is decreased to 4 MHz. It can

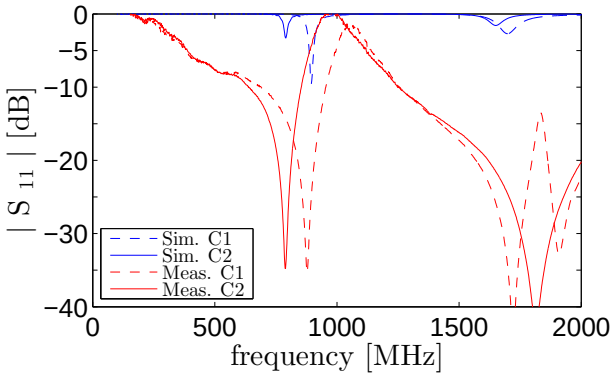

Fig. A.3: Simulated (Sim.) and Measured (Meas.) $|S_{11}|$ parameter for the lowest and highest tuning stages, where C1=0.125 pF and C2=1.875 pF.

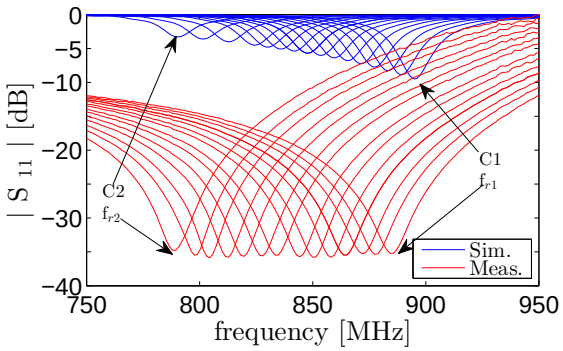

Fig. A.4: Simulated (Sim.) and Measured (Meas.) $|S_{11}|$ parameter throughout its tuning range, between C1=0.125 pF and C2=1.875 pF.

Table A.1: Q and BW of the mock-up in simulations and measurements

f_r [MHz]		Q		BW [MHz]	
sim.	**meas.**	**sim.**	**meas.**	**sim.**	**meas.**
890	891	89	79	10	11
884	883	88	94	10	9
878	878	110	94	8	9
866	870	108	93	8	9
861	863	108	115	8	7
855	855	143	114	6	7
849	846	142	113	6	7
843	840	141	112	6	7
831	831	139	111	6	7
825	823	206	110	4	7
814	816	204	109	4	7
802	801	201	107	4	7
791	793	198	141	4	6

be seen in Fig. A.5 that the Q of the system suffers dramatic discontinuities at three particular frequencies throughout the tuning range. This phenomenon is intrinsic to the Q calculation of narrow-band antennas as showed in [27] and comes from the circuitry chosen at the perfect matching step of the algorithm.

For the highest and the lowest bounds of the tuning range, the total efficiency (e_T) of the mock-up is measured in an anechoic chamber and calculated with 3-D integration technique. At 890 MHz e_T is -1.9 dB, whereas at 790 MHz e_T is -4.8 dB. Mismatch efficiency is negligible as the antenna self-matches itself. A degradation of 3 dB is explained by the increase in conductive losses at low frequencies. Further investigation is needed to identify precisely the cause of loss for the low LTE-700 band.

6 Conclusion

This paper has presented the challenges that can be met while manufacturing a FRA for 4G use. Having a wide and fine tuning range is a trade-off between the accuracy of the tuning component and its location. The dependency between the essential parameters of the FRA design are presented in order to understand the necessary trade-offs before

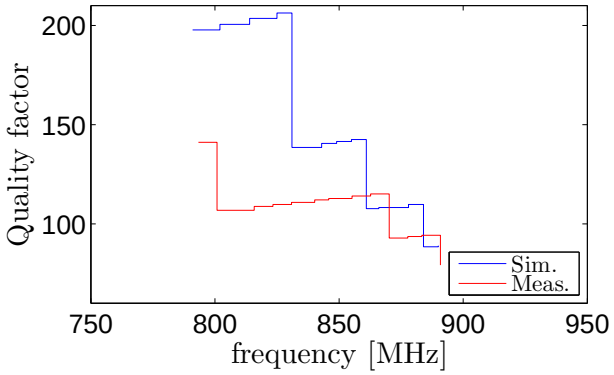

Fig. A.5: Simulated (Sim.) and Measured (Meas.) Q of the prototyped antenna.

manufacturing processes. Continuous tuning could be reached with an RF-MEMS variable capacitor (0.125 pF to 1.875 pF in 14 steps) between 890 MHz and 790 MHz. A frequency ratio f_R of 1.13 was achieved corresponding to a tuning range of 11 %. With higher values of the MEMS capacitor the tuning range can be increased to reach the band 12 of the LTE standard as the mock-up self-matches itself at resonance. However the Q of the antenna dramatically increases when the antenna is tuned towards lower frequencies, which results in narrower bandwidths, coarser tuning range, and poorer efficiency. The measured total efficiency dropped from -2 dB at 890 MHz to -5 dB at 790 MHz. The source of the losses must be further investigated, as it might come from multiple reasons: ESR, soldering tin or copper conductivity for example.

References

[1] 3GPP Technical Report, "Feasibility study for Further Advancements for E-UTRA (LTE-Advanced) - Specification 36.912 - Release 11," 2012. [Online]. Available: http://www.3gpp.org/ftp/Specs/html-info/36912.htm

[2] R. F. Harrington, "Effect of Antenna Size on Gain, Bandwidth, and Efficiency," *Journal of Research of the National Bureau of Standards- D. Radio Propagation*, vol. 64D, no. 1, pp. 1–12, 1960. [Online]. Available: http://archive.org/details/jresv64Dn1p1

[3] K. A. Jose, V. K. Varadan, and V. V. Varadan, "Experimental investigations on electronically tunable microstrip antennas," *Microw. Opt.Technol. Lett.*, vol. 20, no. 3, pp. 166 – 169, 1999.

[4] R. K. Mishra, S. S. Pattnaik, and N. Das, "Tuning of microstrip antenna on ferrite substrate," *IEEE Transactions on Antennas and Propagation*, vol. 41, pp. 230–233, 1993.

[5] P. Panayi, M. Al-Nuaimi, and I. Ivrissimtzis, "Tuning techniques for planar inverted-F antenna," *Electronics Letters*, vol. 37, no. 16, pp. 1003 – 1004, 2001.

[6] P. Bhartia and I. Bahl, "Frequency agile microstrip antennas," *Microwave Journal*, vol. 25, pp. 67 – 70, 1982.

[7] N. Behdad and K. Sarabandi, "A varactor-tuned dual-band slot antenna," *IEEE Transactions on Antennas and Propagation*, vol. 54, pp. 401–408, 2006.

[8] N. Behdad and K. Sarabandi, "Dual-band reconfigurable antenna with a very wide tunability range," *Antennas and Propagation, IEEE Transactions on*, vol. 54, no. 2, pp. 409–416, 2006.

[9] C. Jung, Y. Kim, Y. Kim, and F. De Flaviis, "Macro-micro frequency tuning antenna for reconfigurable wireless communication systems," *Electronics Letters*, vol. 43, pp. 201 – 202, 2007.

[10] S. Kawasaki and T. Itoh, "A slot antenna with electronically tunable length," in *Antennas and Propagation Society International Symposium*, 1991, pp. 130 – 133.

[11] J. Ollikainen, O. Kivekas, and P. Vainikainen, "Low-loss tuning circuits for frequency-tunable small resonant antennas," in *Personal, Indoor and Mobile Radio Communications, Symposium on*, 2002, pp. 1882 – 1887.

[12] R. Valkonen, J. Holopainen, C. Icheln, and P. Vainikainen, "Broadband tuning of mobile terminal antennas," in *IET Seminar Digests*, 2007, pp. 182–182.

[13] E. Erdil, K. Topalli, M. Unlu, O. Civi, and T. Akin, "Frequency tunable microstrip patch antenna using RF MEMS technology," *IEEE Transactions on Antennas and Propagation*, vol. 54, pp. 1193–1196, 2007.

[14] S. Shynu, G. Augustin, C. Aanandan, P. Mohanan, and K. Vasudevan, "C-shaped slot loaded reconfigurable microstrip antenna," *Electronics Letters*, vol. 42, pp. 316 – 318, 2006.

[15] J. Villanen, J. Ollikainen, and P. Vainikainen, "Coupling Element Based Mobile Terminal Antenna Structures," *IEEE Transactions on Antennas and Propagation*, vol. 54, no. 7, pp. 2142–2153, 2006.

[16] J. S. McLean, "A re-examination of the fundamental limits on the radiation Q of electrically small antennas," *IEEE Transactions on Antennas and Propagation*, vol. 44, no. 5, p. 672, May 1996.

[17] A. D. Yaghjian, S. R. Best, and S. Member, "Impedance , Bandwidth , and Q of Antennas," *IEEE Transactions on Antennas and Propagation*, vol. 53, no. 4, pp. 1298–1324, 2005.

[18] S. C. Del Barrio, M. Pelosi, O. Franek, and G. F. Pedersen, "On the currents magnitude of a tunable Planar-Inverted-F Antenna for low-band frequencies," in *2012 6th European Conference on Antennas and Propagation (EUCAP)*, Mar. 2012, pp. 3173–3176.

[19] S. C. Del Barrio, M. Pelosi, O. Franek, and G. F. Pedersen, "Coupling element antenna with slot tuning for handheld devices at LTE frequencies," in *2012 6th European Conference on Antennas and Propagation (EUCAP)*. Ieee, Mar. 2012, pp. 3587–3590.

[20] D. e. a. Anagnostou, "Design, fabrication, and measurements of an RF-MEMS-based self-similar reconfigurable antenna," *IEEE Transactions on Antennas and Propagation*, vol. 54, pp. 422–432, 2006.

[21] G. Huff and J. Bernhard, "Integration of packaged RF MEMS switches with radiation pattern reconfigurable square spiral microstrip antennas," *IEEE Transactions on Antennas and Propagation*, vol. 54, pp. 464–469, 2006.

[22] R. Waterhouse and N. Shuley, "Full characterization of varactor-loaded, probe-fed, rectangular, microstrip patch antennas," *Microwaves, Antennas and Propagation, IEE Proceedings*, vol. 141, pp. 367–373, 1994.

[23] J. Quijano and G. Vecchi, "Optimization of an Innovative Type of Compact Frequency-Reconfigurable Antenna," *IEEE Transactions on Antennas and Propagation*, vol. 57, pp. 9–18, 2009.

[24] R. Valkonen, C. Luxey, J. Holopainen, C. Icheln, and P. Vainikainen, "Frequency-reconfigurable mobile terminal antenna with MEMS switches," in *Antennas and Propagation (EuCAP), 2010 Proceedings of the Fourth European Conference on*, 2010, pp. 1–5.

[25] J. De Luis, A. Morris, Q. Gu, and F. De Flaviis, "Tunable antenna systems for wireless transceivers," in *Antennas and Propagation (APSURSI), 2011 IEEE International Symposium on*, 2011, pp. 730 – 733.

[26] "Samsung Omnia W with Wispry MEMS module, Web Press Release." in *http://evertiq.com/news/21198?utm_source=feedburner&utm_medium=feed &utm_campaign=Feed%3A+EvertiqCom%2FAll+28evertiq.com+%3A%3A +Latest+news%29&utm_content=Google+Reader*

[27] J. Rahola, "Bandwidth potential and electromagnetic isolation: Tools for analysing the impedance behaviour of antenna systems," in *Antennas and Propagation, 2009. EuCAP 2009. 3rd European Conference on*, 2009, pp. 944–948.

Paper B

On the Efficiency of Frequency Reconfigurable High-Q Antennas for 4G Standards

Caporal Del Barrio, S. ; Pelosi, M. and Pedersen, G.F.
Section of Antennas, Propagation and Radio Networking (APNet), Department of Electronic Systems, Faculty of Engineering and Science, Aalborg University, DK-9220, Aalborg, Denmark, {scdb, mp, gfp}@es.aau.dk

The paper has been published in the
Electronics Letters, Vol. 48, Issue 16, pp. 982–983, Aug., 2012.

The layout has been revised.

Abstract

In the actual context of reducing the antenna size and operating in multiple bands tunable antennas are investigated. Moreover high-Q and low-Q tunable antennas are compared with respect to their efficiency. The paper addresses the loss issue that tunable high-Q antennas present. Using a variable capacitor as a tuning mechanism, simulations and measurements of a self-resonating antenna show the mismatch and the radiation efficiencies of the high-Q and the low-Q antennas. The investigated frequencies are in the low band of the 4G standard. Measurements are conducted for different tuning stages and the study shows that the high-Q design performs worse than low-Q one. A 1.4 dB degradation in total efficiency is observed for a high-Q antenna in a tunable system.

1 Introduction

Today the access to a large number of bands with a platform as small as a mobile phone is becoming a requirement for the majority of the consumers. As the fundamental antenna limits relate bandwidth, size and efficiency [1] it is a real challenge to design very compact and broad-band antennas. To overcome this constraint tunable (also named frequency reconfigurable) antennas are investigated. Tunable antennas offer the possibility to have an antenna size that is constant and a reconfigurable resonance frequency with the use of additional lumped components. Nevertheless the overall system complexity remains a challenge for the upcoming 4G-LTE standard as it requires to cover 25 bands from 700 MHz to 2.7 GHz. Unlike low-Q antennas, high-Q antennas are narrow-band. Therefore they have the potential to avoid the use of duplex filters and further to dramatically decrease the complexity of the Front-End architecture [2]. However the loss mechanism of high-Q antennas is not well understood yet. This letter will highlight the efficiency issue of a tunable self-resonating high-Q antenna by comparing it with a low-Q antenna. The investigated frequencies are in the low bands, below 1 GHz.

2 Antenna design

The self-resonating antenna is a Planar Inverted F-Antenna (PIFA) designed for 960 MHz, as it is the upper bound of the low frequencies for the 4G spectrum [3]. The PIFA has the dimensions of 55 x 10 mm^2 over a 55 x 120 mm^2 Ground Plane (GP), as shown in Fig. B.1. The source and the short pins are placed 4 mm apart from each other and the tuning point is placed 45 mm away from the source. The height (H) of the PIFA over the GP will determine its Quality factor (Q).

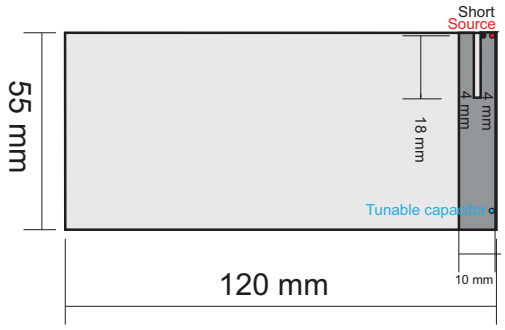

Fig. B.1: Antenna design. Low-Q antenna A1 with H=8mm, High-Q antenna A2 with H=2mm

3 Antenna Q

The Q of a single band self-resonating antenna is defined in [4] using the matched VSWR at the resonating frequency. Two cases are investigated with the above-design, on the one hand the PIFA is placed 8 mm above the GP and exhibits a Q of 6 at 960 MHz and on the other hand the PIFA is placed at 2 mm above the GP and exhibits a Q of 30 at 960 MHz. These designs will be denoted A1 and A2 respectively. In both cases when the antenna is tuned further away from the resonance frequency defined by its design, its Q is increased considerably.

4 Tuning capacitor

The tuning mechanism that is implemented is representing a variable capacitor of 1/8pF steps as it is the state of the art in Micro Electro-Mechanical Systems (MEMS) [5]. The simulation and the measurements are done with fixed capacitors placed between the PIFA and the GP, therefore they are not in a 50 Ω environment and insertion losses can arise. The resonance frequency of the overall system is fine-tuned to provide continuous coverage over different bands and channels, and comply with 4G requirements. The tuning system aims at reaching the frequency 800 MHz as it is one of the lowest LTE band to host 4G.

5 Simulation results

The simulation were realized with a Finite-Difference Time-Domain (FDTD) method. First the tunability of the high-Q and the low-Q designs is investigated and shown in Fig. B.2 and Fig. B.3. Fine-tuning is achieved for both designs showing their ability

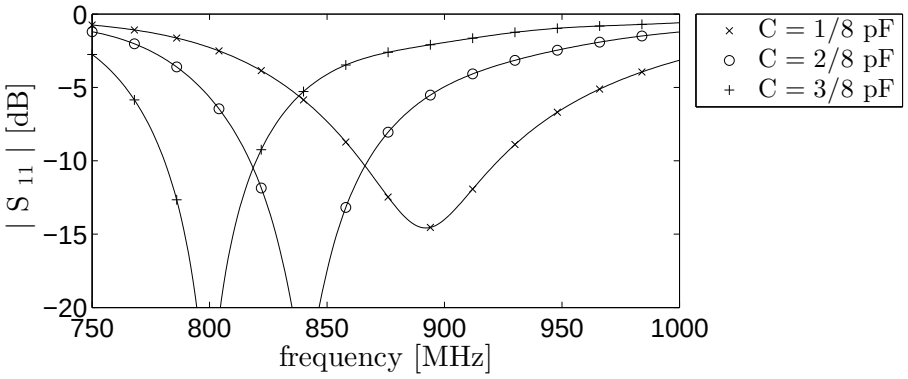

Fig. B.2: Tuning range of the low-Q antenna (A1)

to cover all frequencies in a chosen range. The increase of the Q value for both A1 and A2 is shown in Fig. B.4 with the associated bandwidths (BW) at -6 dB. A1 reaches the resonance frequency 800 MHz in three tuning steps only and its Q increases from 6 at 960 MHz to 14 at 800 MHz, accordingly its BW decreases from 125 MHz to 55 MHz. The high-Q antenna A2 can be tuned to 800 MHz with a total added capacitance of 1 pF. Moreover its Q increases from 30 at 960 MHz to 67 at 800 MHz, accordingly its bandwidth decreases from 30 MHz to 12 MHz. However the reduction of bandwidth is not a issue in tunable systems as it is only needed to cover one channel and not a full band. At 800 MHz A2 exhibits a Q close to 5 times the Q of A1.

6 Measurement results

Mock-ups of the simulated antennas are built and measured in order to calculate their efficiency and estimate its degradation with respect to the increasing Q. In the measurement fixed capacitors (C1 and C2) with low Equivalent Series Resistance (ESR) are used, their ESR is shown in Table B.1. The return loss of A1 and A2 is depicted in Fig. B.5 and the efficiencies are computed from anechoic chamber measurements with a 3D integration method. At 960 MHz A1 and A2 exhibit similar efficiencies whereas at 808 MHz A2 performs worse than A1, as shown in Table B.2.

7 Loss mechanism

At the lowest frequency reached by A1 and A2, the high-Q antenna (A2) performs 1.4 dB worse than the low-Q antenna (A1) even though A2 uses a better (lower ESR) capacitor. In order to understand the loss mechanism of the high-Q antenna a closer look into the currents delivered to the tuning capacitor is taken and the results are

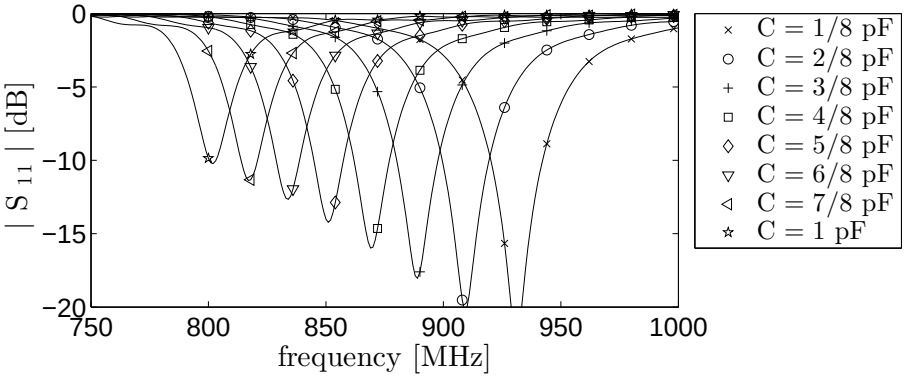

Fig. B.3: Tuning range of the high-Q antenna (A2)

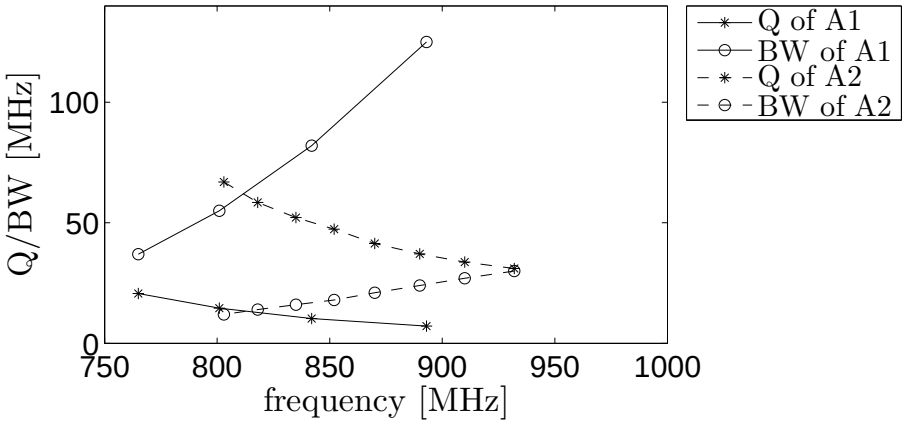

Fig. B.4: Q and BW increment over the tuning stages for A1 and A2

Table B.1: Fixed capacitors used for measurements

	C [pF]	f_r [MHz]	ESR [Ω]	Q
C1	0.3	808	0.9	685
C2	1	808	0.2	925

Table B.2: Measured efficiencies

	C [pF]	f_r[MHz]	η_r[dB]	η_m [dB]	η_T[dB]
A1	x	960	-1.6	-0.4	-2.0
A1	0.3 (C1)	808	-2.2	0.0	-2.2
A2	x	960	-2.2	0.0	-2.2
A2	1 (C2)	808	-3.2	-0.4	-3.6

shown in Table B.3. It shows that at the last tuning stage the current running through C1 (0.3 pF) for A1 is 0.13 A whereas through C2 (1 pF) for A2 it is 0.45 A, both currents are normalized to 1 W input power. As the losses due to the ESR are proportional to the square of the currents, a lower ESR does not lead to an efficiency improvement if the currents delivered to it are more than tripled, as in the presented case.

8 Conclusion

For frequency reconfigurable antenna designs high-Q antennas open the possibilities for finer tuning and higher size reduction of the antenna. However their efficiencies is still lower than low-Q antennas. Measurements showed that the high-Q antenna performs similarly to the a low-Q antenna at the designed frequency (0.2 dB difference in total efficiency) but worse when tuned 150 MHz down in frequency (1.4 dB). This is explained by the antenna Q that is considerably higher (close to quintuple) for the high-Q design and therefore the currents delivered to the capacitor are an issue.

Table B.3: Simulated currents delivered to the tunable capacitor for 1 W input power

C [pF]	1/8	2/8	3/8	4/8	5/8	6/8	7/8	1
Ic_{A1} [A]	0.04	0.08	0.13	x	x	x	x	x
Ic_{A2} [A]	0.05	0.10	0.15	0.21	0.26	0.32	0.38	0.45

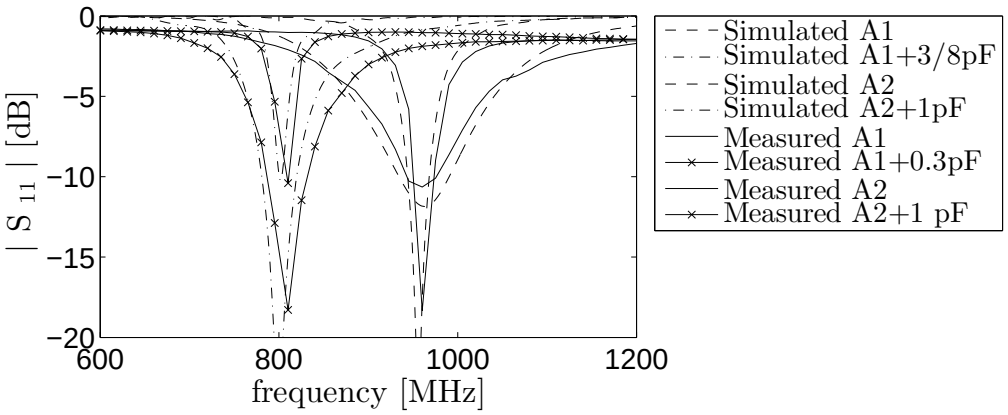

Fig. B.5: Simulated and measured reflection coefficient

References

[1] R. F. Harrington, "Effect of Antenna Size on Gain, Bandwidth, and Efficiency," *Journal of Research of the National Bureau of Standards- D. Radio Propagation*, vol. 64D, no. 1, pp. 1–12, 1960. [Online]. Available: http://archive.org/details/jresv64Dn1p1

[2] M. Pelosi, M. B. Knudsen, and G. F. l. Pedersen, "Decoupled Radiators," *IEEE Transactions on Antennas and Propagation*, vol. 60, no. 2, pp. 503–515, 2012.

[3] 3GPP TS 36.101, "LTE; Evolved Universal Terrestrial Radio Access (E-UTRA); User Equipment (UE) radio transmission and reception," p. V11.3.0 Realease 11, 2013.

[4] A. D. Yaghjian, S. R. Best, and S. Member, "Impedance , Bandwidth , and Q of Antennas," *IEEE Transactions on Antennas and Propagation*, vol. 53, no. 4, pp. 1298–1324, 2005.

[5] WiSpry Tunable Digital Capacitor Arrays (TDCA), "http://www.wispry.com/products-capacitors.php." [Online]. Available: http://www.wispry.com/products-capacitors.php

Paper C

On the Efficiency of Capacitively Loaded Frequency Reconfigurable Antennas

Caporal Del Barrio, S. ; Pedersen, G.F.
Section of Antennas, Propagation and Radio Networking (APNet), Department of Electronic Systems, Faculty of Engineering and Science, Aalborg University, DK-9220, Aalborg, Denmark, {scdb, mp, gfp}@es.aau.dk

The paper has been published in the
International Journal of Distributed Sensor Networks (IJDSN)
Special Issue on Smart and Reconfigurable Antenna Applications in Wireless Sensor Networks, Article ID 232909, June, 2013.

The layout has been revised.

Abstract

The design of a reconfigurable antenna that can be fine tuned to address future communication systems is proposed. The design consists of a capacitively loaded patch antenna for nowadays smart-phone platforms. The antenna is narrow-band and can be fine tuned over the range (700 MHz - 960 MHz). Measurements at 700 MHz with fixed capacitors raise the challenge of the component insertion loss. Distribution of the tuning capacitance is investigated and shows 1 dB improvement in the antenna radiation efficiency.

1 Introduction

The need for bandwidth has been dramatically increased with the standardization of the 4^{th} Generation (4G) of mobile communication systems. Handset devices need to cover an ever-increasing frequency spectrum. Today's specifications fill the spectrum from 700 MHz to 2.6 GHz [1]. The trend shows that further widening of the spectrum towards 600 MHz is likely. Therefore, the need for frequency coverage is urgent and essential to future communication systems. However, electrically small antennas respond to fundamental laws that limit their possibility to increase their bandwidth while simultaneously preserve a small size and a good radiation efficiency. The trade-off between antenna radiation efficiency, size and bandwidth is detailed in [2]. The antenna bandwidth issue is mostly challenging at the low frequencies (below 1 GHz) as the radiating structure is the whole handset, which becomes electrically smaller.
In order to cover the required bandwidth, Frequency Reconfigurable Antennas (FRA) are a promising solution. A FRA is a small and efficient antenna that covers only one band at a time. This element is made reconfigurable in order to choose which band to operate in. In that way, FRA can cover an effectively wide bandwdith − while covering instantaneous narrow bandwidths − and preserve its small size. Further, one can see that the complexity of the RF chain increases with the number of bands to cover ; and an optimal solution is having an antenna pair (separate and flexible transmitting and receiving chains). In that case, one FRA only needs to cover a channel, which decreases even further its bandwidth requirement, highlighting FRA potential for 4G communication systems.
The reconfigurability mechanism can be implemented with various techniques such as switches, p-i-n or varactor diodes [3], or MicroElectroMechanical Systems (MEMS) capacitors. MEMS components are regarded as the best candidates for FRA application as they exhibit a high Quality factor (Q) and excellent linearity. They add little insertion loss in Radio Frequency (RF). For example, RF MEMS tunable capacitors have been successfully implemented in tunable filters, as described in [4], [5] and [6]. Their implementation on mobile phone antenna designs has been investigated in [7] and in [8] for the UHF band (510 MHz - 800 MHz) and in [9] for the PCS and IMT bands. RF

MEMS appeared for the first time on the phone market with the release of Samsung Omnia [10].
The first study on the antenna pair front-end design [11] shows the importance of the Q of the tuning capacitor as it severely affects the FRA radiation efficiency. Further studies on FRA confirm that the limiting criteria to achieve highly efficient systems is the tunable component. In [8], MEMS variable capacitors are used to tune a low-profile antenna in the Digital Terrestrial Broadcasting (DTB) band. The efficiency decreases from -1 dB to -4 dB between 800 MHz and 500 MHz. This study is relevant as the investigated frequencies can be foreseen as the next ones and most challenging ones to be covered with 4G.
The losses in FRA are mainly coming from the tuner and need to be overcome even-though better components are not yet available. This paper investigates the loss mechanism of the FRA at the low-band and proposes a distributed tuning mechanism in order to reduce the loss due to the tuner. The paper will be organized in 5 sections. Section II presents the problem of high-loss for fine-tuned narrow-band antennas. Section III details the distributed-tuning design, and Section IV concludes on the improvements such design brings on the antenna performance. Finally, Section V describes the future implementation of the presented findings.

2 Problem formulation

The FRA must have the ability to be fine-tuned over the bands to cover. This study focuses on the low-band for 4G from 960 MHz to 700 MHz. As detailed in [12], in order to achieve fine-tuning the capacitance steps of the tuner will determine the position of the tuner on the antenna structure. The total tuning range will then be determined by the maximum capacitance the tuner can provide. Moreover the position of the tuner will determine the loss it will cause on the total antenna system. It is important to understand that the optimal position of the tuner − that is determined by its capacitance steps − is not the optimal position from an efficiency point of view [13]. The closer to the antenna feed point the higher the currents delivered to the tuner and the greater the loss. Indeed the tuner has resistive losses, they are modeled with the Equivalent Series Resistance (ESR) and are proportional to the square of the current delivered to it. As a result the measured loss becomes greater as the antenna is tuned further away from its original resonance frequency. This loss issue is a specific problem of fine-tuned narrow-band antennas and it has been documented in [12], [14], [15], [8], [16], [17] with different tuning components. Additionally the work in [18] uses high-Q discrete components instead of a packaged tuner and shows that the same phenomenon happens. The total loss drops from -2.2 dB to -3.6 dB between 960 MHz and 800 MHz. As documented in the literature, the greatest loss happens at the furthest frequency the antenna is tuned to, compared to its natural resonance frequency. Therefore the investigation presented in this paper will focus on the lowest frequency of the tuning range, here 700 MHz.

This section will present two antenna mock-ups and measure their efficiency. The first mock-up includes a discrete high-Q capacitor and the second mock-up includes an built-in air-capacitor. This study will quantify the loss due to the fixed-capacitor. The next section will propose a distributed tuning system in order to reduce that loss.

2.1 Antenna Design

The presented antenna design aims at being assembled with a MEMS tunable capacitor to become a FRA. For that reason the design is made to originally resonate at 960 MHz. Simulations were performed with the transient solver of CST MWS, a Finite Element Method (FEM) based solver [19]. The chosen design is a Planar-Inverted-F Antenna (PIFA) as it is a low-cost and easy to manufacture antenna. The dimensions of the PIFA are shown in Fig. C.1. The ground plane of the structure has dimensions 120 × 55 mm in order to represent nowadays smart-phones. The PIFA is placed 2 mm above the ground plane. The port 1 represents the feeding point of the antenna and the port 2 represents the tuning capacitor. Port 1 and Port 2 are spaced by 14 mm. The short of the PIFA is placed 2 mm below the feeding point. Simulations can determine the position of the tuner in order to achieve fine-tuning with capacitance steps of 1/8 pF - as provided by the tuner in [20]. A key information in the design of a FRA is that the capacitance steps of the tuner will determine the position of the tuner on the antenna structure in order to achieve fine-tuning. To continuously tune the resonance frequency of the proposed antenna to 700 MHz a total capacitance of 5.1 pF is needed, at the position 14 mm away from the source. Simulations of the tunability of the antenna design are shown in Fig. C.2. In loss-less simulations the matching of the antenna varies as more capacitance is added to the structure. In measurements the tuning loss helps preserving the matching [12]. This phenomenon will also be shown in the next subsection.

2.2 Discrete-capacitor-based FRA

The above-described design is built with a discrete capacitor for resonating at 700 MHz and it is shown in Fig. C.3. The mock-up is made out of pure copper and minimum tin is used in order to isolate the loss due to the ESR of the capacitor only. The high-Q Murata [21] fixed capacitor is inserted between the PIFA and the GP. The ESR and Q of the capacitor (Q_c) are summarized in Table C.1. Q_c is calculated according to Eq. (1) where ω is the angular frequency and C is the capacitance.

$$Q_c = \frac{1}{\omega \times C \times ESR} \tag{C.1}$$

Frequency responses of the mock-up are measured with and without fixed capacitor. Fig. C.4 shows that the matching is preserved throughout tuning. Additionally the

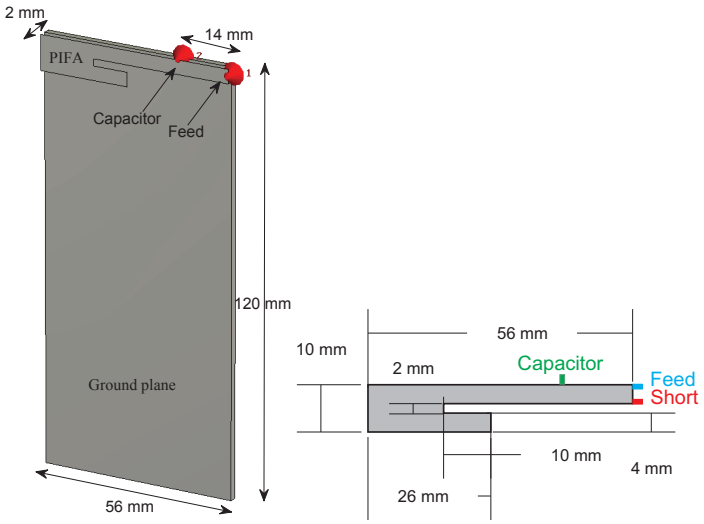

(a) Antenna. **(b)** PIFA dimensions.

Fig. C.1: Antenna design.

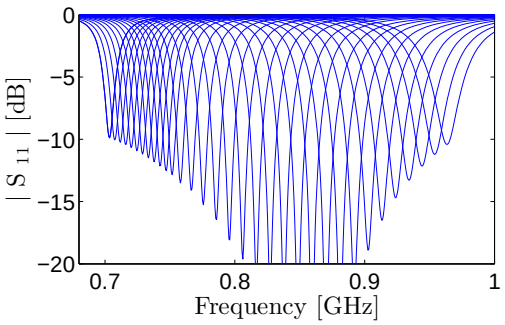

Fig. C.2: Simulated FRA frequency response.

Table C.1: ESR and Q_c of the discrete capacitor at 700 MHz.

C [pF]	ESR [Ω]	Q_c
5.1	0.258	173

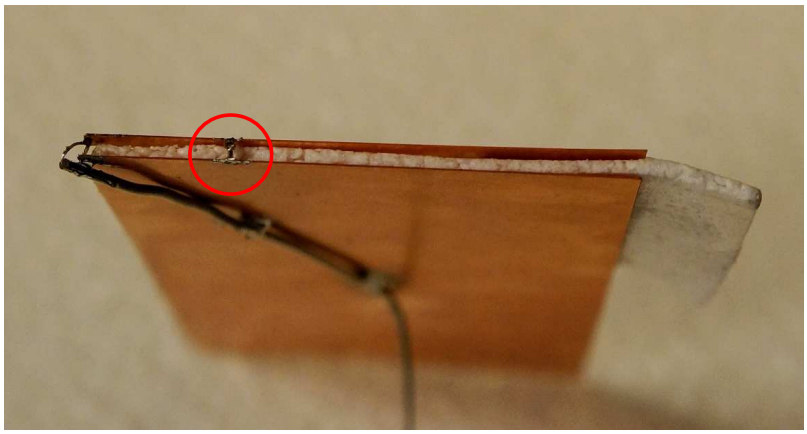

Fig. C.3: FRA mock-up with discrete capacitor.

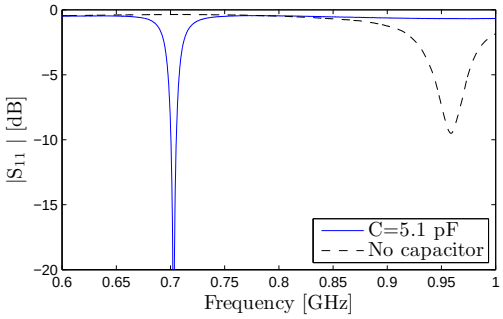

Fig. C.4: Measured FRA frequency response.

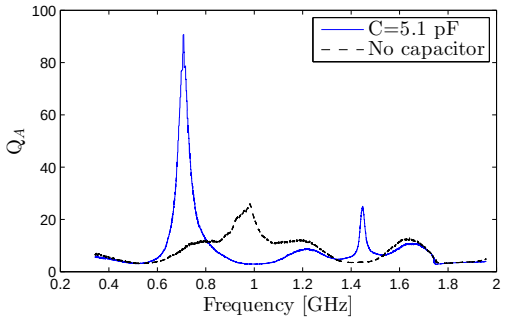

Fig. C.5: Measured Q_A of FRA with and without discrete capacitor.

bandwidth (at -6 dB) is reduced from 25 MHz to 10 MHz. This is a result of the Antenna Q (Q_A) that dramatically increases as the resonance frequency is tuned further away from its natural one, as explained in [22]. The measured Q_A is depicted in Fig. C.5 and shows an increase from $Q_A = 25$ without tuning capacitor to $Q_A = 90$ with tuning component. The mock-up is further measured in anechoic chamber and its peak efficiency at resonance is computed with 3D pattern integration technique. The measured radiation efficiency (η_r) is -3.4 dB. η_r reflects only the thermal loss and the ESR loss. Mismatch and cable losses have been taken out hereafter.

2.3 Air-capacitor-based FRA

Narrow-band antennas have a loss mechanism that is more complex than only the loss due to the ESR of the tuning capacitor, as shown in [12]. In order to isolate the thermal loss due to the narrow-band antenna design itself, the previous mock-up is re-built with an integrated air-capacitor made out of the same copper piece as the rest of the antenna. The air capacitor having an extremely high Q, the efficiency measurement will show the loss due to the copper alone. Fig. C.6 shows the pure copper mock-up. The two relatively small metal plates forming the air-capactior have the dimensions 20 $\times$ 10 mm. The size of the built-in air-capacitor is calculated with Eq. (2) where ϵ is the permittivity, A is the area and d is the distance separating the two plates. The capacitor is supported with additional polystyrene in order to have a stable distance d. Expanded polystyrene foam is commonly used in antenna mock-ups because its effect on measured antenna properties is known to be very low. The relative permittivity of the material used in the following is about 1.03 [23], [24].

$$C = \frac{\epsilon A}{d} \tag{C.2}$$

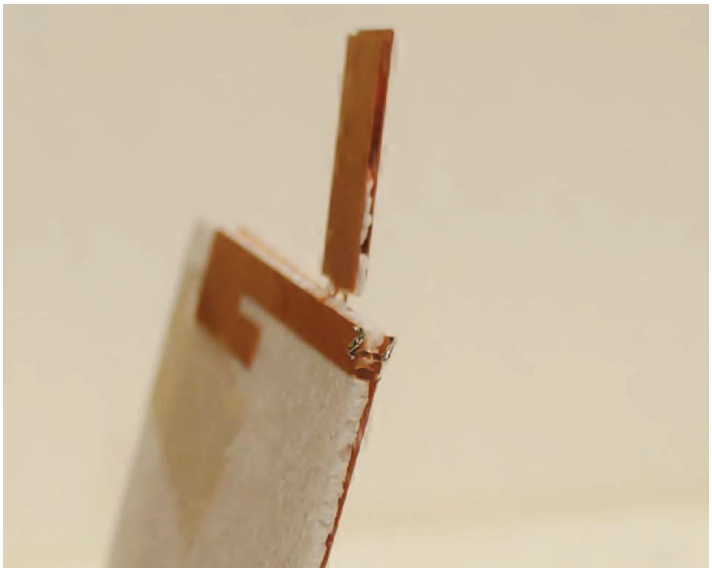

Fig. C.6: FRA mock-up with air-capacitor.

The air-capacitor adds radiation surface to the mock-up and raises the question of comparability between the air-capacitor and the fixed-capacitor mock-ups. In order to verify whether the air-capacitor alters the radiation characteristics of the antenna, the envelope correlation (ρ) is computed, as defined in [25]. It compares the measured pattern of the mock-up with the fixed capacitor and the measured pattern of the mock-up with the built-in air-capacitor. The anechoic chamber measurement is performed with angular steps of 15 degrees and $\rho = 0.988$. It is concluded that both mock-ups are comparable. The air-capacitor only stores energy and does not radiate. Additionally it is located at the top of the mock-up, where the fields are minimum according to dipole radiation mode. The measured radiation efficiency of the air-capacitor-based mock-up is $\eta_r = -0.8$ dB.

2.4 Mock-up resonating at 700 MHz

In order to confirm the existence of high thermal loss for pure-copper-narrow-band antennas, a third mock-up resonating at 700 MHz is built. The modification made to the design shown in Fig. B.1 is lengthening the bottom arm of the PIFA from 26 mm to 56 mm. The new antenna exhibits similar complex antenna impedance and the radiation efficiency measurement shows $\eta_r = -0.8$ dB.

2.5 Interpretation of the results

Antenna thermal loss due to the copper conductivity exists and plays a non-negligible role in narrow-band antenna designs. It cannot be easily simulated as shown in [26]. However it can be isolated and measured. Once this loss is taken out of the FRA radiation efficiency, the loss due to the fixed component only can be evaluated. Comparing the discrete component measurement and the air-capacitor measurement leads to the conclusion that the loss due to the ESR of the tuning capacitor is equal to -2.6 dB $(-3.4-(-0.8))$. This result matches simulated loss due to the ESR. Indeed the currents delivered to the tuning capacitor (I_C) can be computed in the simulator, and according to Eq. (3) it can be calculated that the dissipated power due to the ESR (P_L) equals -2.3 dB. The estimated loss matches well the measurement as the difference between them is within the chamber accuracy.

$$P_L = \frac{{I_C}^2 \times ESR}{2} \tag{C.3}$$

The following section of this paper addresses the possibility of reducing P_L with a distributed capacitance design.

3 Distributed tuning

It is well understood that by distributing the tuning mechanism along the antenna plate the current delivered to each capacitor would be reduced, and so the loss. However how the distribution should be designed is not an obvious choice. This section presents how to place the tuners and investigates the loss reduction with simulations and measurements.

3.1 Design

Two tuning capacitors are used instead of one. They are both placed between the antenna element plate and the GP plate. Their location is chosen according to the capacitance steps the tuners can provide. According to the previous sections a capacitor providing steps of 1/8 pF needs to be placed 14 mm away from the source on the investigated PIFA design in order to achieve fine-tuning over the targeted bands. With a distributed design, one of the capacitors also needs to be placed at 14 mm in order to ensure fine-tuning − given that it provides steps of 1/8 pF as well −. The other capacitor can be placed further away from the source. The additional capacitor will then tune with larger frequency shifts. In that way the first tuner C_1 (placed the closest from the source) will use smaller amounts of capacitance compared to a single tuner design. This will result in less loss due to its ESR. The second tuner C_2 (placed the

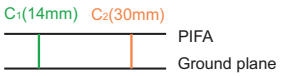

(a) Distributed design.

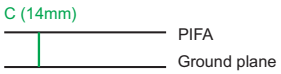

(b) Single tuner.

Fig. C.7: Tuning designs.

furthest from the source) will also exhibit low loss, as it is placed far from the high-current concentration.
Fig. C.7 illustrates the distributed-tuning design that is implemented on the investigated PIFA design. The results obtained with the distributed capacitance design shown in Fig. C.7a will be compared to the case where only one tuning capacitor is used at 14 mm from the source ($C_{pos} = 14$) as shown in Fig. C.7b. This comparison will lead to a fair evaluation of the improvement a distributed-tuning mechanism brings to a FRA. From a reflection coefficient point of view, performances are unchanged with a distributed system compared to a single-capacitor tuning system.

3.2 Simulations

The investigation on the distributed capacitance is first conducted with simulations. The ESR of the simulated capacitors is taken according to the bank of Murata 0402 capacitors from the GRM 15 collection [21], values for the MEMS [20] not being available. All the simulations are normalized to 1 W input power.

Capacitance

Table C.2 and Table C.3 summarize the capacitance and ESR data that will be used throughout the simulations, in order to tune the investigated PIFA design from 960 MHz to 700 MHz. For more clarity the simulated results are only displayed every 50 MHz. Table C.2 and Table C.3 also show that by using the distributed design the amount of capacitance that is needed per capacitor is considerably smaller than with using only one tuning capacitor. Indeed if only one capacitor was used for tuning at the position $C_{pos} = 14$ the amount of required capacitance at this location would be at least twice larger than with the proposed distributed design.

Table C.2: Capacitance and ESR for distributed tuning

	$C_{1pos} = 14$	$C_{2pos} = 30$
	pF/Ω	pF/Ω
900 MHz	0.250/0.863	0.250/0.863
850 MHz	0.375/1.120	0.625/0.282
800 MHz	1.000/0.325	0.875/0.298
750 MHz	1.500/0.230	1.250/0.282
700 MHz	2.000/0.197	1.750/0.244

Table C.3: Capacitance and ESR for single-capacitor tuning

	C_{pos}=14mm
	pF/Ω
900 MHz	1.000/0.336
850 MHz	2.000/0.212
800 MHz	3.000/0.234
750 MHz	4.000/0.243
700 MHz	5.125/0.257

Normalized currents

The surface currents in the case of single-capacitor-tuning and of distributed-tuning are shown in Fig. C.8 for 700 MHz. In the case of the distributed tuning the currents are spread on a larger section. Fig. C.9 depicts the magnitude of the peak current at each capacitor. It compares the distributed system to the single-capacitor tuning system. At 700 MHz in the case of the distributed-tuning, the currents delivered to C_1 are reduced by 65 % compared to the case of the single-capacitor-tuning. The additional capacitor C_2 receives currents that are 50 % reduced compared to the single-capacitor case. This significant current reduction will lead to a significant loss reduction.

Dissipated power in the ESR

The amount each capacitor needs to provide to tune the antenna to a certain frequency is minimized with the use of a distributed-tuning system. Consequently the energy stored in each capacitor is considerably reduced by using a distributed system. This result is plotted in Fig. C.10. Hence the dissipated power in the ESR of each capacitor is also reduced using a distributed system, as depicted in Fig. C.11. At 700 MHz, the power dissipated by the capacitor placed at 14 mm is divided by a factor 4 for the distributed-tuning compared to the single-capacitor tuning mechanism. The simulated η_r can be computed with the ESR values from Table C.2 and Table C.3 and the simulated

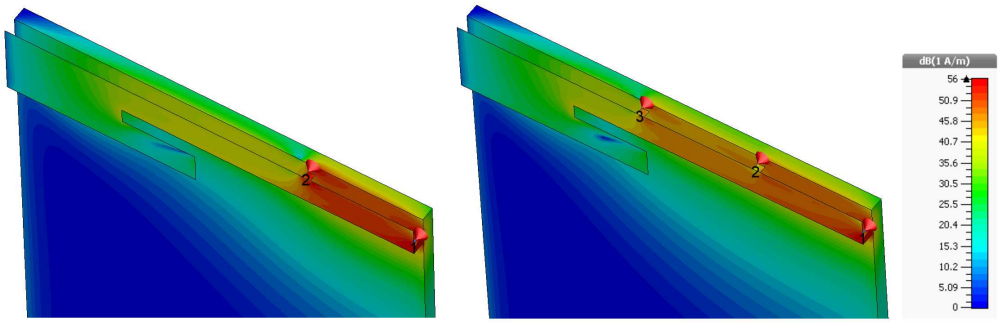

Fig. C.8: Surface currents in a single-capacitor tuning system (left) and a distributed system (right). Port 1 is the feed, port 2 and port 3 represent the capacitors.

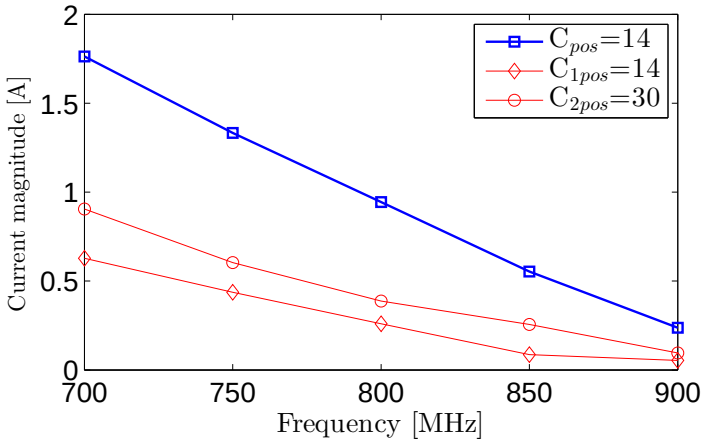

Fig. C.9: Normalized currents in a single-capacitor tuning system and a distributed system.

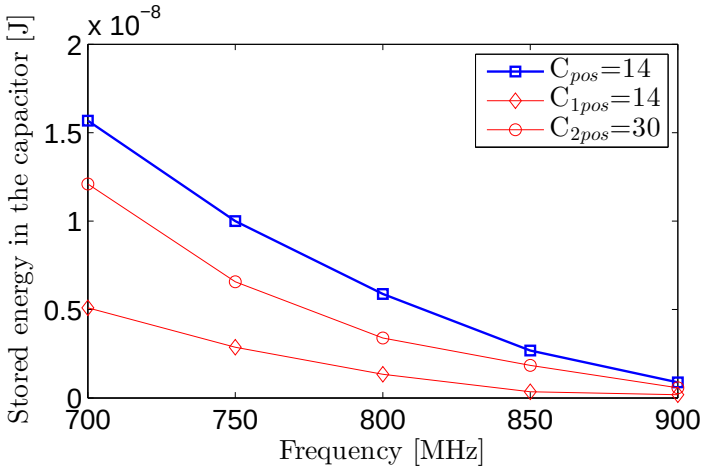

Fig. C.10: Energy stored in each capacitor in a single-capacitor tuning system and a distributed system.

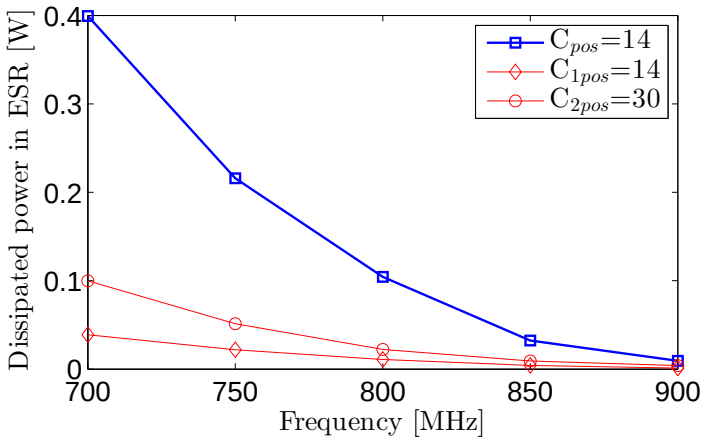

Fig. C.11: Dissipated power per capacitor in a single-capacitor tuning system and a distributed system.

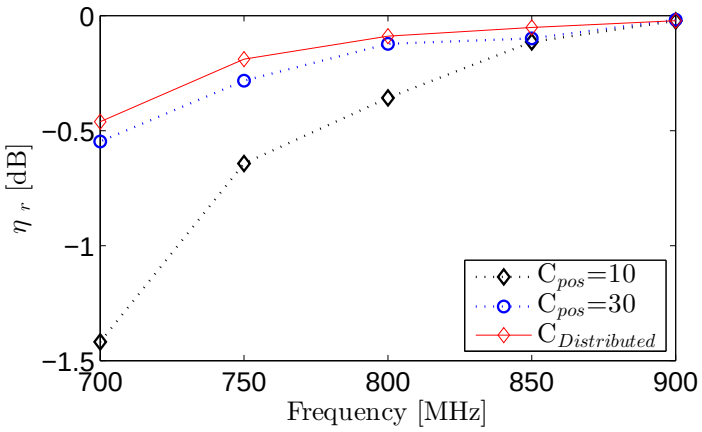

Fig. C.12: Total efficiency in a single-capacitor tuning system and a distributed system.

conductive loss. The conductive loss is a difficult task to model, requiring an extremely fine-mesh in the transient simulator [26]. The Fig. C.12 plots the simulation results of η_r over frequency. For the single-capacitor tuning system, an improvement of 1.5 dB happens due to the ESR loss alone, simulated radiation loss being identical for both mock-ups.

3.3 Interpretation of the results

Distributed-tuning has been compared to single-capacitor-tuning with simulations. Given a capacitance step of the tuner there is only one position (measured in distance to the antenna feed point) that will provide fine-tuning. The same position must be taken by one of the capacitors used for distributed-tuning. The second capacitor can be placed further away from the feed, at an arbitrarily chosen position. The main advantage that distributing the tuning provides to FRA is that the loss reduction increases as the antenna is tuned further away from its natural resonance (here 960 MHz). The further the antenna is tuned, the more relevant the distribution is. At 700 MHz the dissipated power by the ESR is already reduced by a factor 4, and the radiation efficiency is enhanced by 1.5 dB using distributed-tuning. With a trend towards extending the frequency spectrum to even lower frequencies, distributing the tuning will bring significant efficiency improvements. Using more than two capacitors to even further distribute the tuning could be considered. Nevertheless one must to keep in mind that the ESR increases as the capacitance decreases. Therefore it is a trade-off between the reduction of the current density by distributing the tuning, and the increase of the ESR by using smaller amounts of capacitance. Further investigation on the proposed design have shown that

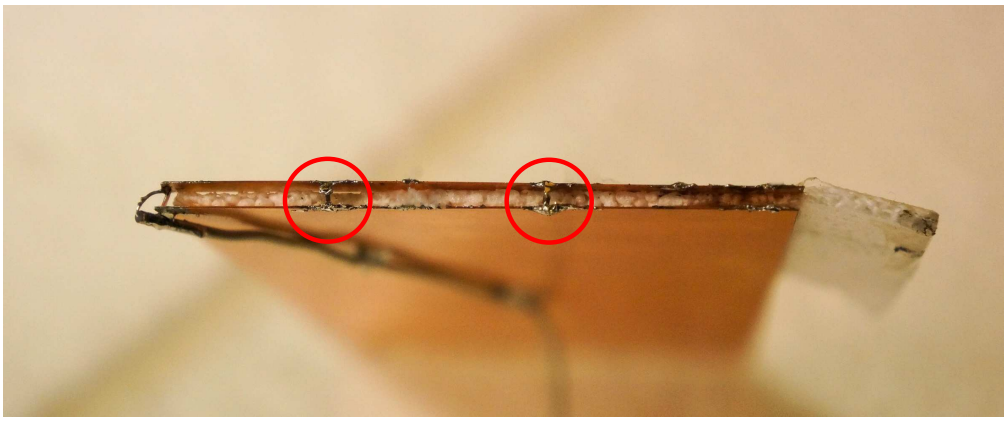

Fig. C.13: FRA mock-up with distributed tuning system.

distribution with two capacitors is the optimal design.

3.4 Measurement

The mock-up shown in Fig. C.3 is modified for the distributed-tuning measurement. Instead of one capacitor of 5.1 pF placed at 14 mm from the feed, two capacitor are used as shown in Fig. C.13. According to the Table C.2 the capacitor placed at 14 mm takes the value 2.0 pF and the capacitor placed at 30 mm takes the value 1.7 pF. The frequency response of the mock-up is comparable to the one of the single-capacitor mock-up in terms of resonance frequency and bandwidth. The unloaded Q_A is not affected by having one or two capacitors on the mock-up. However the measured loaded Q_A is increased by 20%, due to ESR adding in parallel. This increase corresponds to a bandwidth reduction of less than 1 MHz, therefore it is considered negligible. The mock-up is further measured in anechoic chamber and the radiation efficiency equals $\eta_r = -2.1$ dB. With only one capacitor the measured radiation efficiency is $\eta_r = -3.4$ dB. This measurement shows an improvement of 1.3 dB on the antenna efficiency when two capacitors are used instead of one. This result is consistent with the simulated improvement.

4 Conclusion

This work has highlighted the issue of tuning loss for narrowband FRA. This type of antennas can provide continuous tuning over a large frequency range. They have a great potential for 4G communications as only one small element can cover all frequencies in

the low band (700 MHz to 960 MHz), by being tuned to the desired band (or channel if one considers an antenna pair). However, the tuning component cannot be placed in the best location from an efficiency point of view. That is because the position of the tuner ensures the fine tuning. As the loss it causes on the antenna radiation efficiency is significant—due to high fields in narrowband antennas—it is crucial to understand and reduce its impact. This work is specific to fine-tuned narrowband antennas, as for a 2-stage frequency reconfigurability there is more flexibility in the choice of the tuner position. Tuning has been considered to be performed with an MEMS variable capacitor in simulations. For more practicality, measurements have been performed with high-Q fixed components.

The conclusion of this paper is twofold: firstly, it shows the existence of thermal losses for narrowband antennas; secondly the loss due to the ESR of the tuner is quantified and reduced using a distributed-tuning mechanism. The antenna thermal loss (due to conductivity of the copper plate) is nonnegligible for narrowband antennas. This phenomenon happens because narrowband antennas exhibit higher and more confined fields than typical antennas. Additionally, the higher thermal loss needs to be measured, as its estimation using simulators cannot be achieved in reasonable computational time. This paper compares a built-in air capacitor to a fixed high-Q component in order to quantify the loss due to the ESR of the capacitor and the thermal loss. In this way, the measured loss due to the ESR matches the simulated one. The ESR loss was estimated to be 2.6 dB when the antenna was tuned from 960 MHz to 700 MHz. In order to reduce this loss, a distributed-tuning design is proposed. It uses two capacitors placed at two different locations on the antenna. At 700 MHz, the distributed tuning shows 1.3 dB improvement on the total loss compared to the single-tuning mechanism. The loss due to the tuner increases as the operating frequency is tuned towards lower values. Similarly, the loss reduction improves as the frequency is tuned further away from the natural resonance frequency of the design. The wider the tuning range is, the greater the improvement by distributing the tuning.

5 Future Work

Distributing the capacitance reduces the current in each tuner. The voltage will be increased and one needs to ensure that it remains below the breakdown voltage of the tuner. However, with MEMS technology the breakdown voltage and the maximum capacitance are a trade-off. As distributing the tuning involves lowering the maximum capacitance, simultaneously increasing the maximum handled voltage should not be an issue. Moreover, designing a distributed-tuning mechanism increases the degree of complexity of the antenna, as two tuners are needed instead of one. Therefore, the authors suggest to co-design the antenna and the tuner so that only one tuner with two parallel and independent tracks can be used, instead of two tuners. Cost and complexity reduction can then be achieved and an efficient FRA can be manufactured for 4G. In the

future work, the authors will build an FRA with a specifically designed tuner in order to efficiently cover the low band of the 4G spectrum with a single and small antenna.

Acknowledgment

The work is supported by the Smart Antenna Front End (SAFE) Project within the Danish National Advanced Technology Foundation, High Technology Platform.

References

[1] 3GPP Technical Report, "Feasibility study for Further Advancements for E-UTRA (LTE-Advanced) - Specification 36.912 - Release 11," 2012. [Online]. Available: http://www.3gpp.org/ftp/Specs/html-info/36912.htm

[2] R. F. Harrington, "Effect of Antenna Size on Gain, Bandwidth, and Efficiency," *Journal of Research of the National Bureau of Standards- D. Radio Propagation*, vol. 64D, no. 1, pp. 1–12, 1960. [Online]. Available: http://archive.org/details/jresv64Dn1p1

[3] S.-k. Oh, H.-s. Yoon, and S.-o. Park, "A PIFA-Type Varactor-Tunable Slim Antenna With a PIL Patch Feed for Multiband Applications," *Antennas and Wireless Propagation Letters*, vol. 6, no. 11, pp. 103–105, 2007.

[4] A. Abbaspour-Tamijani, L. Dussopt, and G. M. Rebeiz, "Miniature and Tunable Filters Using MEMS Capacitors," *IEEE Transactions on Microwave Theory and Techniques*, vol. 51, no. 7, pp. 1878 – 1885, 2003.

[5] D. Peroulis, S. Pacheco, K. Sarabandi, L. P. B. Katehi, and A. Arbor, "Tunable Lumped Components with Applications to Reconfigurable MEMS Filters," in *Microwave Symposium Digest, IEEE MTT-S International*, 2001, pp. 341 – 344.

[6] Y. Liu, A. Borgioli, A. S. Nagra, and R. a. York, "Distributed MEMS transmission lines for tunable filter applications," *International Journal of RF and Microwave Computer-Aided Engineering*, vol. 11, no. 5, pp. 254–260, Sep. 2001.

[7] M. Nishigaki, T. Nagano, T. Miyazaki, T. Kawakubo, K. Itaya, M. Nishio, and S. Sekine, "Piezoelectric MEMS Variable Capacitor for a UHF Band Tunable Built- in Antenna," in *Microwave Symposium IEEE/MTT-S International*, 2007, pp. 2079–2082.

[8] Y. Tsutsumi, M. Nishio, S. Obayashi, H. Shoki, T. Ikehashi, H. Yamazaki, E. Ogawa, T. Saito, T. Ohguro, and T. Morooka, "Low Profile Double Resonance

Frequency Tunable Antenna Using RF MEMS Variable Capacitor for Digital Terrestrial Broadcasting Reception," in *IEEE Asian Solid-State Circuits Conference*, 2009, pp. 125–128.

[9] J. R. De Luis, A. Morris, Q. Gu, and F. de Flaviis, "Tunable Duplexing Antenna System for Wireless Transceivers," *IEEE Transactions on Antennas and Propagation*, vol. 60, no. 11, pp. 5484–5487, Nov. 2012.

[10] "Samsung Omnia W with Wispry MEMS module, Web Press Release," p. http://evertiq.com/news/21198?utm%20source=feedbur.

[11] A. James, "Reconfigurable Antennas for Portable Wireless Devices," *IEEE Antennas and Propagation Magazine*, vol. 45, no. 6, pp. 148–154, 2003.

[12] S. Caporal, D. Barrio, M. Pelosi, G. F. Pedersen, and A. Morris, "Challenges for Frequency-Reconfigurable Antennas in Small Terminals," in *IEEE Vehicular Technology Conference (VTC Fall)*, 2012, pp. 1–5.

[13] S. C. Del Barrio, M. Pelosi, O. Franek, and G. F. Pedersen, "On the currents magnitude of a tunable Planar-Inverted-F Antenna for low-band frequencies," in *2012 6th European Conference on Antennas and Propagation (EUCAP)*, Mar. 2012, pp. 3173–3176.

[14] M. G. S. Hossain and T. Yamagajo, "Reconfigurable Printed Antenna for a Wideband Tuning," in *European Conference on Antennas and Propagation (EuCAP)*, vol. 1, 2010, pp. 1– 4.

[15] A. Suyama and H. Arai, "Meander Line Antenna Built in Folder-Type Mobile," in *International Symposium on Antennas and Propagation (ISAP)*, 2007, pp. 294–297.

[16] V.-a. Nguyen, R.-a. Bhatti, and S.-o. Park, "A Simple PIFA-Based Tunable Internal Antenna for Personal Communication Handsets," *IEEE Antennas and Wireless Propagation Letters*, vol. 7, pp. 130–133, 2008.

[17] N. Behdad, S. Member, and K. Sarabandi, "A Varactor-Tuned Dual-Band Slot Antenna," *IEEE Transactions on Antennas and Propagation*, vol. 54, no. 2, pp. 401–408, 2006.

[18] S. C. D. Barrio, M. Pelosi, and G. F. Pedersen, "On the efficiency of frequency reconfigurable high-Q-antennas for 4G standards," *Electronics Letters*, vol. 48, no. 16, pp. 982– 983, 2012.

[19] Computer Simulation Technology (CST) http://www.cst.com, "CST Microwave Studio," 2012.

[20] WiSpry Tunable Digital Capacitor Arrays (TDCA), "http://www.wispry.com/products-capacitors.php."

[21] Murata, "Chip Monolithic Ceramic Capacitors," 2012. [Online]. Available: http://www.murata.com/products/catalog/pdf/c02e.pdf

[22] O. Kivekäs, J. Ollikainen, and P. Vainikainen, "Frequency-tunable Internal Antenna for Mobile Phones," in *12th International Symposium on Antennas (JINA)*, vol. 2, no. November, 2002, pp. 53–56.

[23] M. A. Plonus, "Theoretical Investigations of Scattering from Plastic Foams," *IEEE Transactions on Antennas and PropagationAntennas and Propagation*, vol. 13, no. 1, pp. 88–94, 65.

[24] E. Knott, "Dielectric constant of plastic foams," *IEEE Transactions on Antennas and Propagation*, vol. 41, no. 8, pp. 1167–1171, 1993.

[25] J. Pierce and S. Stein, "Multiple Diversity with Nonindependent Fading," *Proceedings of the I.R.E.*, vol. 48, pp. 89–104, 1960.

[26] S. Caporal Del Barrio and G. F. Pedersen, "High-Q Antennas : Simulator limitations," in *European Conference on Antennas and Propagation (EuCAP)*, no. 1, 2013.

Paper D

Loss Limitations of Frequency Reconfigurable Antennas

Caporal Del Barrio S.[1], Bahramzy P.[1,2], Svendsen S.[2], Jagielski O.[2] and Pedersen G.F.[1]

[1]Section of Antennas, Propagation and Radio Networking (APNet), Department of Electronic Systems, Faculty of Engineering and Science, Aalborg University, DK-9220, Aalborg, Denmark, {scdb, mp, gfp}@es.aau.dk

[2] Intel Antenna Business, Lindholm Brygge, Noerresundby, 9400, Denmark, {pevand.bahramzy, simon.svendsen, ole.jagielski}@intel.com

The paper has been submitted to the *Transaction on Antennas and Propagation* Aug., 30^{th} 2013.

The layout has been revised.

Abstract

Antenna volume has become a critical parameter in mobile phone antenna design, as broader bandwidths are required for high connectivity between users. Shrinking the antenna size affects its efficiency, if one does not sacrifice bandwidth. This paper proposes an architecture to address the need for small and wide-band antennas. The study focuses on the low-frequencies (700 MHz - 960 MHz) in order to address a tough scenario for small platforms. An investigation of the loss mechanism in a tunable architecture is proposed, and presents the limitations of efficient antenna miniaturization.

1 Introduction

During the last decade the development of wireless communication has been major. The user's demand for ever increasing data rates has driven the development of the 4^{th} Generation (4G) of mobile communication standards. 4G will provide speeds up to 1 Gbit/s for low-mobility users and 100 Mbit/s for high-mobility users of mobile devices [1]. In order to achieve these requirements 4G specifies the use of Multiple-Input Multiple-Output (MIMO) technology where several antennas are operating simultaneously at both ends of the radio link. Each of these antennas should also support a significantly large number of frequency bands.

The challenges that 4G raises for the mobile phone antenna designers are complex and inter-dependent. Firstly, multiple antennas that work simultaneously in transmitting or receiving mode must be decoupled and decorrelated in order to benefit from a maximum power transfer and from multipath [2]. This can be ensured when the antennas are separated with a distance equal or greater than $\lambda/2$, where λ is the wavelength. At 700 MHz $\lambda/2$ means 43 cm, and this separation is not feasible in hand-held devices. Secondly the Frequency Division Duplexing (FDD) spectrum has been already extended for 4G to 25 bands ranging from 700 MHz to 2.7 GHz [1]. The new standard started a trend to ever increase the number of bands and to target lower frequencies, towards 400 MHz (new bands being the re-allocation of the old TV-bands). Such large bandwidth including such low frequencies means very large antenna designs, because size, bandwidth and efficiency at a given frequency are a trade-off [3]. However the antennas must be integrated in smartphones where the available space is ever reducing, in order to embed more chips, cameras, speakers and various components.

In order to address the bandwidth issue multi-band antennas have been investigated in the past years, covering up to 9 different bands [4], [5], [6]. However they require additional arms for every new frequency band, thus increasing the antenna volume proportionally with the number of bands and making this technique not suitable for a long-term solution on hand-held 4G platforms. Parasitic elements have been used for the same purpose [7], though increasing the antenna volume. The board resonances

can also be exploited to obtain a broad frequency response, with the use of matching networks [8], [9], [10], [11], [12], at the cost of space and efficiency as well as antenna decoupling limitations [13], [14]. Frequency Reconfigurable Antennas (FRAs) are good candidates to provide a wide bandwidth. An additional active component (often switch or tunable capacitor) will change the equivalent reactance of the resulting antenna and modify its resonance frequency. A tunable reactance can continuously shift the resonance frequency of the antenna across a very wide range of consecutive frequencies, i.e. fine-tuning. The FRA can achieve an equivalent large bandwidth exhibiting an instantaneous narrow bandwidth.

Typically, a FRA is designed at its highest frequency of operation, meaning a small resonator. Afterwards the tuning mechanism shifts its resonance towards lower frequencies. The main advantage of using FRA is the possibility of having only *one* element that is *small* and can operate in all the bands. The immediate question that comes to ones mind is, how small can the element get while preserving acceptable performances. The size reduction of the element is limited by the increase in Quality factor (Q) and the allowed loss in the antenna structure. Understanding the loss mechanism of small, high-Q and tunable antennas has been driving the research presented in this paper. Efficiency is a critical parameter in applications where Electrically Small Antennas (ESAs) are required and transmitter power is limited.

Much interest has been given to ESA technologies. Wheeler [15] initiated the study of the effect of antenna size reduction and proved the relation between antenna volume and the product of its efficiency and bandwidth. Chu [16] generalized the previous work, relating the antenna volume to the Q and later Harrington [3] determined the maximum achievable gain for ESAs. Hansen [17] and McLean [18] have also shown the relation between impedance bandwidth and antenna volume. Next, James investigated the loss impact of dielectric loading of the antenna element, highlighting the trade-off between compactness and efficiency in [19]. Following, Smith [20] derived the efficiency of ESAs combined with matching networks, necessary components for ESAs as they exhibit very small radiation resistances. More recently genetic algorithms [21] have been developed in order to optimize the antenna geometry for a given parameter, radiation resistance for example. Independently, geometries considering height over a ground plane have been optimized for radiation efficiency of wire antennas in [22] and of patches in [23]. Meandered lines efficiencies, for a given small volume, are optimized in [24], [25] and [26] for Radio Frequency Identification (RFID) applications.

In the scope of fine-tuned FRA for mobile phone application, this paper investigates the loss mechanism of high-Q antennas. All investigations are made at 700 MHz, being the lowest frequency bound 4G requires nowadays, thus the toughest for small platforms. Section 2 presents the Q formulations that will be used throughout the paper. A high-Q design fit for small mobile-phone application is then presented in Section 3. That design is compared to a large high-Q design in Section 4, and to a small tunable loop antenna in Section 5 and Section 6. Finally discussions and conclusions from all three designs

are disclosed in Sections 7 and 8 respectively.

2 Antenna Quality factor

The Antenna Quality factor (Q_A) is a measure of the stored energy relative to the accepted power in the radiating structure. FRA have a Q_A that increases considerably as the resonance frequency is tuned further away from its original resonance frequency [27]. Along with this increase in Q_A comes a significant radiation efficiency drop, as reported in [28]. The Q_A can also be expressed as a measure inversely proportional to the bandwidth (BW). Dependent on the Voltage-Standing-Wave Ratio (VSWR), Q_A can be expressed as follows [27]:

$$Q_A(\omega) = \frac{2\sqrt{\beta}}{FBW_V(\omega)}, \sqrt{\beta} = \frac{s-1}{2\sqrt{s}},$$

where FBW_V is the matched VSWR fractional bandwidth and s is a specific value of the VSWR.
In practical antenna design, one can distinguish the unloaded Q_A ($Q_{A,unoad.}$) from the loaded Q_A ($Q_{A,load.}$). The $Q_{A,unload.}$ values are found through simulation of a loss-less structure and describe the relation between reactance and resistance in the element itself. They give a worst case scenario, however these values are useful for directly comparing one antenna to another. The $Q_{A,load.}$ values are found through measurements and include the loss in the structure. Evidently $Q_{A,load.}$ values will always be lower than $Q_{A,unload.}$ values. The difference between unloaded and loaded Q_A gives an insight into the amount of loss in the antenna structure. For this purpose the authors will introduce the Ratio of loaded to unloaded Q_A values: R_{Q_A}. This ratio will be used to characterize antenna designs in the following sections.
Simple Q_A calculations on today's bandwidth requirements highlight the challenge of ESA design. In the low-band of 4G communications, the antenna must cover frequencies ranging from 960 MHz to 699 MHz, which corresponds to a Q_A of 3.25. In the case of a FRA with an instantaneous bandwidth of 10 MHz, the corresponding Q_A is 70 at 704 MHz. With these considerations in mind the authors will also name FRA, high-Q antennas.

3 Small monopole for handset operation

In this section the design of a novel architecture for FRA on a small handset is described, and its performances are presented.

3.1 Framework of the design

To comply with the next generation of mobile communication, mobile phone antennas need to be operating in frequencies as low as 700 MHz, for the current release [1]. From fundamental limitations on antenna design [3] one cannot increase the antenna bandwdith, and decrease its volume, without affecting its efficiency. However the room left for the each antenna on the mobile phone decreases, as the number of required antennas increases. In order to address the issues raised by the new standard, FRA are a promising solution, as they allow a single antenna element to be narrow-band and to operate in a wide frequency spectrum. Thus low frequencies can be reached while the size of the element is kept small and constant.
Furthermore with the addition of bands to operate in, the front-end design increases dramatically in complexity. One realizes that in order to build a long term solution that can handle the need for bandwidth, flexible and independent receiving (RX) and transmitting (TX) chains need to be built [29]. Separating the TX from the RX into two autonomous and tunable chains will provide a long term solution to address the expansion of bands added to the spectrum of the next communication generations. In that respect the design proposed in this section has two antennas, operating in TX and RX frequencies of band 12 with 30 MHz duplex distance, as specified in [1]. The main advantage of this novel architecture is the possibility to remove the duplex filter, which will save cost and space. However enough isolation needs to be then provided by the antennas − typically 25 dB.

3.2 Geometry

The geometry of the proposed antennas is depicted in Fig. D.1. In this section the design is presented without tunability, as its scope is to characterize the performances of small and isolated antennas at 700 MHz on a small platform. The Ground Plane (GP) is chosen to be a candy-bar type in order to create a tough scenario at the chosen frequency, and its dimensions are 100×40 mm^2, which represents about $\lambda/4$ at 700 MHz. The largest dimension of the GP is slightly smaller than $\lambda/4$ at 700 MHz. The antenna type − for both TX and RX − is a slot-fed monopole placed 3 mm above the GP. The monopole is an inductively loaded wire, exhibiting a length of 60 mm. The feeding happens through coupling with a small slot, cut into the GP. This slot is capacitively loaded and controls the matching − to the 50 Ω impedance feed line − of the resulting design. The slot is filled with FR-4 and placed under the end of the monopole and has dimensions 10×1.5 mm. The inductive loading of the monopole allows a smaller element and the coupled feeding results in a wider bandwidth. Hereafter the authors distinguish the tuning from the matching components used in the proposed design. The tuning components are the inductors and effectively change the resonance frequency of the monopoles; the matching components are the capacitors at the feed that only affect how well the antennas are matched to the feed lines. Both RX and TX antennas have

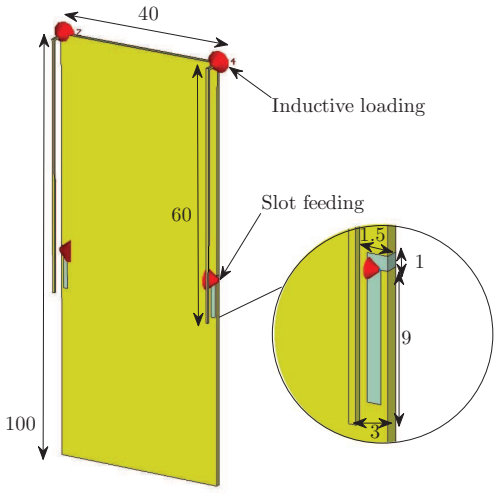

Fig. D.1: Small antenna design for handset. Dimensions are given in mm.

Table D.1: Tuning and matching values.

	TX	RX
L [nH]	34.4	30.0
C_1 [pF]	1.0	1.0
C_2 [pF]	10.0	9.0

the same length, thus the inductors and matching components have different values in each antenna in order to provide resonances that are 30 MHz apart. These values are summarized in Table D.1 for a resonance in band 12 and the schematic is represented in Fig. D.2. Simulations were run with the Finite Element Method (FEM) solver in CST [30].

3.3 Measurements

A mock-up of the above-described design was built for band 12, and it is shown in Fig. D.3. Measurements of the two isolated resonances at 700 MHz and 730 MHz are plotted in Fig. D.4. The isolation between the TX and RX antennas reaches -20 dB, for bandwidths of 25 MHz and 30 MHz for TX and RX respectively. However with bandwidth of about 10 MHz it is reasonable to expect an isolation below -25 dB. For the proposed architecture, bandwidths of 10 MHz are sufficient in band 12 [31], as

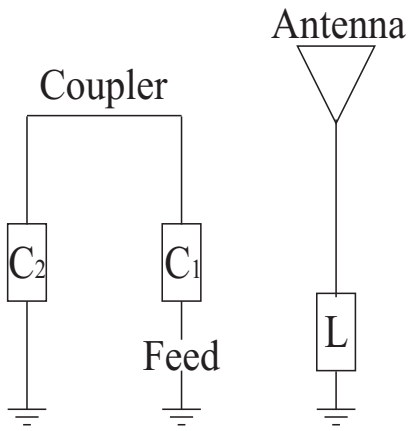

Fig. D.2: Antenna diagram.

Table D.2: Loss decomposition of the TX slot-fed monopole

η_T [dB] / $Q_{A,load.}$	-5.0 / 55
L_L [dB] / Q_c	1.8 / 88
L_{C_1} [dB] / Q_c	0.1 / 725
L_{C_2} [dB] / Q_c	2.7 / 57

the antenna only needs to cover a channel, as opposed to a full band. The differences between the simulations and the measurements lie in a high precision required for the dimensions and placement of the slot and the components. The mock-up was measured in anechoic chamber to evaluate its efficiency with 3D radiation pattern integration technique, and the total efficiency (η_T) is summarized in Table D.2. The measured η_T of the mock-up with FR-4, tuning and matching components is -5.0 dB for each antenna. Same efficiencies − within the chamber accuracy − are measured for TX and RX antennas. The power lost in the lumped elements can be evaluated in the simulations. The power lost in L (L_L), in C_1 (L_{C_1}) and in C_2 (L_{C_2}) are normalized to 1 W input power and shown in Table D.2 for the TX antenna. From the simulations it can be evaluated that the components are responsible for 4.5 dB of loss in total. The Q values of the components (Q_c) used in the mock-up are also summarized in Table D.2. It is concluded that most of the loss comes from the matching capacitor C_2, which is placed across the matching slot. Indeed it is placed in a very high current location, even-though it is also placed at the feed. Additionally, because of the high capacitance value needed to match the antenna, its Q_c is very poor. The resulting $Q_{A,load.}$ of the antenna is also summarized in Table D.2.

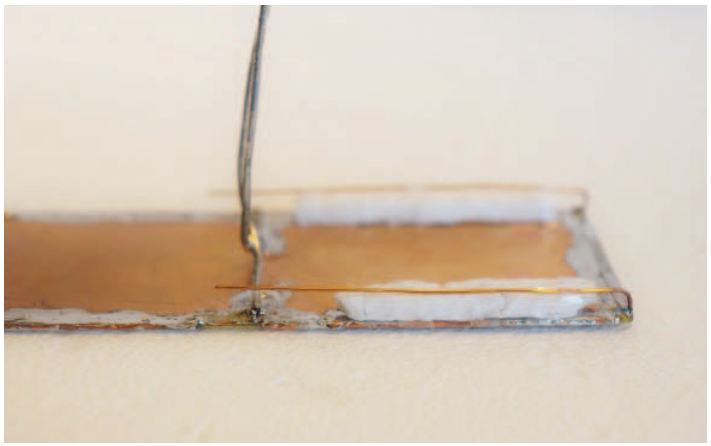

Fig. D.3: Mock-up of the small antenna design for handset.

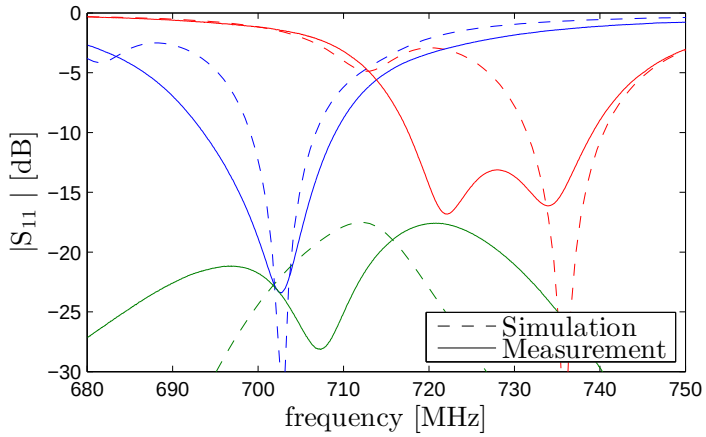

Fig. D.4: Simulated and measured frequency responses of the slot-fed monopole in band 12.

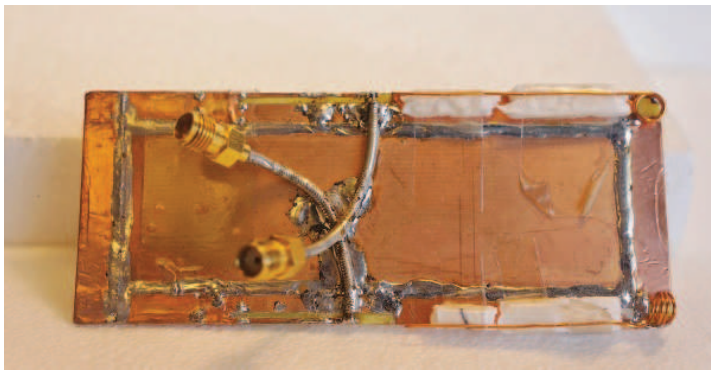

Fig. D.5: Improved mock-up with air-inductor (top view).

Table D.3: Total efficiency and loaded Q_A of the TX slot-fed monopole with air-inductors

η_T [dB]	-3.0
$Q_{A,load.}$	125

As an attempt to reduce the loss in the mock-up, the fixed inductors are replaced by air-inductors made out of the same copper piece as the monopole. The new mock-up is shown in Fig. D.5. The inductor consists of only 3 turns as the height of the monopole should remain low. The maximum allowed height is 3 mm, if one wants to keep the height of the monopole identical to the mock-up containing the fixed inductors and not alter the coupling to the matching slot. For this reason the monopole needs to be extended to both sides of the PCB, as shown in Fig. D.6. In order to minimize the antenna isolation the inductors are placed orthogonally. As a result, the η_T has improved almost 2 dB, as summarized in Table D.3, together with the measured $Q_{A,load.}$ value. This result was expected from the loss decomposition summarized in Table D.2. However the isolation has worsen to 18 dB. The reason of the drop in isolation between the antennas is twofold: the fields generated by the air-inductors are not as confined as in the case of chip inductors and couple more to each other; and the antennas are more efficient (typically isolation improves with losses, when the antennas are made more efficient more power is radiated, and is likely to couple into the other antenna). The measured S parameters of the mock-up with the air-inductors are shown in Fig. D.7.

3.4 Results

The high-Q antenna measurements performed in this section show that even using pure copper antennas loaded with air-inductors, a small antenna design at low-frequency is

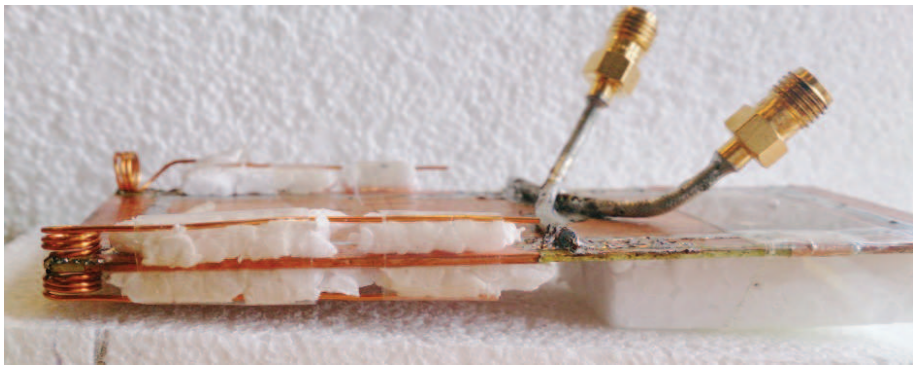

Fig. D.6: Improved mock-up with air-inductor (side view).

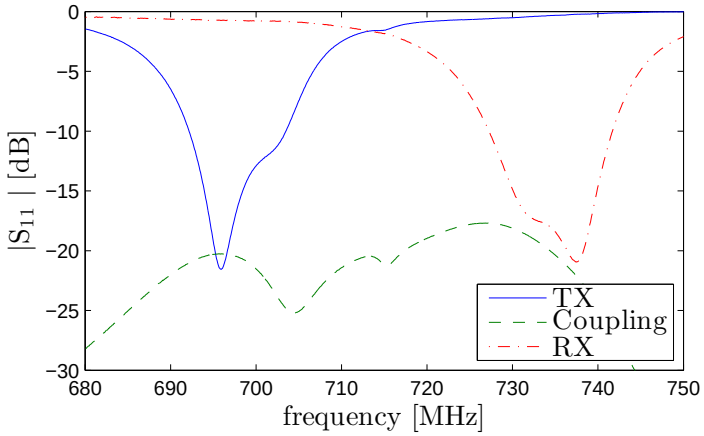

Fig. D.7: Measured S parameters of the slot-fed monopole with air-inductors.

Table D.4: Design dimensions

	Area [mm^2]
Ground	300 × 300
Slot	2 × 38
Patch	196 × W

still lossy. This phenomenon is intrinsic to ESAs, when matching and tuning components are needed, as they cause the loss to increase. In the proposed design, size reduction required capacitive matching, which lead to high currents in the matching slot (including components and FR-4), thus high losses. In the next sections the authors will try to understand further the loss mechanism in high-Q antennas and ESAs, in order to further understand the loss mechanism of FRA.

4 Electrically Large High-Q antennas

In this section the authors investigate the loss mechanism of a high-Q antenna. It is important to bear in mind that a high-Q antenna is not necessarily an ESA. Therefore the authors will dedicate this section to the investigation of a large high-Q antenna, consisting of a slot-fed patch. The antenna resonates at 700 MHz. The proposed design has the advantage of allowing to control the Q_A while keeping its other parameters constant (height of the patch and resonance frequency).

4.1 Geometry

The geometry of the proposed design is shown in Fig. D.8. The large squared ground has a rectangular slot in its center. The feeding is positioned across the slot, in its center along $+z$ axis. The patch is placed 10 mm above the ground ($+x$ direction). The length of the patch controls the resonance frequency. The patch width W controls only the Q_A value whereas the height of the patch controls the matching. The strength of the presented design is that the width parameter only affects the Q_A without modifying its resonance frequency. Therefore comparisons can be made between antennas without using any lumped element, thus avoiding external losses. The mock-ups are made out of pure copper only, in order to investigate the possibility of loss due to conductivity of lossy metals. W varies from 2 to 25 mm and all the other dimensions of the design are fixed and summarized in Table D.4. The length of patch is about $\lambda/2$ at 700 MHz, and the side of the GP equivalent to $5\lambda/7$ at 700 MHz.

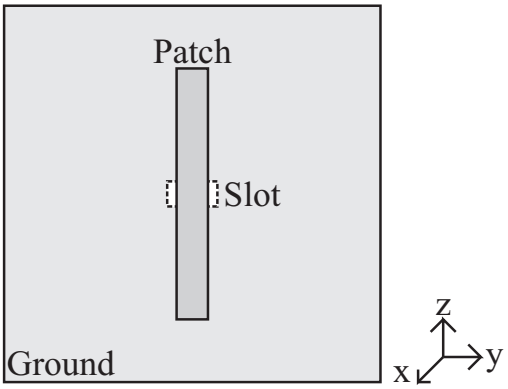

Fig. D.8: Design of the high-Q antenna on a large GP.

4.2 Measurements

The above-described mock-up is simulated using the Finite Element Method (FEM) solver in CST [30] and built with pure copper. The mock-up is shown in Fig. D.9 for $W = 25$ mm. Polystyrene spacers are used to stabilize the mock-up. Alignment of the plates is ensured, as it affects the resonance frequency of the mock-up. The large GP limits the interaction between the radiator and the coaxial measuring cable. Measurements of the three patches reveal varying bandwidths depending on the width of the patch. Absolute and complex frequency responses of the mock-ups can be seen in Fig. D.10 and Fig. D.11 respectively. The center frequency for the three mock-ups is 698 MHz. The absolute response shows a bandwidth enhancement as the patch width increases and the complex response shows the comparability between the mock-ups as the curves cross very similar points in the smith chart. This figure also shows the entering and exiting frequencies (rounded to 1 MHz) of the VSWR circle. Simulated and measured Q_A values as well as measured η_T are summarized in Table D.5. The measurements show that the measured $Q_{A,load.}$ values of the electrically large high-Q antenna − made with pure copper and polystyrene − is close to the simulated $Q_{A,unload.}$ values − resulting from simulations with Perfect Electric Conductor (PEC). The ratios R_{Q_A} are about 0.9 and the presented antenna design exhibits a low loss, even for $Q_{A,load.}$ values as high as 225.

4.3 Results

On the measurements of the presented large high-Q antenna made out of pure copper, one can observe that even high-Q antennas can be made efficient, if they can be large enough. Nevertheless the structure becomes lossier as its Q_A increases, exhibiting a con-

Fig. D.9: Front (left) and back (right) views of the mock-up.

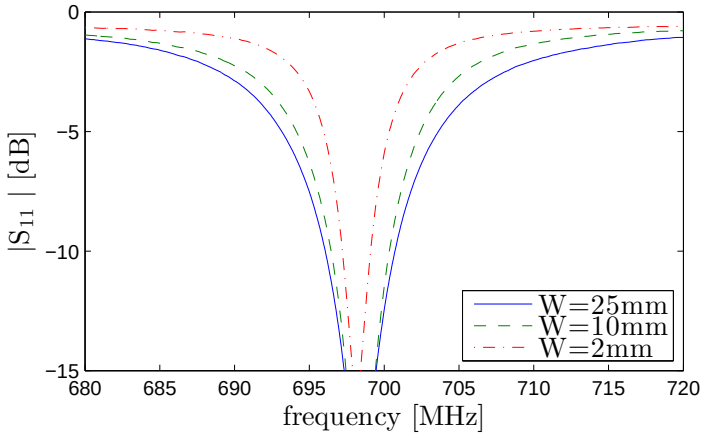

Fig. D.10: Measured frequency response for different widths of the patch.

Table D.5: Total efficiency comparison between different widths of the patch

	$Q_{A,unl}$	$Q_{A,l}$	R_{Q_A}	η_T [dB]
W=25mm	90	81	0.90	-1.1
W=10mm	175	160	0.91	-1.3
W=2mm	260	225	0.87	-2.0

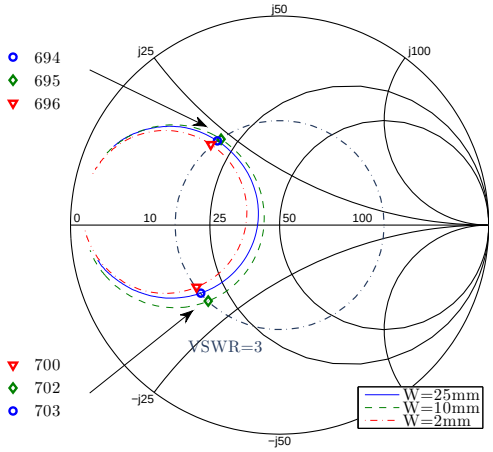

Fig. D.11: Measured frequency response for different widths of the patch. Entering and exiting frequencies of the VSWR circle are given in MHz.

ductive loss phenomenon in high-Q antennas. This source of loss is further investigated in the next section.

5 Loop antennas with tuning

In this section the authors investigate small high-Q antennas and the effect of miniaturization on the efficiency. The choice of loop antennas for this investigation lies on their analytically well defined characterization [32], [33], their easiness to manufacture, and to tune by placing a capacitor in a cut of the loop. The diameter of the loop being directly related to its resonance frequency, a discrete capacitor is used to force the loops to resonate at the same frequency. The consequences of drastically reducing the antenna volume is described in the following, comparing total efficiencies at 700 MHz.

5.1 Geometry

The presented designs are electrically small, as can be seen in the Table D.6 showing the areas of the four loops L1, L2, L3 and L4. The $Q_{A,unload.}$ values − showing the behavior of the structure itself independently of the amount of loss − are also summarized in this table. For their calculation each structure is simulated with PEC and an ideal capacitor, using the Finite Element Method (FEM) solver in CST [30]. As the loop diameter shrinks its $Q_{A,unload.}$ value at 700 MHz increases, as well as its natural resonance frequency and the amount of capacitance needed to tune the antenna back to

700 MHz. The fixed capacitors used to tune the antennas have a low Equivalent Series Resistance (ESR) in order to minimize their insertion loss. Table D.7 summarizes the natural resonance frequencies (f_r) of the four loops and describes the capacitors used for each of the four loops, with their ESR and their Q_c values at 700 MHz.

Table D.6: Antenna dimensions

	Area [mm^2]	Diameter [λ]	$Q_{A,unload.}$
L_1	2000	1/8	74
L_2	1000	1/12	202
L_3	350	1/20	524
L_4	180	1/28	850

Table D.7: Antenna tuning comparison

	Natural f_r [MHz]	C [pF]	ESR [Ω]	Q_c
L_1	782	0.2	0.60	1895
L_2	1060	0.5	0.31	1516
L_3	1780	1.3	0.19	874
L_4	2690	2.7	0.09	935

5.2 Measurements

The four proposed loops have been built and are shown in Fig. D.12. The feed structure and the capacitor position are detailed in Fig. D.13. The feeding of the loops is made through a thin coaxial cable, which is carefully placed in order to avoid its participation into the radiation characteristics of the loops. As shown in Fig. D.14 the feeding cable does not carry any currents, therefore it is not part of the radiation pattern and the loops can be measured and compared fairly. The measured reflection coefficient of the four loops is shown in Fig. D.15. The plot shows shrinking bandwidth for loops of smaller areas, assessing of an enhancing Q_A. The four mock-ups have also been measured in anechoic chamber and their efficiency was computed with 3D pattern integration technique. Measured $Q_{A,load.}$ values and η_T are summarized in Table D.8. A significant drop in efficiency is observed as the size of the loop decreases. As a result the loss has increased 9 dB when the loop diameter has been reduced by a factor of 3.5. The R_{Q_A} drops from 0.95 for L1 to 0.34 for L4, accordingly with the significant loss increase.

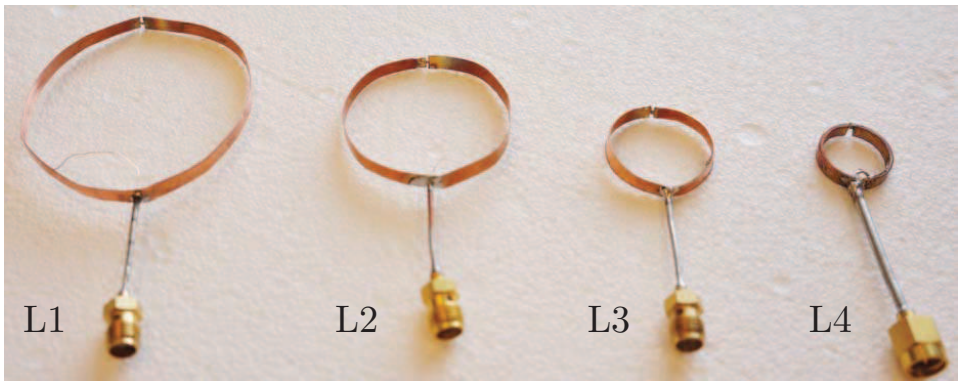

Fig. D.12: Loop antennas of four diffenrent sizes.

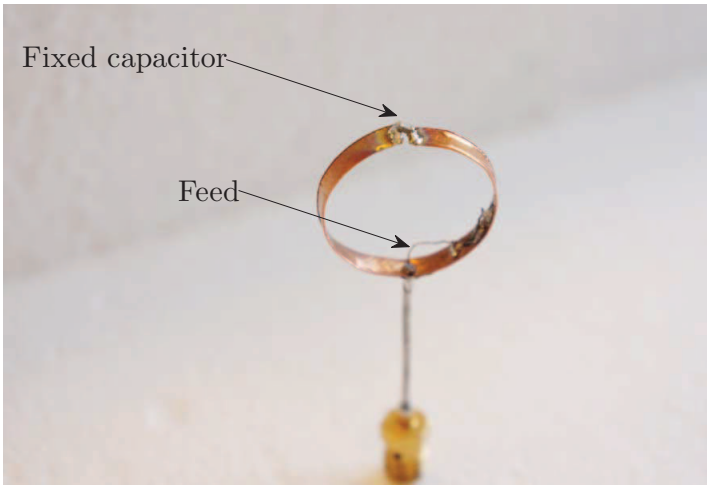

Fig. D.13: Structure of the antenna.

Table D.8: Efficiency comparison of the loops.

	$Q_{A,load.}$	R_{Q_A}	ESR_{Loss} [dB]	η_T [dB]
L_1	70	0.95	0.1	-0.7
L_2	195	0.96	0.2	-1.2
L_3	272	0.52	1.2	-4.6
L_4	292	0.34	2.6	-9.7

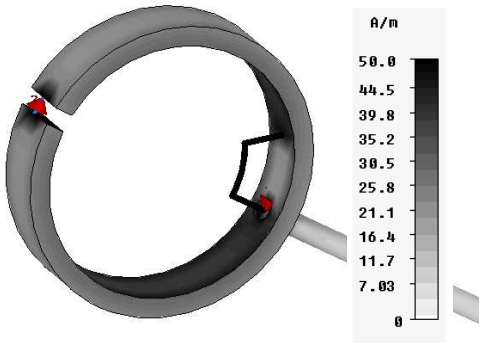

Fig. D.14: Current distribution on the loops.

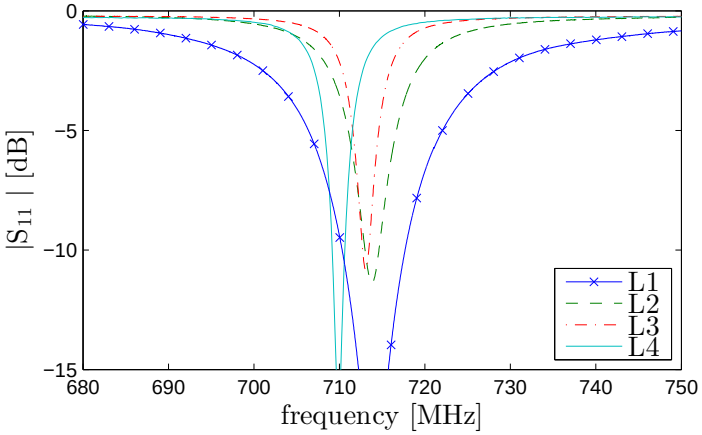

Fig. D.15: Measured absolute frequency response of the four loops.

5.3 Results

The measurements presented in this section have shown that, when dealing with ESAs, the efficiency drops significantly when the Q_A is increased. A lumped element, used to tune the resonance frequency of the antennas, carries only some of the loss. The source of loss can be separated into losses due to the ESR of the tuning component and conductive losses. The insertion loss due to the ESR of the tuning capacitors (ESR_{Loss}) can be computed at the simulation stage [34]. Its participation is summarized in Table D.8. Given the low ESR values of the capacitors, insertion loss is not the main source of loss. The capacitors are only responsible for a loss of 14 % to 27 %. The conductive losses play a significant role in the loss mechanism of small antennas, as testified by the measurements of L4. Indeed for a diameter of $\lambda/28$ and a R_{QA} of 0.34, the conductive loss is estimated to 7 dB. The component loss is only causes a loss of 2.6 dB, given its Q_c.

6 Thermal loss investigation

6.1 Analytical investigation

In order to appreciate the impact of the conductive loss into the total measured loss, a theoretical analysis of the radiation mechanism of the loop antennas is performed. Loop antennas can be analytically described [33] and their efficiency is calculated according to the following formulas:

$$\eta_r = \frac{R_r}{R_r + R_L} \tag{D.1}$$

$$R_r = 20\pi^2 \left(\frac{C}{\lambda}\right)^4 \tag{D.2}$$

$$R_L = \frac{C}{2\pi b}\sqrt{\frac{\omega\mu_0}{2\sigma}} \tag{D.3}$$

where η_r is the radiation efficiency, R_r is the radiation resistance, R_L is the loss resistance, C is the circumference of the loop, λ is the wavelength, b is the thickness of the wire, ω is the angular frequency, μ_0 is the permeability of free-space and σ the conductivity of metal. Eq. (2) is based on the small loop approximation and holds for a loop circumference up to 2 λ [33]. Therefore the above-formulations are valid in the presented investigation. Eq. (3) gives the R_L for a uniform current distribution. In the case of a sinusoidal distribution the values of R_L are halved. In the following, the efficiency is calculated according to Eq. (1) for the dimensions of L4. The values plotted for the conductivity of the copper ($\sigma = 5.8 \times 10^7$ S/m). Fig. D.16 shows the

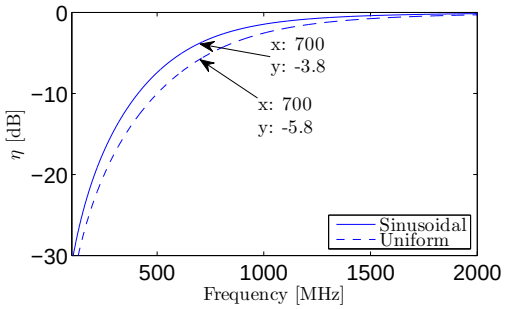

Fig. D.16: Analytical calculation of the efficiency of L4 for uniform and sinusoidal current distributions for copper.

theoretical efficiency of a copper loop antenna with the dimensions of L4, where the only source of loss is the metal conductivity. The plot shows both uniform and sinusoidal current distributions, knowing that the experimental distribution will be somewhere in between. These two curves are then the lower and the upper bounds of the conductive losses on the small loop. The curves show a loss between -3.8 dB and -5.8 dB only due to the copper in L4 at 700 MHz. The analysis was performed with a round wire of diameter 1.3 mm. However the mock-ups were made out of cylindrical sections of 1-by-3 mm, which can explain slight differences between measured and predicted copper loss. In order to further understand the efficiency drop in the loop antenna radiation mechanism, its radiation resistance and loss resistance are also plotted, see Fig. D.17. One can observe that as the frequency decreases, the radiation resistance is reduced at a faster rate than the loss resistance, leading to a degradation of the radiation efficiency. One can note that in the range 900-800 MHz − depending on the current distribution − the R_L and R_r curves cross in Fig. D.17, corresponding in Fig. D.16 to the start of a rapid efficiency degradation.

6.2 Experimental investigation

To further test the participation of conductive loss in the electrically small loop antennas, two more experiments were run. In the first one the ESR of the capacitor is changed in order to assess its impact on the η_T. In the second one the conductivity of the loop itself is changed and the degradation of η_T is appreciated.

Variation of the ESR

The loop antenna L4 is rebuilt with a capacitor exhibiting a higher ESR. In this new measurement the ESR of the capacitor is raised to 0.218 Ω. Therefore the Q_c has dropped to 386 and as a consequence the $Q_{A,load.}$ has dropped to 193. In the simulation

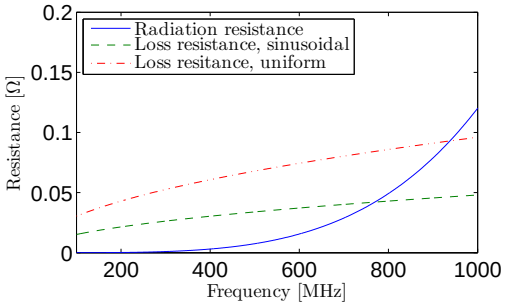

Fig. D.17: Analytical calculation of the radiation resistance and the loss resistance of L4 for uniform and sinusoidal current distributions on copper.

tool [34] the ESR_{Loss} is then estimated to -5.0 dB and the measured η_T is found to be -12.5 dB. This experiment shows a good agreement with the predicted loss (initially L4 was measured to have a loss of 9.7 dB and the new capacitor was estimated to further deteriorate the efficiency by 2.4 dB, leading to an estimated loss of 12.1 dB). Additionally this experiment shows the repeatability of the loss prediction and builds trust in the existence of conductive loss for reconfigurable-high-Q antennas.

Variation of the metal conductivity

The loop L4 is mocked-up in brass, aluminum, copper and silver. The conductivities of the materials are summarized in Table D.9. The loops are tuned with a 2.7 pF capacitor that has a Q of 935 at 700 MHz, as previously. A picture of the mock-ups is shown in Fig. D.18. The capacitor are placed in the gap of the loop and held with the forces of the metal, so that no soldering tin is used. On the silver antenna the feed line is also connected to the metal and held in place without using tin. In this way the losses due to the metal itself can be isolated. Fig. D.19 depicts the antenna structure minimizing the use of tin. The Fig. D.20 and D.21 show the frequency responses of the four loops. These responses are very narrow-band and the entering and exiting frequencies of the VSWR circle are rounded to 1 MHz. A more accurate way to compare the antennas is to use the $\mathrm{Q}_{A,load.}$ values, which are plotted in Fig. D.22. The measured $\mathrm{Q}_{A,load.}$ curves rank the antennas according to the conductivity values of the investigated metals. The loops are further measured in anechoic chamber and the radiation efficiencies are summarized in Table D.10. However the amount of current flowing into the capacitor is not identical for different metal conductivities, nor is the surface current concentration on the metallic ring. For this reason comparing the antennas including the tuning capacitor is a delicate task. One can rely on the simulation tool to calculate out the loss due to the ESR of the capacitor and conclude on the loss due to the metal (Metal_{Loss}). These results are shown in Table D.10 as well. Differences between silver and copper are expected to be

Fig. D.18: Loop antenna mock-ups with fixed capacitors.

very small as their difference in conductivity is also very small. The difference between the silver and the copper measurement reported in Table D.10 belongs to the chamber uncertainty.

Table D.9: Metal conductivities

Metal	σ [10^7 S/m]
Pure silver	6.30
Annealed copper	5.80
Aluminium 6060	3.12
Brass alloy	1.70

In order to fairly compare and determine the conductive loss of the antennas, an air-capacitor is built-in the antenna structure. The air-capacitor is made out of the same metal piece than the antenna and its dimensions are 5 × 8 mm with a spacing of 0.1 mm. The air-capacitor adds metal surface, however the envelope correlation (ρ) between simulated patterns is high (ρ=0.9985), which leads to the interpretation that the air-capacitor does act as a capacitor storing energy, rather than a radiator. A picture of the four air-capacitor mock-ups is shown in Fig. D.23. The frequency responses are shown in Fig. D.24 and D.25 and are comparable to the responses of the mock-ups with the chip capacitors. The $Q_{A,load.}$ curves are significantly increased by using air-capacitors, as shown in Fig. D.26. The radiation efficiencies of the four loop are summarized in Table D.11. The efficiency values classify the antennas accordingly to their conductivities and $Q_{A,load.}$ values. The antennas are now compared in a fair way and the results show high losses.

Fig. D.19: Antenna structure minimizing the use of tin.

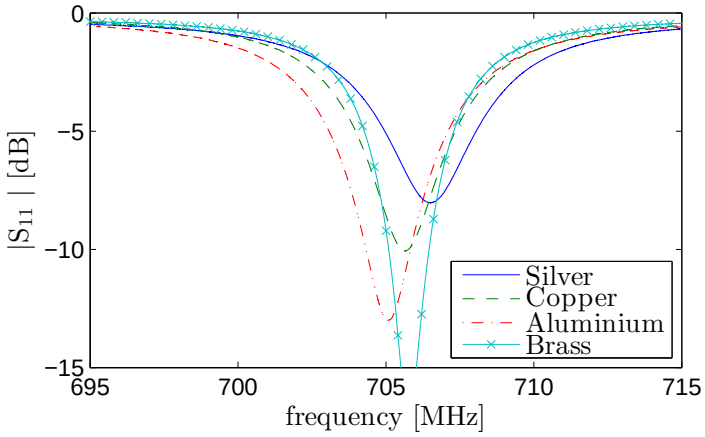

Fig. D.20: Magnitude of the frequency response of the loop antennas with fixed capacitors.

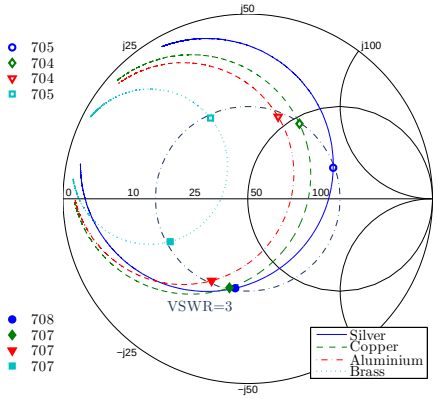

Fig. D.21: Complexe frequency response of the loop antennas with fixed capacitors.

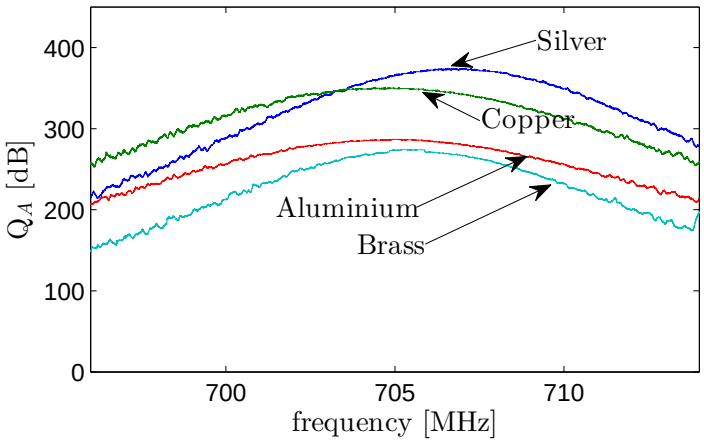

Fig. D.22: Q_A of the loop antennas with fixed capacitors.

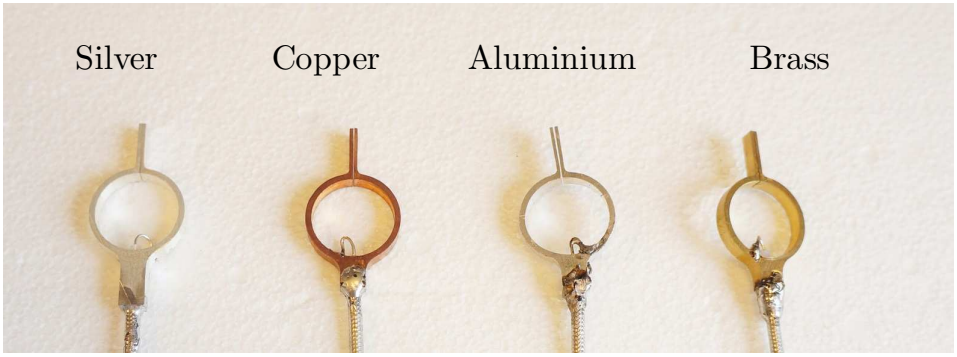

Fig. D.23: Loop antenna mock-ups with air capacitors.

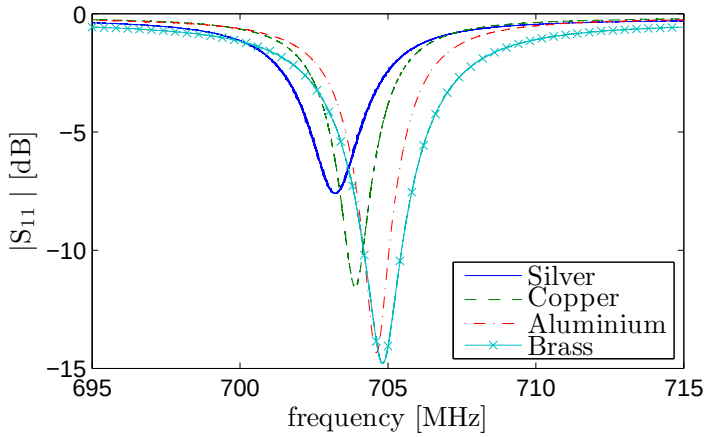

Fig. D.24: Magnitude of the frequency response of the loop antennas with air capacitors.

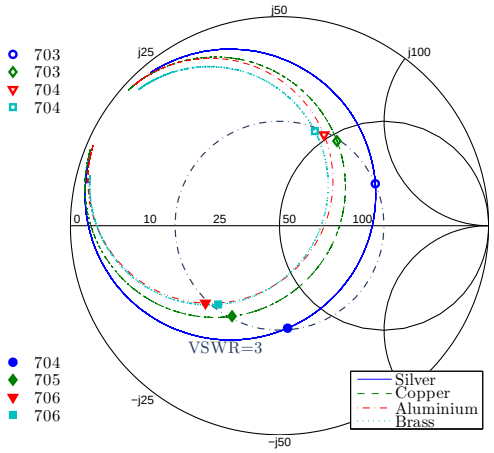

Fig. D.25: Complexe frequency response of the loop antennas with air capacitors.

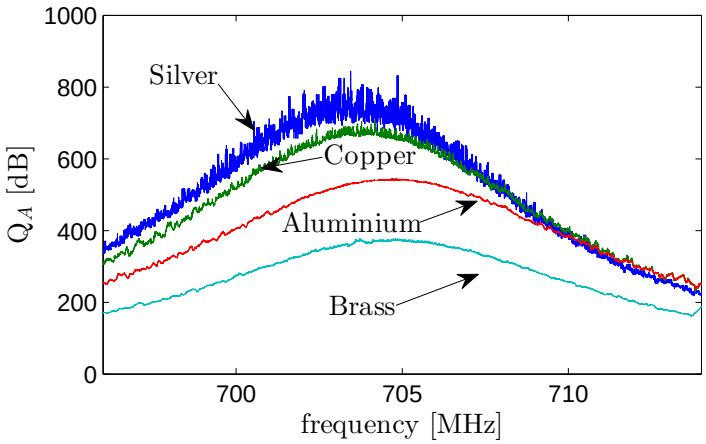

Fig. D.26: Q_A of the loop antennas with air capacitors.

Table D.10: Radiation efficiency of the loop antennas with fixed capacitors

Metal	η_r	ESR_{Loss} [dB]	Metal_{Loss} [dB]
Silver	-10.0	2.81	7.2
Copper	-9.8	2.68	7.1
Aluminum	-11.5	2.53	9.1
Brass	-10.9	2.07	8.9

Table D.11: Radiation efficiency of the loop antennas with air capacitors

Metal	η_r
Silver	-7.8
Copper	-8.2
Aluminum	-8.7
Brass	-10.3

6.3 Results

The conductive loss of the ESA investigated in this section − tuned from 2.7 GHz to 700 MHz, in pure silver, and with an air-capacitor − is -7.8 dB. This investigation shows that even with the best material and without component loss or soldering tin in high current locations, the efficiency of tunable antennas is limited by its conductive loss.

7 Summary and discussion

Section 3 presented a promising architecture with two independent and tunable chains for RX and TX on a candy-bar phone, addressing the need for broad bandwidths required by 4G. The design comprised high-Q ESA and lumped elements that resulted in a loss of 5 dB at 700 MHz. The results of this section raised the loss issue for tunable high-Q antennas. The main questions are whether high-Q antennas are necessarily lossy, and what are the sources of loss. Component loss certainly is one of them but thermal loss may also play a significant role.

Section 4 presented an electrically larger design for high-Q antennas. This design has shown that high-Q antennas are not necessarily lossy antennas, as long as they are large enough. The antenna with a loaded Q_A of 225 exhibited a loss of -2 dB at 700 MHz for a 300 × 300 mm ground plane.

Section 5 showed that there is an intrinsic loss for tunable ESAs. Even with the best conductor available nowadays, the antenna exhibited a thermal loss of -7.8 dB, when

tuned from 2.7 GHz to 700 MHz. This tuning range is the spread of frequencies that LTE shall cover so far [31]. Conductive loss plays a major role in tunable high-Q antennas.
Moreover presenting three antenna types throughout the loss investigation also raised the challenge of comparability of antennas. Size-wise estimating the radiating surface is a delicate task. The presence of a GP and its participation blur the antenna volume definition. However it has been considered that in the first design (Section 3) the 100 $\times$ 40 mm^2 GP being the main radiator at 700 MHz, the antenna volume is given by the GP ($\lambda/4$). In the second design (Section 4) the patch is the main radiator, therefore the antenna volume is determined by the length ($\lambda/2$) and the height of the patch. The last design (Section 5) does not include a GP, therefore the antenna volume is simply the volume occupied by the loop. The antennas can be compared in that way. Another system that can compare antennas in a more straightforward way is the use of R_{Q_A}, as introduced in this paper. It directly compares the $Q_{A,unload.}$ to the $Q_{A,load.}$. It relies on the radiation characteristics of the antennas and gives a clue on the amount of loss to expect from the antenna design. Additionally antenna losses have to be compared and put into perspective of nowadays products in the market [35] and system architecture requirements.

8 Conclusion

In this paper the authors have chosen to compare three antenna types in order to understand the loss mechanism of tunable ESAs. The source of loss is two-fold: the components used in the antenna structure and the conductivity of the metal. In order to improve the component loss one can use better components, with low-ESR. However engineers are limited by the available components on the market and the maximum allowed size on the board, or on the antenna. The conductive loss is difficult to predict, and to compensate for. It is significant for antennas with a very small volume, and dramatically increases as they are tuned down in frequency. Its behavior increases exponentially when the loss resistance curve against frequency crosses the radiation resistance curve. This loss mechanism limits how much an antenna can be tuned away from its natural resonance frequency and opens the door for new manufacturing materials offering higher conductivities.

References

[1] 3GPP TS 36.101, “LTE; Evolved Universal Terrestrial Radio Access (E-UTRA); User Equipment (UE) radio transmission and reception,” p. V11.3.0 Realease 11, 2013.

[2] R. G. Vaughan and J. B. Andersen, "Antenna diversity in mobile communication," *IEEE Trans. Veh. Technol.*, vol. 36, no. 4, pp. 149–172, 1987.

[3] R. F. Harrington, "Effect of Antenna Size on Gain, Bandwidth, and Efficiency," *Journal of Research of the National Bureau of Standards- D. Radio Propagation*, vol. 64D, no. 1, pp. 1–12, 1960. [Online]. Available: http://archive.org/details/jresv64Dn1p1

[4] K. R. Boyle and P. J. Massey, "Nine-band Antenna System for Mobile Phones," *Electronics Letters*, vol. 42, no. 5, pp. 5–6, 2006.

[5] P. Ciais, R. Staraj, G. Kossiavas, and C. Luxey, "Compact internal multiband antenna for mobile phone and WLAN standards," *Electronics Letters*, vol. 40, no. 15, pp. 3–4, 2004.

[6] I. Strip, S.-b. Wwan, Y.-l. Ban, C.-l. Liu, J. L.-w. Li, and R. Li, "Small-Size Wideband Monopole With Distributed Mobile Phone," *IEEE Antennas and Wireless Propagation Letters*, vol. 12, pp. 7–10, 2013.

[7] A. Cihangir, F. Ferrero, C. Luxey, G. Jacquemod, and P. Brachat, "A Bandwidth-Enhanced Antenna in LDS Technology for LTE700 and GSM850 / 900 Standards," in *European Conference on Antennas and Propagation (EUCAP)*, no. Eucap, 2013, pp. 2706–2709.

[8] B. K. Lau, J. r. B. Andersen, L. Fellow, G. Kristensson, S. Member, and A. F. Molisch, "Impact of Matching Network on Bandwidth of Compact Antenna Arrays," *IEEE Transactions on Antennas and Propagation*, vol. 54, no. 11, pp. 3225–3238, 2006.

[9] J. Ilvonen, P. Vainikainen, R. Valkonen, and C. Icheln, "Inherently non-resonant multi-band mobile terminal antenna," *Electronics Letters*, vol. 49, no. 1, pp. 11–13, Jan. 2013.

[10] J. Villanen, J. Ollikainen, and P. Vainikainen, "Coupling Element Based Mobile Terminal Antenna Structures," *IEEE Transactions on Antennas and Propagation*, vol. 54, no. 7, pp. 2142–2153, 2006.

[11] A. Andújar, S. Member, J. Anguera, S. Member, and C. Puente, "Ground Plane Boosters as a Compact Antenna Technology for Wireless Handheld Devices," *Antennas and Propagation, IEEE Transactions on*, vol. 59, no. 5, pp. 1668–1677, 2011.

[12] F. Sonnerat, R. Pilard, F. Gianesello, F. L. Pennec, C. Person, and D. Gloria, "Innovative LDS Antenna for 4G Applications," in *European Conference on Antennas and Propagation (EUCAP)*, no. Eucap, 2013, pp. 2696–2699.

[13] H. Li, Y. Tan, B. K. Lau, Z. Ying, and S. He, "Characteristic Mode Based Tradeoff Analysis of Antenna-Chassis Interactions for Multiple Antenna Terminals," *IEEE Transactions on Antennas and Propagation*, vol. 60, no. 2, pp. 490–502, Feb. 2012.

[14] H. Li, S. Member, B. K. Lau, S. Member, and Z. Ying, "Decoupling of Multiple Antennas in Terminals With Chassis Excitation Using Polarization Diversity , Angle Diversity and Current Control," *IEEE Transactions on Antennas and Propagation*, vol. 60, no. 12, pp. 5947–5957, 2012.

[15] H. A. Wheeler, "Fundamental Limitations of Small Antennas," *Proceedings of the I.R.E.*, vol. 35, no. 12, pp. 1479–1484, 1947.

[16] L. J. Chu, "Physical Limitations of Omni-directional Antennas," *Journal of Applied Physics*, vol. 19, no. 64, pp. 1163–1175, 1948.

[17] R. C. Hansen, "Fundamental limitations in Antennas," *Proceedings of the IEEE*, vol. 69, no. 2, pp. 170–182, 1981.

[18] J. S. McLean, "A re-examination of the fundamental limits on the radiation Q of electrically small antennas," *IEEE Transactions on Antennas and Propagation*, vol. 44, no. 5, p. 672, May 1996.

[19] J. R. James, A. J. Schuler, and R. F. Binham, "Reduction of antenna dimensions by dielectric loading," *Electronics Letters*, vol. 10, no. 13, pp. 263–265, 1974.

[20] G. S. Smith, "Efficiency of Electrically Small Antennas Combined with Matching Networks," *IEEE Transactions on Antennas and Propagation*, vol. 25, no. 3, pp. 369 – 373, 1977.

[21] E. E. Altshuler and L. Fellow, "Electrically Small Self-Resonant Wire Antennas Optimized Using a Genetic Algorithm," *IEEE Transactions on Antennas and Propagation*, vol. 50, no. 3, pp. 297–300, 2002.

[22] S. R. Best, "The Performance Properties of Electrically Antennas," *IEEE Antennas and Propagation Magazine*, vol. 47, no. 4, pp. 13–27, 2005.

[23] C. S. Lee and K.-h. Tseng, "Radiation Efficiency of Electrically Small Microstrip Antennas With Width Discontinuities," *IEEE Transactions on Antennas and Propagation*, vol. 53, no. 2, pp. 871–873, 2005.

[24] A. Galehdar, D. V. Thiel, and S. G. O. Keefe, "Antenna Efficiency Calculations for Electrically Small, RFID Antennas," *IEEE Antennas and Wireless Propagation Letters*, vol. 6, no. 2, pp. 156–159, 2007.

[25] M. Randall, A. Lewis, A. Galehdar, and D. Thiel, "Using Ant Colony Optimisation to Improve the Efficiency of Small Meander Line RFID Antennas," in *Third IEEE International Conference on e-Science and Grid Computing*, 2007, pp. 345–351.

[26] A. Galehdar, S. Member, D. V. Thiel, S. Member, and S. G. O. Keefe, "Tapered Meander Line Antenna for Maximum Efficiency and Minimal Environmental Impact," *IEEE Antennas and Wireless Propagation Letters*, vol. 8, pp. 244–247, 2009.

[27] A. D. Yaghjian, S. R. Best, and S. Member, "Impedance , Bandwidth , and Q of Antennas," *IEEE Transactions on Antennas and Propagation*, vol. 53, no. 4, pp. 1298–1324, 2005.

[28] S. Caporal, D. Barrio, M. Pelosi, G. F. Pedersen, and A. Morris, "Challenges for Frequency-Reconfigurable Antennas in Small Terminals," in *IEEE Vehicular Technology Conference (VTC Fall)*, 2012, pp. 1–5.

[29] A. James, "Reconfigurable Antennas for Portable Wireless Devices," *IEEE Antennas and Propagation Magazine*, vol. 45, no. 6, pp. 148–154, 2003.

[30] Computer Simulation Technology (CST) http://www.cst.com, "CST Microwave Studio," 2012.

[31] 3GPP Technical Report, "Feasibility study for Further Advancements for E-UTRA (LTE-Advanced) - Specification 36.912 - Release 11," 2012. [Online]. Available: http://www.3gpp.org/ftp/Specs/html-info/36912.htm

[32] G. S. Smith, "Chapter 5: Loop Antennas," in *Antenna Engineering Handbook*, 2nd ed. New-York: McGraw-Hill Book Co., 1984, pp. 69–109.

[33] C. A. Balanis, "Chapter 5: Loop Antennas," in *Antenna theory: Analysis and design*, 3rd ed. Hoboken, New Jersey: John Wiley & Sons, 2005, pp. 231–281.

[34] Agilent EEsof EDA, "Advanced Design System (ADS)."

[35] S. Caporal, D. Barrio, and G. F. Pedersen, "Correlation Evaluation on Small LTE Handsets," in *Vehicular Technology Conference (VTC Fall)*, 2012, pp. 1–4.

Paper E

The Effect of the User's Body on High-Q and Low-Q Planar Inverted F Antennas for LTE Frequencies

Caporal Del Barrio, S. ; Pelosi, M. ; Franek, O. and Pedersen, G.F.
[1]Section of Antennas, Propagation and Radio Networking (APNet), Department of Electronic Systems, Faculty of Engineering and Science, Aalborg University, DK-9220, Aalborg, Denmark, {scdb, mp, gfp}@es.aau.dk

The paper has been published in the
75 th Vehicular Technology Conference (VTC Spring), 6-9 May, 2012,
Yokohama, Japan, pp. 1–4.

The layout has been revised.

Abstract

The influence of the user's body degrades small antenna performances. This paper investigates the detuning and the losses on high-Q planar antennas for small devices due to user proximity. The results at low frequencies for the Long Term Evolution (LTE) standard are compared to the results for a low-Q antenna. Two hand grips are studied and combined to a SAM (Specific Anthropomorphic Mannequin) phantom. It is shown that using the high-Q antennas the loss due to the mismatch is reduced but the absorption loss is increased.

1 Introduction

Today's antenna designers have to deal with size challenges while building antennas for hand-held devices. The phone market is evolving towards smaller and slimmer designs which are contradictory with antenna limitations for more bandwidth at lower frequencies, in a limited space [1]. Another major constraint that antenna designers have to deal with for portable devices is the interaction with the user's body. The hand effect has been investigated, mainly in [2], [3] and [4], and it has been found to detune the resonance frequency in an inductive way. The proximity of the user's head further disturbs the antenna near fields , causing more degradation of the resonance characteristics.

The Long Term Evolution (LTE) frequency spectrum extends mobile communication channels on 23 bands over frequencies between 700 MHz and 2.7 GHz. One way to cover the whole spectrum is to use tunable antennas - also called reconfigurable antennas. These antennas exhibit a narrow instantaneous bandwidth that can be tuned to resonate at different frequencies. In this sense they cover a large bandwidth.

Tuning techniques can refer to PIN diodes switches, Field Effect Transistors (FET) or Micro-Electro-Mechanical Systems (MEMS) switches among others. In all cases these mechanisms are used to change the current path on the antenna and introduce an additional reactance that will change the resonance frequency of the resulting antenna. In the following a variable capacitor connecting the antenna element and the Ground Plane (GP) is used.

This paper presents the effect of the user's body on a tunable Planar Inverted F-Antenna (PIFA) for frequencies between 700 MHz and 2 GHz. Low-Q and high-Q antennas are compared with respect to the detuning in frequency (Δf_r), the Absorption Loss (L_A) and the Mismatch Loss (L_M). Different hand grips are studied and further added to a SAM phantom. Section II presents the simulation parameters and the models used for the analysis. The results are presents in Section III and conclusions are disclosed in Section IV.

2 Simulation Parameters

2.1 Method

The following simulations are performed with a Finite-Difference Time-Domain (FDTD) software, using 1 mm space step size and an energy-based termination criterion. The handset was modeled with Perfect Electric Conductor (PEC) for the GP and the PIFA. The housing of the handset is simulated with a non lossy plastic : the relative permittivity ϵ_r is set to 3 and the conductivity σ to 0 S/m, in order to exclusively take into consideration the effect of the user's body. A capacitor is used to tune the antenna resonance frequency. The capacitor is also simulated as ideal, that is to say without an Equivalent Series Resistance (ESR).

2.2 Quality Factor (Q)

The investigated antennas are compared using their Q. The Q value that is considered hereafter is the Q for a perfectly matched antenna response at its resonance frequency. The antenna Q refers to the matched VSWR Q and it relates to the Matched Bandwidth (MBW) as shown in eq. 1 [5]:

$$Q_{fr} = \frac{2\sqrt{\beta}}{MBW_{fr}} \text{ , with } \sqrt{\beta} = \frac{VSWR - 1}{2\sqrt{VSWR}}, \tag{E.1}$$

where the characteristic impedance of the antenna is perfectly matched to the 50 Ω antenna's feed point resistance at the tuned frequency.
As tunable antennas are narrow-band in each operating frequency they are tuned to, their Q is rather high. Moreover the further away the antenna is tuned from its original resonance frequency, the higher its Q gets. This phenomenon is due to over-coupling with the GP, which resonates around 1.2 GHz when 100 mm long.

2.3 Antenna Models

The hand-held device used throughout the simulations is a candy-bar type, with a GP of dimensions 40 × 100 × 2 mm^3. Firstly a dual band PIFA is designed to operate at 900 MHz and 1800 MHz, covering the GSM bands.The antenna occupies a volume of 40 × 22 × 5 mm^3 and has a Q equal to 16. The antenna geometry is detailed in [6]. A lossless capacitor is placed between the PIFA and the GP. As there is no ESR modeled with the capacitor, its position only influences the frequency shift that can be obtained and the antenna Q. The distance between the feeding point and the tuning point is arbitrarily set to 20 mm. This set-up describes the first antenna model (A1), with the capacitor in the off-state.
Secondly the Q of this antenna is increased by reducing the distance between the PIFA and the Ground Plane (GP). This is the geometry of the second antenna model (A2).

Table E.1: Antenna Model Geometries

Model	Volume occupied	Capacitance	Q
A1	40 x 22 x 5 mm^3	OFF	16
A2	40 x 22 x 2 mm^3	OFF	56
A3	40 x 22 x 2 mm^3	1 pF	360

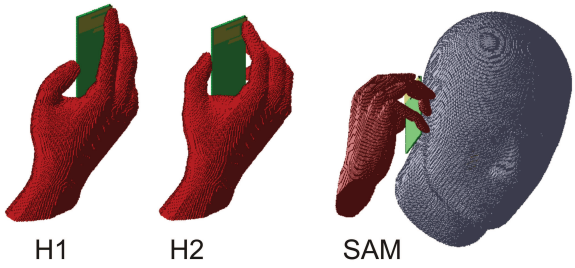

Fig. E.1: Phantoms [7].

The initial distance separating the PIFA from the GP is reduced from 5 mm to 2 mm, which results in a Q for A2 raised to 56. Further the high-Q antenna is tuned to the LTE-700 band by switching to the on-state of the capacitor, where it provides a capacitance equal to 2 pF. The resultant antenna (A3) resonates at 720 MHz and has a Q of 360.
A1 will be denoted as a low-Q antenna whereas A2 and A3 will be high-Q antennas. The antenna geometries and characteristics are summarized in TABLE I. As the whole antenna structure is modeled as a PEC and the lumped component and phone housing are lossless, the source of all losses can only be in the lossy dielectric material used to model the user's hand and head.

2.4 Phantoms

The investigation uses realistic phantom head and hands, with a relative permittivity of the body tissue $\epsilon_r = 36$ and a conductivity $\sigma = 0.8$ S/m at 900 MHz [2]. Two hand grips are used : the "firm" grip (H1) and the "soft" grip (H2). These two grips differ by the distance between the palm and the ground plane. In the "firm" grip case the center of the palm is at a distance of 20 mm from the PCB whereas in he "soft" grip the distance is twice larger. Fig. E.1 shows the two grip models and the SA. In both grips, H1 and H2, the index finger is located in the antenna radiation area and in contact with the phone housing. Therefore it is responsible for the largest degradation of the antenna performance. The casing of the phone is not shown in the figures as it would mask the

Table E.2: Distances Separating Phantoms and Radiating Elements [mm]

Antenna	$D_{GP,F}$	$D_{GP,H1}$	$D_{GP,H2}$	$D_{GP,SAM}$
A1	9	20	40	5
A2 and A3	6	17	37	8

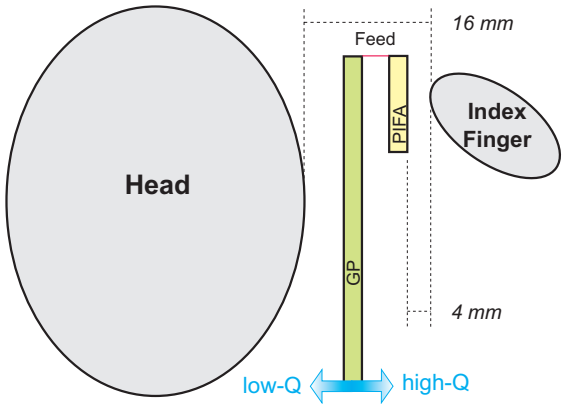

Fig. E.2: Simulation set-up.

antenna description. In order to be able to compare the different antenna models the distance separating the SAM and the index finger in fixed for all the simulations and cases.

2.5 Simulation Set-up

In the proposed PIFA design the height of the antenna varies with the Q of the antenna. The higher the Q the smaller the height. It is known that most of the degradation due to the user's hand comes from the index finger, which is placed over the radiating element. In the proposed set-up the distance separating the index finger from the radiating element is fixed for all scenarios: 4 mm. In order to have comparative interactions from the index finger and the SAM a constant distance separates them: 16 mm. The set-up is shown in Fig. E.2. Therefore the element that is "moving" to modify the antenna Q is indeed the GP. The GP thickness is 2 mm. The evolution of the antenna performances, with respect to its Q, considering the GP location is relevant since it is the main radiator at the low frequencies. To sum-up, when the Q gets higher the distance between the palm and the GP is reduced and the distance between the GP and the SAM is increased. TABLE II presents the set-ups for every grip and antenna model. The distances between the GP and the index finger, the GP and the palm of H1, the

GP and the palm of H2 and the GP and the SAM are denoted $D_{GP,F}$, $D_{GP,H1}$, $D_{GP,H2}$ and $D_{GP,SAM}$ respectively.

3 Simulation Results

The three above-described antennas are simulated. The user's effect on the return loss is shown in Fig. E.3 and Fig. E.4. It is further analyzed, with respect to the free space (FS) case in Tables III-V. The detuning (Δf_r), the bandwidth at -6 dB (BW) and the total loss (L_T) are compared to each other.
On the one hand the distance of the GP to the palm changes with the antenna model and affects differently the radiation, since at low frequencies the GP is the main radiator. On the other hand the distance of the GP to the SAM changes with the antenna model as well, which further disturbs the radiation. The position of the finger is kept unchanged with respect to the antenna throughout the simulations. The simulation results will show if when the GP is closer to the hand but further from the head the effect of the user on the antenna performances is: unchanged, higher or lower. Furthermore this results will compare the user's effect on high-Q and low-Q antennas, thus on narrow-band and wide-band antennas.
As expected the "firm" and the "soft" grip disturb the antennas in the same way, but not up to the same level. In all cases the disturbance introduced by H1 is much larger than the degradation caused by H2. Two cases are studied: hand only and hand with SAM. The phone is placed beside the SAM and the hand in order to simulate the use case: "talk-mode". The SAM is then removed in order to isolate the effect of the hand alone.

3.1 Frequency Detuning

Low-Q case

In the low band A1 suffers an important detuning and mismatch from the addition of the user's hand and head. With H1 alone the antenna resonance is detuned more than 70 MHz whereas with H2 alone the detuning is reduced to 20 MHz. This difference is due to the tighter grip design that H1 exhibits. Mismatch to the 50 Ω feed line is due to the lossy material used to simulate the user's hand. Nevertheless the reflection coefficient is still match to an acceptable value: below the usual -6 dB threshold. The SAM adds further detuning on the case with H2, lowering the resonance frequency 35 MHz off the original one.
In the high band both grips and SAM detune the resonance frequency in the same way and to the same level.

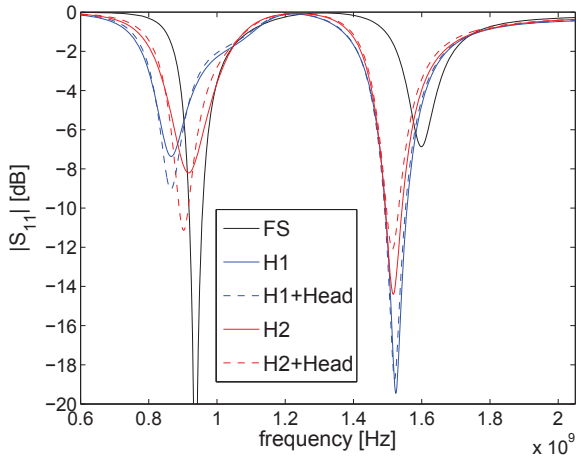

Fig. E.3: |S11| parameter of the low-Q antenna with user's effect.

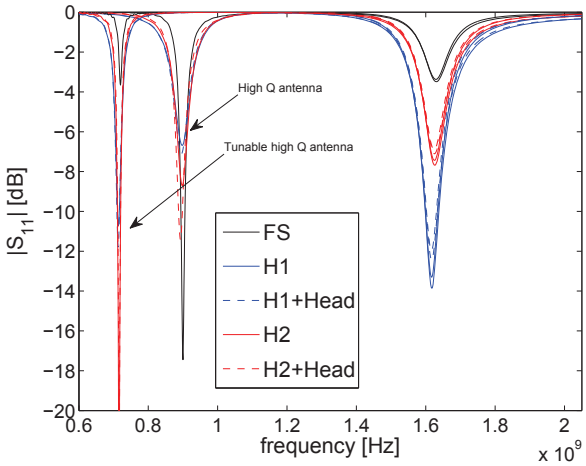

Fig. E.4: |S11| parameter of the high-Q antennas with user's effect.

High-Q cases

The detuning is significantly reduced for both high-Q antenna models, A2 and A3. The proposed high-Q designs experience in the low band a detuning of only 2 to 4 MHz for both grips, and 4 to 7 MHz with the SAM model. The high band resonance frequency is also almost unaffected by the addition of the user. Additionally for the high resonance frequency, the matching is improved and the bandwidth enlarged.

Tuned High-Q case

When the high-Q antenna is tuned to the LTE-700 band, its impedance response is above the conventional limit of -6 dB. However with the user interaction the matching is improved and the bandwidth enlarged. Even though the design seemed to not work in such low frequencies the user interaction actually helps without detuning. The tuning component does not degrade the observed high-Q performances with respect to detuning and matching.

3.2 Absorption and Mismatch Losses in the Low Band

The performances of the low-Q antenna, the high-Q antenna and the tuned high-Q antenna are compared in the TABLE III-V, with respect to losses. A1 and A2 have different locations, with respect to the user, and different Q values. A2 and A3 are placed in the same locations and only the Q is increased, due to the 2 pF capacitor.

Losses due to grips

The Absorption Loss (L_A) due to H1 increases from 4.7 dB to 8.8 dB, from the lowest antenna Q to the highest. As from A1 to A2 the GP is placed 3 mm closer to the palm, higher losses are expected. Between A2 with a Q=56 and A3 with a Q=360 the L_A increase is not significant, the jump occurs between A1 with a Q=16 and A2. With the other grip H2, the L_A level is similar to the one with H1 for the low-Q model. The loss increases significantly between the antenna models A2 and A3. In general H2 absorbs less power than H1 because of its looser grip.

Losses due to SAM and the grips

In the low-Q antenna model the L_A is unchanged whether it is the "firm" or the "soft" grip that is used as long as the SAM is included in the simulation. The user's head accounts for 5 dB of the total losses (9.8 - 4.7 or 9.8 - 4.3 , see TABLE III). In the high-Q designs the absorption loss due to the user (SAM and hand) is increased. However the participation of the SAM is actually decreased to $\sim$3 dB as the distance between the GP and the SAM is increased and the Q gets higher (11.4 - 8.3 or 11.5 - 8.8, see TABLE IV and TABLE V). The total absorption loss due to the user with H1 is greater

Table E.3: User's Effect on the Low-Q Antenna A1

	FS	**H1**	**H1+SAM**	**H2**	**H2+SAM**
$\mathbf{f}_r$ **[MHz]**	937	866	865	917	902
$\Delta\mathbf{f}_r$ **[MHz]**	0	71	72	20	35
BW [MHz]	70	64	64	87	81
$\mathbf{L}_A$ **[dB]**	0.0	4.7	9.8	4.3	9.8
$\mathbf{L}_M$ **[dB]**	0.0	2.3	2.5	0.8	0.9
$\mathbf{L}_T$ **[dB]**	0.0	7.0	12.3	5.1	10.7

Table E.4: User's Effect on the High-Q Antenna A2

	FS	**H1**	**H1+SAM**	**H2**	**H2+SAM**
$\mathbf{f}_r$ **[MHz]**	900	898	895	898	893
$\Delta\mathbf{f}_r$ **[MHz]**	0	2	5	2	7
BW [MHz]	20	20	24	30	30
$\mathbf{L}_A$ **[dB]**	0.0	8.3	11.4	4.8	9.6
$\mathbf{L}_M$ **[dB]**	0.0	1.0	0.9	0.6	0.5
$\mathbf{L}_T$ **[dB]**	0.0	9.3	12.3	5.4	10.1

than 11 dB and there is not any degradation due to the further increase of the Q (that is to say to the increase of the capacitance of the tuning component). In the soft grip case H2 the total absorption loss increases only 1 dB between A2 and A3.

Total Loss (L_T)

In the low-Q design the Mismatch Loss (L_M) is higher than in the high-Q designs and the L_A is smaller than in the high-Q designs. Nevertheless in the talk mode (SAM and hand) the total loss is equal to 12 dB for H1 and SAM on the three antenna models, and to ∼11 dB for H2. The effect of the hand alone exhibits the L_T 2 dB higher for the high-Q designs compared to the low-Q design with H1. Moreover the lumped component does not affect the losses with H1, up to 9 dB. In the case of H2 alone, 5 dB total loss are observed in both A1 and A2. They are increased to 7 dB for the highest antenna Q model.

Table E.5: User's Effect on the tuned High-Q Antenna A3

	FS	**H1**	**H1+SAM**	**H2**	**H2+SAM**
$\mathbf{f}_r$ **[MHz]**	720	714	713	716	716
$\Delta\mathbf{f}_r$ **[MHz]**	0	4	7	4	4
BW [MHz]	0	20	20	15	15
$\mathbf{L}_A$ **[dB]**	0.0	8.8	11.5	7.0	10.8
$\mathbf{L}_M$ **[dB]**	0.0	0.6	0.7	0.2	0.2
$\mathbf{L}_T$ **[dB]**	0.0	9.4	12.2	7.2	11.0

4 Conclusion

In this paper high-Q and low-Q antennas where designed and compared with respect to their interaction with the user. The simulated antenna is a PIFA and its surface is unchanged from one model to another. The Q is modified by first reducing the height of the PIFA with respect to the GP, and then increasing the value of the tuning capacitor. Reducing the height of the PIFA of only 3 mm results in a significant increase of the Q. Two hand grips are compared, one is holding the phone tight and the other is more loose. The simulations with only a hand isolate the effect of the user's hand alone, as it is responsible for most of the degradation of the antenna performance. A SAM is further added to the simulations to reproduce a "talk mode" operation of the device.
It is observed that the high-Q antennas have a very reduced detuning when held, and in close proximity of the user - in both low and high bands. The L_M of the high-Q antennas is below 1 dB. Nevertheless the total loss is not improved because the absorption loss in the high-Q models is higher than in the low-Q model. With H1 the L_A is significantly higher for the high-Q antennas. This results in quasi-equal total loss for the three antenna models in all simulation environments: 11 to 12 dB of total loss in "talk mode" for both grips and three different antenna Q, from 16 to 360.
The response of a tunable high-Q antenna for the low LTE frequency bands is investigated when the user is located in the close proximity. The comparison with a typical low-Q antenna shows that the detuning is reduced by 95%, and the mismatch loss does not exceed 1 dB for high-Q antennas. However, the absorption loss is larger; hence the total loss remains similar in all cases.

References

[1] R. F. Harrington, "Effect of Antenna Size on Gain, Bandwidth, and Efficiency," *Journal of Research of the National Bureau of Standards- D. Radio Propagation*, vol. 64D, no. 1, pp. 1–12, 1960. [Online]. Available: http://archive.org/details/jresv64Dn1p1

[2] M. Pelosi, O. Franek, M. Knudsen, M. Christensen, and G. Pedersen, "A grip study for talk and data modes in mobile phones," *Antennas and Propagation, IEEE Transactions on*, vol. 57, no. 4, pp. 856–865, 2009.

[3] C.-H. Li, E. Ofli, N. Chavannes, and N. Kuster, "Effects of hand phantom on mobile phone antenna performance," *Antennas and Propagation, IEEE Transactions on*, vol. 57, no. 9, pp. 2763–2770, 2009.

[4] J. Ilvonen, O. Kivekas, J. Holopainen, R. Valkonen, K. Rasilainen, and P. Vainikainen, "Mobile terminal antenna performance with the user's hand: Effect of antenna dimensioning and location," *Antennas and Wireless Propagation Letters, IEEE*, vol. 10, pp. 772–775, 2011.

[5] A. D. Yaghjian, S. R. Best, and S. Member, "Impedance , Bandwidth , and Q of Antennas," *IEEE Transactions on Antennas and Propagation*, vol. 53, no. 4, pp. 1298–1324, 2005.

[6] S. Del Barrio, M. Pelosi, O. Franek, and G. Pedersen, "Tuning range optimization of a planar inverted f antenna for the lte low frequency bands," in *Vehicular Technology Conference (VTC Fall), 2011 IEEE*, 2011, pp. 1–5.

[7] M. Pelosi, O. Franek, M. Knudsen, G. Pedersen, and J. Andersen, "Antenna proximity effects for talk and data modes in mobile phones," *Antennas and Propagation Magazine, IEEE*, vol. 52, no. 3, pp. 15–27, 2010.

Paper F

Coupling element antenna with slot tuning for handheld devices at LTE frequencies

Caporal Del Barrio, S. ; Pelosi, M. ; Franek, O. and Pedersen, G.F.
[1]Section of Antennas, Propagation and Radio Networking (APNet), Department of Electronic Systems, Faculty of Engineering and Science, Aalborg University, DK-9220, Aalborg, Denmark, {scdb, mp, gfp}@es.aau.dk

The paper has been published in the
6th European Conference on Antennas and Propagation (EuCAP), 26-30 March, 2012, Prague, Czech Republic, pp. 3587–3590.

The layout has been revised.

Abstract

Tunable antennas are a promising way to overcome bandwidth limitations for the new communication standards. Since it is the chassis that resonates in the low frequencies, its tuning is pertinent and allows for more compact size designs. This paper proposes a coupling element based antenna. A reconfigurable slot is inserted in the ground plane in order to lower its resonance frequency. The tuning is done by a capacitor across the slot. It is shown that covering all frequencies between the 900-GSM band and the 700-LTE band can be achieved. The radiating structure also presents a resonance in the high LTE band which is unaffected by the tuning mechanism of the lower band. Moreover, the efficiency can be optimized by an analysis of the currents across the slot. The study also shows that holding the device does not lead to additional mismatch losses which will further improve the overall efficiency.

1 Introduction

A strong trend in the mobile telecommunication technology is to significantly decrease the size of the handsets. Miniaturization can be achieved by efficient designs as multi-band structures, high dielectric loading or non-resonant antennas [1], [2], [3], [4], [5], [6], [7]. The non-resonant antennas are designed in order to properly excite certain radiation modes of the ground plane rather than self resonance [8], [9], [10]. Their main advantage is to be low-volume and low-profile. Nevertheless separate matching circuitry has to be used to match the resulting antenna to the 50 Ω feed line at the desired resonance frequency. Thus a drawback of such technique is the losses introduced by the lumped components [6], [7], [11], especially for low frequencies as 700 MHz.
For the next Long Term Evolution (LTE) standard, the mobile terminals will need to operate in 23 frequency bands between 700 MHz and 2.6 GHz. Among other techniques, reconfigurability provides tuning over a wide range of frequencies without requiring additional space for the antenna. Slot antennas are a good candidate for compact tunable antennas and have the convenience of tuning the resonance frequency across the slot.
This paper presents a compact and simple reconfigurable antenna combining coupling elements and slot tuning techniques. In Section II, the geometry of the radiating structure is described. Simulated results are presented in Section III investigating the tuning range and influence of the tuning capacitor on the losses. Section IV presents the user's influence on the design. Finally conclusions are drawn in Section V.

2 Antenna Design

Even though the proposed design is based on a coupling element excitation, there is no external matching circuitry. A slot in the Ground Plane (GP) is used instead. This

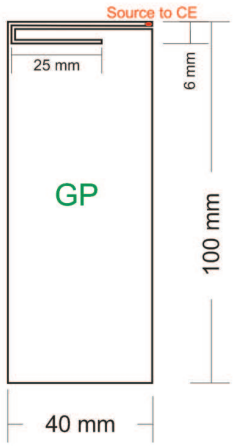

Fig. F.1: Ground plane geometry.

is done in order to lower the resonance frequency of the radiating structure preventing losses from lumped components, overall when the structure is being tuned.

2.1 Geometry

The GP size is 100×40 mm^2 and it has a resonance close to 1.1 GHz. These dimensions correspond to the ones of a typical "candy-bar" phone. A coupling element (CE) is placed at a distance of 2 mm above the GP. The CE is a square of 4x4 mm^2. A slot is inserted in the GP to lower the resonance frequency of the overall structure. The slot is not directly fed, the source is connected to the CE. The designed slot is an open-ended slot type since with the same physical length of the slot the resonant frequency can be doubled by opening one of its ends [12]. Additionally, the slot itself resonates which creates a second resonance covering the high LTE band around 2.6 GHz. The resulting dual band radiating structure is shown in Fig.1 and has a Quality factor (Q) of 26 at 1 GHz. Between the 700-LTE band and the 900-GSM band the coverage is ensured by a tuning mechanism. The resonance frequency is tuned towards lower values when the capacitance is increased.

2.2 Tuning

The slot in the GP is not fed by the source, therefore the currents running along the slot result from the coupling with the CE. The tuning capacitor is placed across the slot and in this configuration the currents running through the lumped component are expected to be small. This means that the losses due to the lumped component will be reduced,

when increasing the capacitance and thus tuning towards lower frequencies. Because losses are expected when the capacitance value increases, having low currents through the capacitor is important from an efficiency point of view. Nevertheless, the frequency shift ability is preserved and the tuning range wide. In order to achieve fine-tuning over the frequency bands, capacitance values below 1 pF are needed. The proposed design covers bands from 700-LTE to 900-GSM with 8 steps of 1/8 pF.

3 Simulations

3.1 Method

The described design was simulated with a Finite-Difference Time Domain (FDTD) method. Considering a uniform cubic lattice, a space step size of 1 mm was chosen, using perfectly matched layer absorbing boundary conditions. The Printed Circuit Board (PCB) and the CE were modeled as perfect electric conductors. The tuning capacitor was modeled as lossless.

3.2 Fields

Fig. 2 shows the **H** field magnitude normalized to 1 W on the chassis at 1 GHz. The scale is given in dBA/m so that the small variations of the field can be distinguished. From this plot it can be inferred that the tuning capacitor should be placed in a location close to the open end of the slot in order to minimize the currents running through it and therefore the losses due to the Equivalent Series Resistance (ESR) of the lumped component. However the frequency shift depends on the position of the capacitor as well. The lower the currents through it, the larger the shifts [13]. Hence, the tuning capacitor is placed at 15 mm from the open end of the slot on the PCB. The achievable tuning range is depicted in Fig. 3, also showing fine tuning between 1 GHz and 760 MHz.

3.3 Currents

The currents running through the capacitor vary with the capacitance value. In this section the currents will be calculated from the fields for different tuning stages and compared to one another. The goal is to see how much of the degradation of the efficiency is due to the tuning component, in both bands. For this reason the study focuses only on the first and the last tuning stages, i.e. 1/8 pF at 1 GHz and 1 pF at 760 MHz. The fields are simulated for a lossless component and the power loss will be calculated with an Equivalent Series Resistant (ESR). Since today's handsets transmit at a power between 1/4 W and 2 W [14] all values are normalized to 1 W input power hereafter.

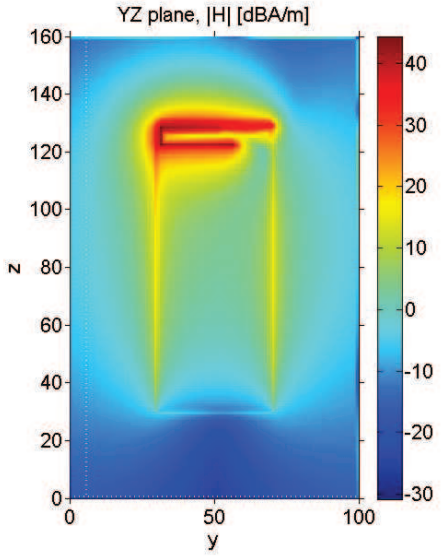

Fig. F.2: |**H**| field on the PCB at 1 GHz.

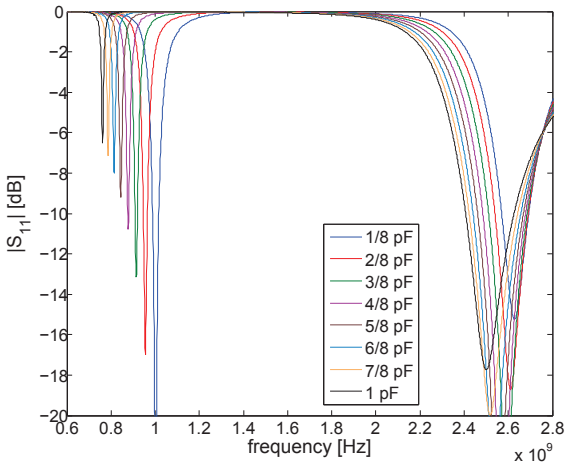

Fig. F.3: Tuning range of the proposed radiating structure.

High Band

For the first tuning stage the currents running through the 1/8 pF capacitor are :

Table F.1: Losses of the proposed antenna due to the tuning capacitor

	1/8 pF		**1 pF**	
$\mathbf{f}_r$	1 GHz	2.6 GHz	760 MHz	2.6 GHz
$\mathbf{P}_{IN}$ **[W]**	1	1	1	1
$\mathbf{P}_L$**[mW]**	2.2	0.5	350	7.8
η_r**[dB]**	$\ll$ -0.1	$\ll$ -0.1	-1.9	$\ll$ -0.1
$\mathbf{V}_{bd}$**[V]**	79	$\ll$ 0.1	190	$\ll$ 0.1

$$I_{C(1/8pF)} = 35 \text{ mA, at 2.6 GHz.}$$

At the last tuning stage the currents running through the 1 pF capacitor are :

$$I_{C(1pF)} = 140 \text{ mA, at 2.6 GHz.}$$

Low Band

In the case where the lower resonance frequency is tuned to 1 GHz with the 1/8 pF capacitor the currents through the capacitor are :

$$I_{C(1/8pF)} = 75 \text{ mA, at 1 GHz.}$$

Typical values of ESR for high-Q series with capacitances below 1 pF are in the order of 0.4 ohms [15], which leads, for a practical case of 1 W input power, to a power loss in the capacitor of:

$$P_{L(1/8pF)} = 2.2 \text{ mW, at 1 GHz.}$$

At 750 MHz, when the lower resonance frequency is tuned with the 1 pF capacitor, the currents running through it are higher :

$$I_{C(1pF)} = 930 \text{ mA, at 760 MHz,}$$

leading thus to a power loss of :

$$P_{L(1pF)} = 350 \text{ mW, at 760 MHz.}$$

The radiation efficiency (η_r) is shown in TABLE I and the presented results are summarized.

3.4 Voltages

Breakdown voltage should also be taken into consideration while placing a capacitor for tuning. The breakdown voltage V_{bd} is defined as :

$$V_{bd} = |E| \times \mathcal{D},$$

where $\mathcal{D}$ stands for the distance separating the two plates of the capacitor. In this section the V_{bd} will be calculated for the tuning range boundaries : for the 1/8 pF case at 1 GHz and the 1 pF case at 760 MHz. The dimension of the tuning capacitor is 1 mm in the length and the width.

1/8 pF

With a 1/8 pF capacitor the dielectric strength $|E_z|$ in the YZ plane leads to a voltage across the capacitor of 79 V. The breakdown voltage for the 1/8 pF capacitor in the proposed design, for 1 W input power is :

$$V_{C(1/8pF)} \geq 79 \text{ V}.$$

1 pF

At 760 MHz the $|E_z|$ component in the YZ plane gives a voltage across the capacitor of V :

$$V_{C(1pF)} \geq 190 \text{ V}.$$

Typical values are between 40 V and 200 V [13]. The results are presented in TABLE I.

3.5 Measurements

The proposed antenna design has been built and the mock-up is shown in Fig. 4. The measurements were made in an anechoic chamber. The radiation efficiency was measured without tuning capacitor at 1 GHz and with a 1 pF fixed capacitor at 800 MHz. The efficiency is computed from a 3-D pattern integration technique, $\eta_{r(1GHz)}$ = -1.5 dB and $\eta_{r(800MHz)}$ = -3.2 dB.

4 User Influence

As it is shown in [16] it is the user's hand that has the highest influence on the deterioration of the antenna performance in the proximity of a user, thus its influence is

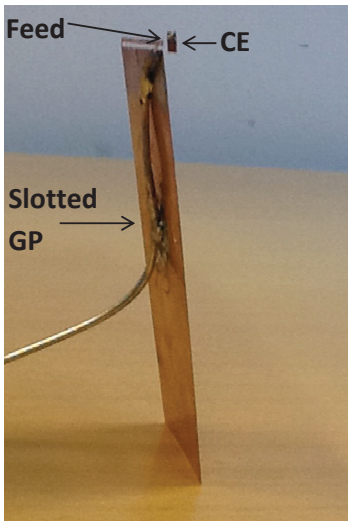

Fig. F.4: Mock-up.

investigated on the proposed design. The results are computed for three cases: the high band, the high bound of the low band and the low bound of the low band. The High Band (HB) case is measured at 2.6 GHz, and the two low band cases are measured one at 990 MHz with a 1/8 pF capacitor and the other at 758 MHz with a 1 pF capacitor.

4.1 Hand Phantom

The study uses a realistic phantom hand with a relative permittivity of the body tissue $\epsilon_r = 36$ and a conductivity $\sigma = 0.8$ S/m at 900 MHz [16]. The distance between the slot and the index finger is set to 10 mm, as the distance between the bottom of the GP and the palm, in order to model a typical thickness of a handset. The index finger is in a high E-field position due to the PCB geometry and additionally in a high H-field position due to the slot. Fig. 5 shows the hand grip on the coupling element based antenna with slotted ground plane.

4.2 Simulation Results

The absorption loss (L_A), the mismatch loss (L_M) and the total loss (L_T) are depicted in TABLE II. The capacitor is simulated as lossless to isolate the losses resulting from the user hand, for different frequencies and tuning stages. In all the cases L_M is smaller or equal to 0.1 dB which means that the antenna resonance frequency does not suffer detuning from holding the phone. The HB and the smallest capacitance value 1/8 pF

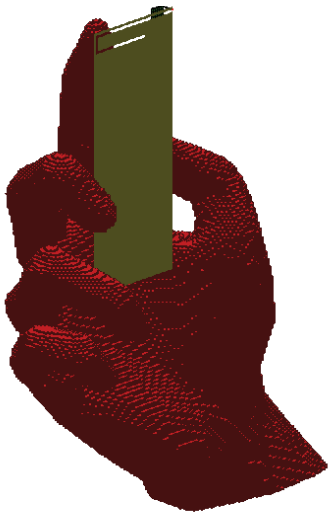

Fig. F.5: Hand model.

Table F.2: Losses of the proposed antenna due the user hand

	HB	1/8 pF	1 pF
f_r	2.6 GHz	990 MHz	760 MHz
L_M [dB]	0.1	$\ll 0.1$	$\ll 0.1$
L_A[dB]	2.3	2.5	4.7
L_T[dB]	2.4	2.6	4.8

create a similar absorption loss about 2.5 dB but this value dramatically increases when the resonance frequency is tuned to the 700-LTE band. In the worst case the L_T is 4.8 dB.

5 Conclusion

In This paper a coupling element based antenna structure with slot tuning of the ground plane has been investigated. The chosen ground plane is a candy bar size one and the investigated frequencies are the low GSM and LTE bands, and the high 2.6 GHz LTE band. The coupling element is very compact, its dimensions are reduced to a square of 4x4 mm^2. The simulations show that fine tuning from the 900-GSM band to the 700-LTE band can be achieved with a capacitance range of 1 pF and steps of 1/8 pF. The

tuning capacitor position is carefully chosen across the slot with a field investigation in order to reduce the losses it could generate. The currents running through the tuning capacitor are investigated since they are a source of loss in the radiation efficiency of the antenna structure.
The losses due to the tuning capacitor are calculated for a transmission power 1W, usual in today's use. The study shows that the highest losses are for the lowest tuned frequencies and therefore the highest capacitance values. Moreover the 1 pF capacitor is responsible for 1.9 dB of losses in the radiation efficiency at 760 MHz. This value is rather high and it is expected that the capacitor will be an important source of degradation of the handset performances.
The breakdown voltage is investigated as well, since it also determines the feasibility of the design. The expected voltages are below 200 V which is not an issue with the available components nowadays. Additionally a user's hand investigation is shown. The mismatch losses are below 0.1 dB and are negligible. The proposed design does not suffer from detuning when held. The absorption losses are up to 4.7 dB at the lowest tuned frequency. The design reaches more than 250 MHz fine tuning, at 760 MHz the 1 pF capacitor is responsible for 1.9 dB of losses and the user's hand contributes to the total losses with 4.8 dB.
Measurements have been made for the low frequencies of the tuning range. The predicted efficiency in TABLE I only took into account the possible losses coming from the capacitor. The measured efficiency is lower than the prediction therefore other causes of losses are to be taken into account. Very low frequencies on small ground plane and high Q of the structure can lead to extra losses, as the poor Q of the components, the soldering or the irregularities of the mock-up.

References

[1] P. Ciais, R. Staraj, G. Kossiavas, and C. Luxey, "Design of an internal quad-band antenna for mobile phones," *Microwave and Wireless Components Letters, IEEE*, vol. 14, no. 4, pp. 148–150, 2004.

[2] C.-W. Chiu and Y.-J. Chi, "Planar hexa-band inverted-f antenna for portable device applications," *Antennas and Wireless Propagation Letters, IEEE*, vol. 8, pp. 1099–1102, 2009.

[3] C.-M. Peng, I.-F. Chen, and C.-T. Chien, "A novel hexa-band antenna for mobile handsets application," *Antennas and Propagation, IEEE Transactions on*, vol. 59, no. 9, pp. 3427–3432, 2011.

[4] S. Yoon, C. Park, M. Kim, K. Kim, and Y. Yang, "Multiband internal antenna for mobile phones using a high dielectric material," in *Microwave Conference Proceedings (APMC), 2010 Asia-Pacific*, 2010, pp. 219–222.

[5] J. Villanen, J. Ollikainen, O. Kivekas, and P. Vainikainen, "Coupling element based mobile terminal antenna structures," *Antennas and Propagation, IEEE Transactions on*, vol. 54, no. 7, pp. 2142–2153, 2006.

[6] A. Andujar, J. Anguera, and C. Puente, "Ground plane boosters as a compact antenna technology for wireless handheld devices," *Antennas and Propagation, IEEE Transactions on*, vol. 59, no. 5, pp. 1668–1677, 2011.

[7] H. Zhao, G. Lin, and C. Beckman, "Design of a coupling element based penta-band mobile phone antenna," in *Antennas Propagation Conference, 2009. LAPC 2009. Loughborough*, 2009, pp. 209–212.

[8] R. F. Harrington and J. Mautz, "Theory of characteristic modes for conducting bodies," *Antennas and Propagation, IEEE Transactions on*, vol. 19, no. 5, pp. 622–628, 1971.

[9] E. Newman, "Small antenna location synthesis using characteristic modes," *Antennas and Propagation, IEEE Transactions on*, vol. 27, no. 4, pp. 530–531, 1979.

[10] P. Vainikainen, J. Ollikainen, O. Kivekas, and I. Kelander, "Resonator-based analysis of the combination of mobile handset antenna and chassis," *Antennas and Propagation, IEEE Transactions on*, vol. 50, no. 10, pp. 1433–1444, 2002.

[11] J. Rahola, "Estimating the performance of matching circuits for antennas," in *Antennas and Propagation (EuCAP), 2010 Proceedings of the Fourth European Conference on*, 2010, pp. 1–3.

[12] H. Li, J. Xiong, Y. Yu, and S. He, "A simple compact reconfigurable slot antenna with a very wide tuning range," *Antennas and Propagation, IEEE Transactions on*, vol. 58, no. 11, pp. 3725–3728, 2010.

[13] S. Del Barrio, M. Pelosi, O. Franek, and G. Pedersen, "Tuning range optimization of a planar inverted f antenna for the lte low frequency bands," in *Vehicular Technology Conference (VTC Fall), 2011 IEEE*, 2011, pp. 1–5.

[14] 3GPP TS 36.101, "LTE; Evolved Universal Terrestrial Radio Access (E-UTRA); User Equipment (UE) radio transmission and reception," p. V11.3.0 Realease 11, 2013.

[15] Murata, "Chip Monolithic Ceramic Capacitors," 2012. [Online]. Available: http://www.murata.com/products/catalog/pdf/c02e.pdf

[16] M. Pelosi, O. Franek, M. Knudsen, M. Christensen, and G. Pedersen, "A grip study for talk and data modes in mobile phones," *Antennas and Propagation, IEEE Transactions on*, vol. 57, no. 4, pp. 856–865, 2009.

Paper G

Antenna design exploiting duplex isolation for 4G communication on handsets

Caporal Del Barrio, S. and Pedersen, G.F.
[1]Section of Antennas, Propagation and Radio Networking (APNet), Department of Electronic Systems, Faculty of Engineering and Science, Aalborg University, DK-9220, Aalborg, Denmark, {scdb, mp, gfp}@es.aau.dk

The paper is published in
Electronics Letters, Vol. 49, Issue 19, pp 1197–1198, Sept., 2013.

The layout has been revised.

Abstract

This letter presents a novel design addressing the antenna bandwidth issue for the future communication standards on handsets. It consists of a tunable-antenna-pair for operation with a tunable front-end. The antennas are narrow-band and frequency-reconfigurable. The study focuses in the low communication bands. Measurements of the design are shown in band 12, and exhibit a receiver-transmitter isolation above 25 dB at 700 MHz.

1 Introduction

Covering the frequency spectrum required for the 4^{th} Generation (4G) of mobile communication is a major challenge for antenna designers. Passive wide-band antennas often become too bulky, as their volume increases proportionally with the number of bands to support, for example [1]. A promising solution is the use of active Frequency-Reconfigurable Antennas (FRA), allowing a unique, small and efficient element to cover an overall wide bandwidth. The FRA can be instantaneously tuned to the targeted band with Radio Frequency (RF) Switches, as in [2], or with tunable capacitors, as in [3]. Besides the antenna bandwidth challenge, 4G also increased the complexity of the RF Front-End (FE) with the bands expansion. Component duplication in the RF-FE lead to higher power consumption, cost and volume on an already tight boards. In this study the authors consider the use of FRA with tunable capacitors, and demonstrate the support of all low-bands of the 4G spectrum, until 699 MHz [4]. Low communication bands are addressed as they are the toughest to cover on small platforms, due to intrinsic physical limitations of antennas [5]. Additionally the authors propose the use of two narrow-band and independent antennas, one transmitter (TX) and one receiver (RX), thus eliminating the need for duplex filters in the RF-FE. The antennas are not only used as radiators but also as filters, giving the opportunity to design simpler and smaller FE architectures.

2 Antenna Geometry

The proposed narrow-band antenna is designed for the integration of a Micro-Electro-Mechanical systems (MEMS) tunable capacitor, that will continuously tune its resonance frequency in the low-band of 4G (699 MHz to 960 MHz). The antennas are mounted on a ground plane of dimensions 120 × 55 mm, representing nowadays smartphones. The design consists of a coupler, fed and placed on top of a slot. The antenna was designed to fit nowadays phone designs, where slimness and wide screens are essential. For this purpose only 1mm was allowed for the height of the antenna and 4 mm for its width. A fixed capacitor (C1=1pF) is placed at the end of the slot to force the initial

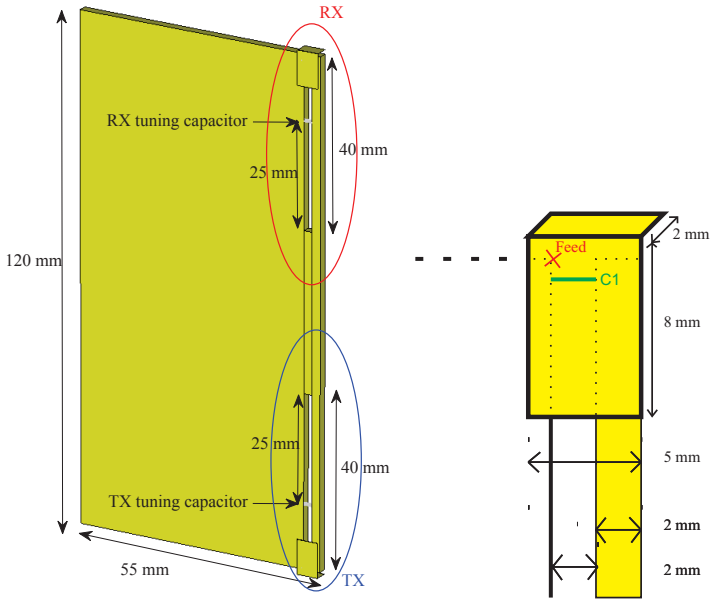

Fig. G.1: Antenna geometry, full board (left) and zoom on the dimensions of the CE and the slot (right).

resonance frequency to 960 MHz. The tunable capacitor is placed at a distance from the source determined by its minimum tuning step. Here 25 mm corresponds to steps of 0.06 pF, according to the commercial MEMS tunable capacitor in [6]. The detailed geometry of the antenna is shown in Fig. G.1.

3 Simulation results

Simulations show, in Fig. G.2, the tunability of the TX and RX antennas, throughout all frequencies of the LTE low-band. It is observed that the impedance is very stable throughout tuning, and minimal mismatch loss is expected. The impedance bandwidth (at -6 dB) shrinks from 10 MHz at 960 MHz to 5 MHz at 700 MHz, as a result of tuning. Indeed as the antenna is tuned further away from its original resonance frequency, more energy is stored in the antenna structure. Consequently the Antenna Quality factor (Q_A) increases and the antenna bandwidth shrinks [7]. However narrow-band antennas are not an issue when an antenna pair is considered, the antennas only need to cover a channel, as opposed to a full band. The loss-less simulations show antenna isolation below 20 dB.

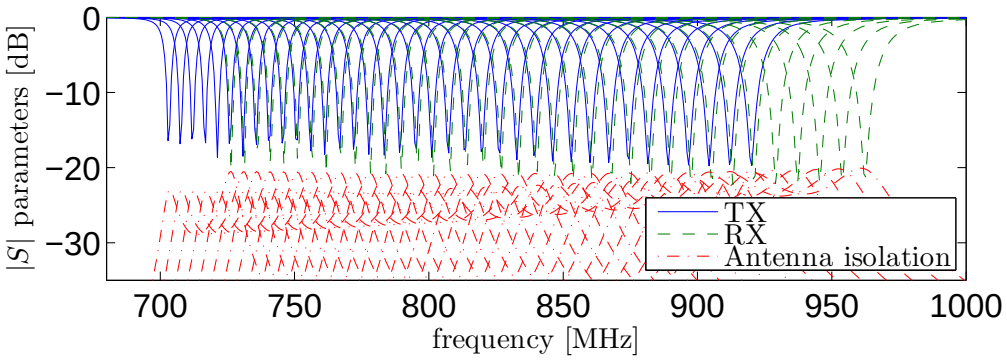

Fig. G.2: S parameters of the antenna-pair with tuning steps of 0.06 pF.

Isolation and efficiency in small platforms are most challenging for low frequencies, as the antennas share the same ground, and the ground itself is a significant part of the radiation [8]. Thus antennas at resonating at low-bands on a small platform are inherently coupled. The concept of antenna-pair appeared in [9]. Later studies have investigated TX/RX isolation, mostly with cancellation techniques as in [10] and [11], needing a separation of several wavelengths, or multiple antennas. The proposed design achieves duplex isolation in a small volume, with means of frequency separation (30 MHz in band 12), spatial separation (40 mm) and opposite direction of the surface currents, see Fig. G.3. The results are shown for band 12, where transmitting frequencies are [699 MHZ - 716 MHz] and receiving frequencies are [729 MHz - 746 MHz]. It is inferred from the plot that high isolation will be achieved between TX and RX channels, as minimal current is leaking from one antenna to the other.

4 Measurement results

A mock-up of the presented design is built and shown in Fig. G.4. It will be used to demonstrate high antenna isolation in band 12. For more practicality, the mock-up uses fixed capacitors instead of tuners. They are offset, 1.8 pF and 1.5 pF, in order to cover both TX and RX RF chains respectively. They exhibit a low Equivalent Series Resistance (ESR) in order to minimize insertion loss, 0.15 Ω and 0.12 Ω. Simulated and measured isolation curves between TX and RX antennas are shown in Fig. G.5. The measured isolation is improved compared to the simulated curve, due to mock-up losses, showing a duplex isolation above 25 dB.

The Q_A of the mock-up is shown in Fig. G.6 for three different stages. Firstly without any tuning capacitor, at its original resonance frequency, secondly with C1, setting the resonance to 960 MHz, and finally with the tuners, here fixed capacitors set

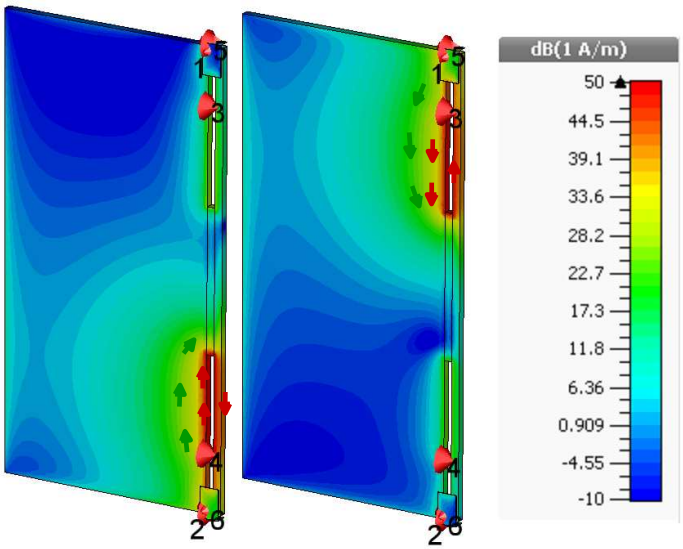

Fig. G.3: Surface currents at 699 MHz (left) and 729 MHz (right).

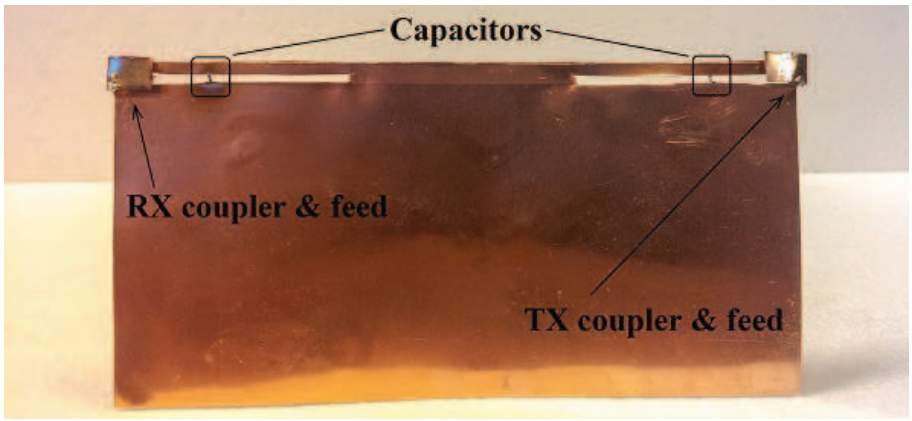

Fig. G.4: Mock-up of the proposed antenna design, using fixed capacitors.

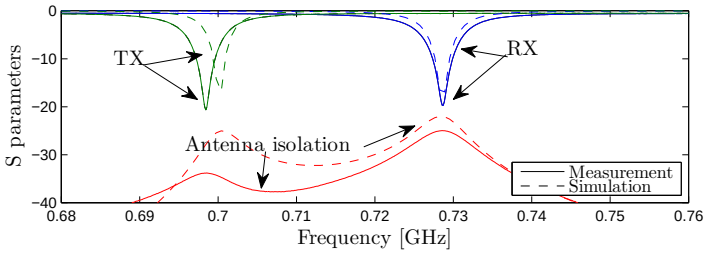

Fig. G.5: Measured and simulated frequency responses in band 12.

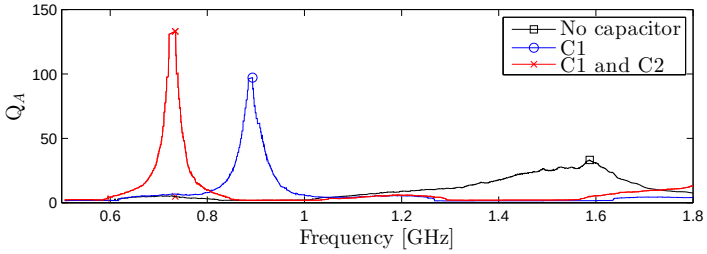

Fig. G.6: Measured Q_A of the RX antenna in different tuning stages.

to band 12. The Q_A is relevant for FRA because of its relation to stored energy and bandwidth. Bandwidth and Q_A relate to the Voltage-Standing-Wave Ratio (VSWR) [7]:

$$Q_A(\omega) = \frac{2\sqrt{\beta}}{FBW_V(\omega)}, \sqrt{\beta} = \frac{s-1}{2\sqrt{s}},$$

where FBW_V is the matched VSWR fractional bandwidth and s is a specific value of the VSWR. The measured Q_A values of the RX antenna are plotted in Fig. G.6. The loaded Q_A increases from 33 at its original resonance frequency, to 97 at 960 MHz, to 133 at 730 MHz. Being multiplied by 4 throughout the tuning. Q_A values are similar for the TX.

The radiation efficiency e_r was measured in anechoic chamber and computed with 3D integration pattern. The TX antenna exhibited e_r=-4.4 dB at 699 MHz, and the RX antenna exhibited e_r=-3.2 dB at 730 MHz. The insertion loss due to the capacitors can be computed and accounts for 2 dB of the measured loss. Thus it is inferred that a high thermal loss, due to high-Q_A and metal conductivity, is present in tunable antennas and may limit their efficiency. Nevertheless the measured values are still acceptable given the performances of nowadays handsets, at these frequencies [12].

5 Conclusion

FRA can operate in a large range of frequencies and easily cope with future addition of bands. Their potential is fully exploited when one considers their narrow-band characteristic and uses it to have a filtering antenna-pair, thus eliminating the need for duplex filters in the FE. A slim and simple design was presented to address this architecture, achieving 25 dB of duplex-isolation in band 12. The antenna efficiency relies mainly on the tunable components. In the future work a mock-up with MEMS tunable capacitors and MEMS tunable filters will be built, in order to appreciate the overall system performance. The proposed antenna-pair is a promising design for 4G communication implementation.

References

[1] P. Ciais, R. Staraj, G. Kossiavas, and C. Luxey, "Compact internal multiband antenna for mobile phone and WLAN standards," *Electronics Letters*, vol. 40, no. 15, pp. 3–4, 2004.

[2] K. R. Boyle and P. G. Steeneken, "A Five-Band Reconfigurable PIFA for Mobile Phones," *IEEE Transactions on Antennas and Propagation*, vol. 55, no. 11, pp. 3300–3309, Nov. 2007.

[3] J. R. De Luis, A. Morris, Q. Gu, and F. de Flaviis, "Tunable Duplexing Antenna System for Wireless Transceivers," *IEEE Transactions on Antennas and Propagation*, vol. 60, no. 11, pp. 5484–5487, Nov. 2012.

[4] 3GPP TS 36.101, "LTE; Evolved Universal Terrestrial Radio Access (E-UTRA); User Equipment (UE) radio transmission and reception," p. V11.3.0 Realease 11, 2013.

[5] R. F. Harrington, "Effect of Antenna Size on Gain, Bandwidth, and Efficiency," *Journal of Research of the National Bureau of Standards- D. Radio Propagation*, vol. 64D, no. 1, pp. 1–12, 1960. [Online]. Available: http://archive.org/details/jresv64Dn1p1

[6] WiSpry Tunable Digital Capacitor Arrays (TDCA), "http://www.wispry.com/products-capacitors.php."

[7] A. D. Yaghjian, S. R. Best, and S. Member, "Impedance , Bandwidth , and Q of Antennas," *IEEE Transactions on Antennas and Propagation*, vol. 53, no. 4, pp. 1298–1324, 2005.

[8] P. Vainikainen, J. Ollikainen, O. Kivekäs, and I. Kelander, "Resonator-Based Analysis of the Combination of Mobile Handset Antenna and Chassis," *IEEE Transactions on Antennas and Propagation*, vol. 50, no. 10, pp. 1433–1444, 2002.

[9] A. James, "Reconfigurable Antennas for Portable Wireless Devices," *IEEE Antennas and Propagation Magazine*, vol. 45, no. 6, pp. 148–154, 2003.

[10] T. Snow, S. Member, C. Fulton, W. J. Chappell, and S. Member, "Transmit - Receive Duplexing Using Digital Beamforming System to Cancel," *IEEE Transactions on Microwave Theory and Techniques*, vol. 59, no. 12, pp. 3494–3503, 2011.

[11] O. N. Alrabadi, A. D. Tatomirescu, M. B. Knudsen, M. Pelosi, and G. F. Pedersen, "Breaking the Transmitter-Receiver Isolation Barrier in Mobile Handsets with Spatial Duplexing," *IEEE Transactions on Antennas and Propagation*, vol. 61, no. 4, pp. 2241–2251, 2013.

[12] S. Caporal, D. Barrio, and G. F. Pedersen, "Correlation Evaluation on Small LTE Handsets," in *Vehicular Technology Conference (VTC Fall)*, 2012, pp. 1–4.

Paper H

Novel Architecture for World-phones

Caporal Del Barrio, S.[1] ; Pedersen, G.F.[1] and Morris, A.[2]
[1]Section of Antennas, Propagation and Radio Networking (APNet), Department of Electronic Systems, Faculty of Engineering and Science, Aalborg University, DK-9220, Aalborg, Denmark, {scdb, mp, gfp}@es.aau.dk
[2]Wispry Inc, Irvine, USA art.morris@wispry.com

The paper has been submitted to the
Antennas and Wireless Propagation Letters, Special Cluster on
Terminal Antenna Systems for 4G and Beyond, Oct. 8^{th} 2013.

The layout has been revised.

Abstract

The new standard of mobile communications came with new challenges, on the antenna bandwidth and on the front-end architecture, of mobile phones. This letter proposes a novel architecture overcoming these challenges. It includes narrow-band tunable antenna, jointly with a tunable front-end. Simulations and measurements are demonstrated at the low and high bands of the communication spectrum.

1 Introduction

With the standardization of the 4th Generation (4G) of mobile communication, came along a significant broadening of the Radio Frequency (RF) spectrum. Heretofore, 4G has allocated 26 bands supporting Frequency Division Duplexing (FDD) operation, ranging from 700 MHz to 2.7 GHz [1]. The number of mobile communication bands has been expanded in order to provide higher data rates. However, there is a direct correlation between the number of bands to support and the number of RF components needed on the Printed Circuit Board (PCB). These components are part of the RF Front-End (FE) of the mobile handset, which includes Power Amplifiers (PA), Low-Noise Amplifiers (LNA), switches and filters. Better data rates also initiated a need for larger screens, processors and batteries, for a given form factor, all increasing the pressure on PCB space. Practically no room is left to include all the components needed for global LTE roaming, and a very high degree of integration is required in future mobile phones. The ever-increasing number of RF components on the PCB also has a significant impact on the battery life [2].

The challenges brought by the spectrum expansion do not affect only the FE of the handset but also its antennas. Their integration is limited by physical limitations, restricting their impedance bandwidth to their size and efficiency [3]. With the band proliferation there is a need for Frequency-Reconfigurable Antennas (FRA), in order to match previous generations antennas, volume-wise and efficiency-wise.

The antenna concepts addressing the bandwidth issue include on the one hand broad-band antennas and on the other hand FRA. The main difference between these two concepts lies in the antenna natural bandwidth. Broad-band antennas are combined with tunable matching networks, as in [4–8]; whereas FRA exhibit a narrow-band resonance that is tuned to a wide range of frequencies, as in [9–13]. The authors use FRA, where the radiator is also used as filter, relaxing the complexity of the FE. In this contribution, the authors propose a novel FE architecture co-designed with FRA, that covers all 4G bands from 700 MHz to 2.7 GHz, consideration is also given to the future bands towards 600 MHz [14]. Splitting the Transmitting (TX) from the Receiving (RX) chains [15], enables the suppression of the duplex filters in the FE. The proposed architecture reduces the PCB area needed, the power consumption and the overall loss.

Section 2 details the proposed FE architecture, designed for narrow-band FRA. Section III presents the dual-band antenna design. Section IV presents the simulated and measured results and Section V draws the conclusions.

2 Front-end Architecture

2.1 Conventional architecture

The RF FE groups all the radio frequency components located between the transceiver and the antenna, including the Power Amplifier (PA), the Low Noise Amplifier (LNA), the filtering (Surface-Acoustic-Wave (SAW) filters and duplex filters) and the switches. The modern 2G/3G/4G radios typically include a broadband antenna with a band-selecting switch and a FE, comprising one filtering chain per band. Therefore multiple-band support has a significant impact on the RF component count in the FE. A jump from 5 UMTS bands to 40 LTE bands has to be addressed for the next phones on the market. With the band proliferation, the conventional FE architecture leads to component duplication, hence a lack of board space and an ever-increasing power consumption. An example of a conventional multi-band multi-mode RF FE is shown in Fig. H.1. One can see that the main component added by 3G and 4G standards is the duplex filter, as these standards rely on half-duplex communication. One duplex filter is needed per band, which makes this component very inefficient from the perspective of board space and battery life.
With the awareness of the challenges that band expansion brought into FE design, also emerged a number of techniques to address it, from research groups in the academia [16], [17], [18] and from the industry. The major challenge of a world-wide 4G phone is to figure out a design that will support all bands, in a small enough form factor, while improving throughput, battery life and heat dissipation. Power envelope tracking techniques have been developed [19] to reduce the power consumption and extend battery life. 3D packaging [19] has emerged in order to save PCB space, by stacking up modules. Filter banks and broadband PA are also part of the new solutions [20]. However, the component count is still high. Nowadays data rates and future trends call for a complete shift in FE architecture in order to meet the market requirements.

2.2 Smart Antenna Front-End (SAFE) architecture

In this letter, the authors describe a novel FE architecture, which will not include duplex filters, main actors of the component duplication. This architecture has been patented [21, 22]. In order to achieve the RX/TX filtering, two distinct antennas will be used in connection with two independent RF chains. The rejection typically provided by duplex filters, is provided here partly by filters in the RF chain and partly by the antennas. The key feature of this design is to separate the TX and the RX into two

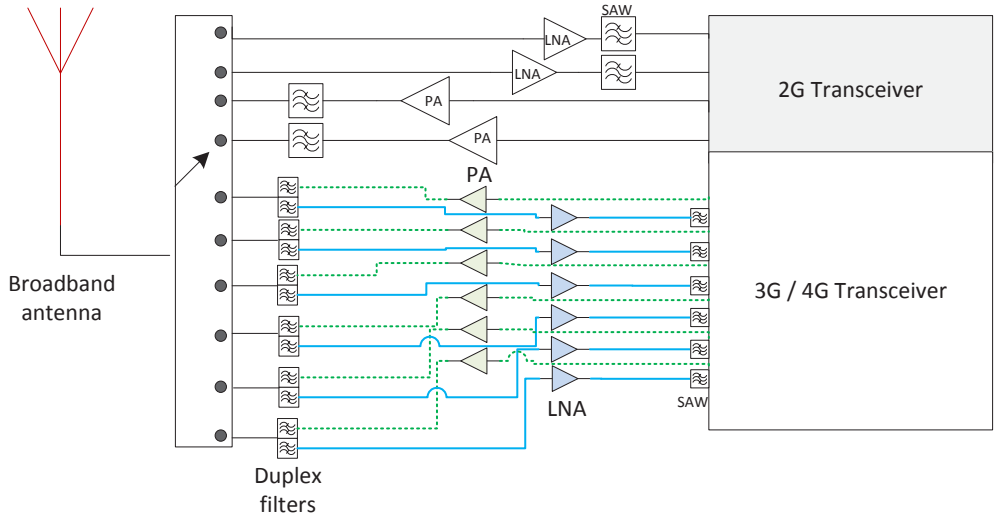

Fig. H.1: Conventional 2G/3G/4G FE architecture.

different antennas, each of them being narrow-band, i.e. covering only a channel instead of a full band. Thus, their narrow-band property is also exploited for its filtering effect. Additionally, both the antennas and the RF filters will be tunable, in order to cover the full 4G frequency spectrum. Another advantage of having two separated narrow-band tunable antennas is in the case of bands with a very large duplex spacing, e.g. band 4 with 400 MHz. The proposed architecture is shown in Fig. H.2. This architecture reduces redundancies, eliminating the antenna switch and all duplex filters. The single RX or TX paths decrease the component count, which decreases the power consumption, therefore the battery life. PCB area is also reduced with the proposed architecture, as well as complexity. Furthermore, the antenna tunability will ensure minimal mismatch loss, saving battery life too, as the PA will not have to compensate for the antenna mismatch. The FE challenge is now shifted to the antennas and the filters, they each need to provide a duplex rejection of 25 dB in order to remove the duplex filters. This level of antenna isolation is particularly challenging at the low frequency bands (below 1 GHz), as the full board is the main radiator.

The proposed architecture was first conceptualized in 2003 [15]. [13] demonstrated the concept at the high bands (1.8 GHz - 2.1 GHz) and this letter will show the performances of the duplex antenna throughout the whole 4G frequency spectrum, with a tunable dual-band element.

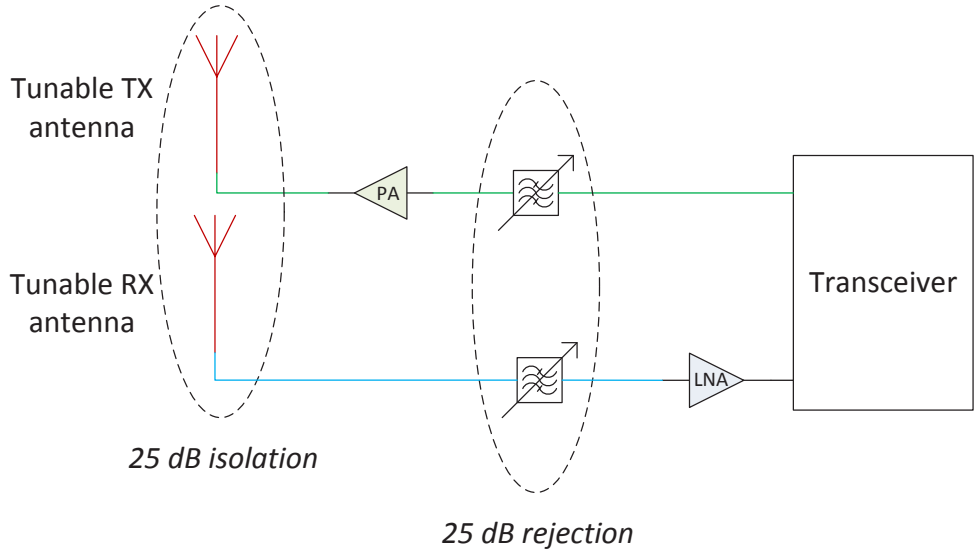

Fig. H.2: Proposed SAFE architecture.

3 Antenna and Tuning Design

3.1 Duplex antennas

The proposed antenna design comprises a coupler connected to the feed line and two radiators, one for the high-band (HB) and one for the low-band (LB). The radiators are fed through electromagnetic coupling with the coupler. They are connected to the tuners in order to change their electrical length, thus their resonance frequency. The antenna is a single-feed tunable dual-band antenna. The geometry of the antenna is depicted in Fig. H.3a. The LB radiators occupy a volume of 0.75 cc, and are placed as extension of the chassis to provide enough bandwidth (BW). The HB radiators occupy a volume of 0.06 cc and are placed on top of the chassis to reach a narrow-band design, i.e. an Antenna with a high Quality factor (Q_A). In order to achieve isolation of the LB radiators, the TX and RX are placed orthogonally, exciting two different modes on the ground plane. The HB radiators are isolated when placed at both ends of the ground plane, having a large enough electrical distance and confined fields due to their high Q_A. The Fig. H.3b shows the antenna schematics and the connections to the feed and the tuner. The feed line is connected to the coupler through a matching capacitor C_m. The radiators are connected to each of the independent banks of the tuner, through the capacitors C_1 and C_2. These fixed capacitors in series with the tuner allow to reduce

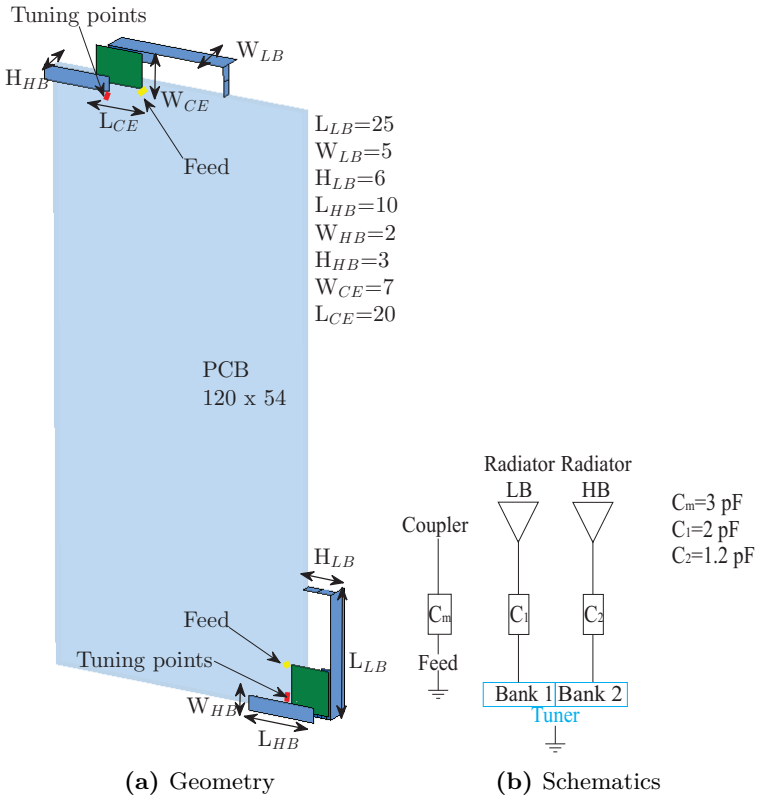

(a) Geometry **(b)** Schematics

Fig. H.3: Antenna Design.

the voltages across it, which can be critical for MEMS.

3.2 MEMS Tunable capacitors

MEMS Tunable capacitors consist of a CMOS-integrated movable mechanical structures. The structure is actuated with electrostatic force to provide capacitance. Each MEMS beam is a pair of metal traces separated by either a dielectric, either an air-gap. This two configurations define the off, and on states respectively. Several beams are combined, forming an array that can provide many states, e.g. a tunable capacitor.
The tuner [23] used for the design of the proposed antennas has two independent banks of 3.875 pF each, with tuning steps of 0.125 pF. The breakdown voltage is above 120 V and the component quality factor (Q_c) reaches 90 at 2 GHz amd 180 at 1 GHz.

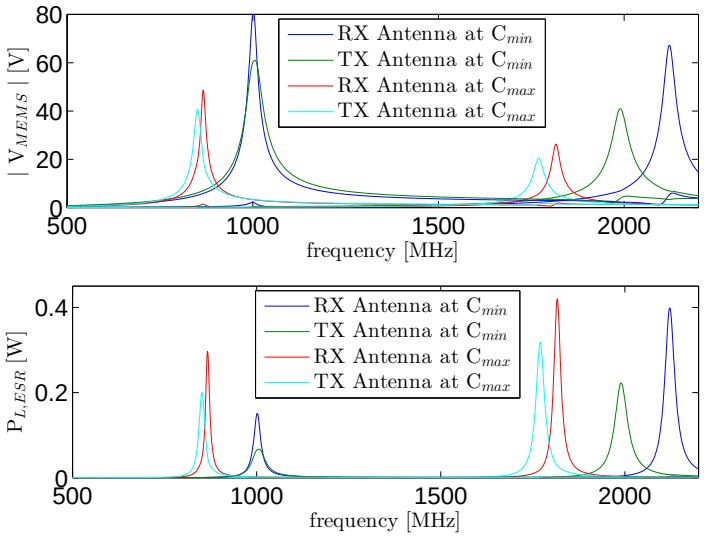

Fig. H.4: Voltages across the MEMS and power lost in the ESR for the lowest and highest tuning steps.

4 Simulated and Measured Performances

4.1 Voltage handling and power lost in the resistance

In order to best utilize the tuner, it is placed at the end of the radiators, which is a low-current location. Nevertheless it is also a high-voltage location, which can be an issue regarding the voltage break-down of MEMS. The introduction of the capacitors C_1 and C_2 provides an additional degree of freedom to the voltage across the tuner. However there is a trade-off between their value and the achievable tuning range, which is also a trade-off with the size of the elements. The proposed design is optimized for compactness. The resulting voltage magnitudes across the tuner ($| V_{MEMS} |$) are depicted in Fig. H.4. This figure also shows the power lost in the total Equivalent Series Resistances (ESR) ($P_{L,ESR}$) of the chain of MEMS and capacitors. Hence it is calculated that, on the RX antenna for example, the loss due to the total ESR is -2.5 dB at the high-band and -1.5dB at the low-band. This frequency difference of the ESR loss is due to the Q of the tuner, which is higher at the low-band. The TX antenna has a lower Q_A than the RX, due to its location on the board. Therefore the $P_{L,ESR}$ is half-dB lower. The increasing loss, as the antenna is tuned further away from its original resonance is due to an increasing Q_A of the element, as will be shown below.

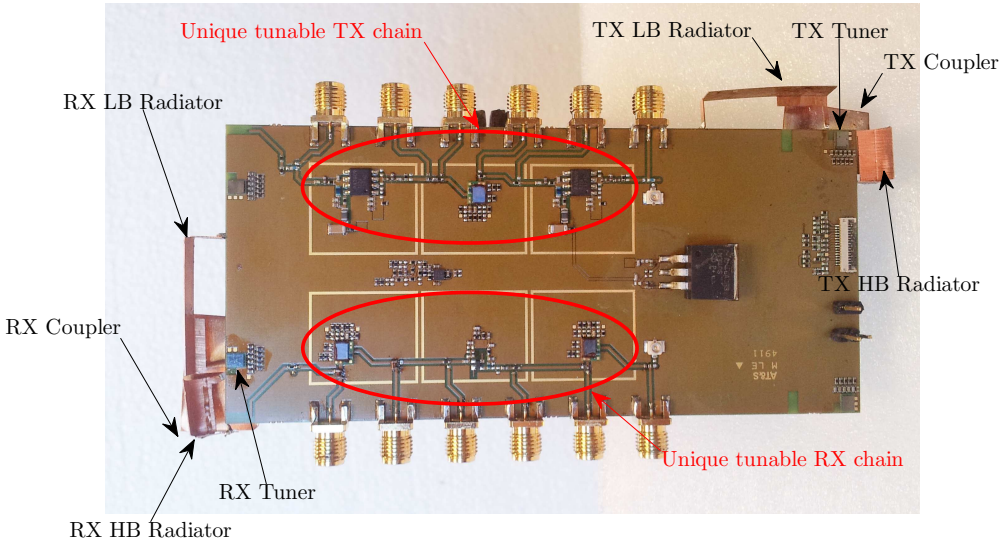

Fig. H.5: Measurement board.

4.2 Tunability and efficiency

A printed circuit board, with the two unique RX and TX chains is built. It also includes the MEMS Tunable capacitors and the duplex antenna. A picture of the board is shown in Fig. H.5. The tuner used on the board only had one bank, so the antennas were measured independently. The measured S parameters of the low-band elements are shown in Fig. H.6, and the high-band elements are shown in Fig. H.7. In order to show the tunability of the low band until 600 MHz, C1 was omitted. The plots show impedance coverage at -6 dB of all frequencies of the targeted bands. Indeed the tuning resolution depends on the minimum step of the tuner and its placement on the antenna design. In both figures, it can also be observed that the isolation between the TX and RX antennas is below-25 dB. The loaded Q_A is shown for the LB antennas, exhibiting higher values for the TX than the RX and an increasing peak value as the tuned frequency is shifted down. The Q_A values at the HB show a similar trend, with peak values at 70 for the RX and 50 for the TX.

The mock-up was measured in Satimo Star-Lab to calculate its total efficiency (η_T) with 3D pattern integration technique. Values are summarized in Table H.1 for bands 8, 5, 1 and 4.

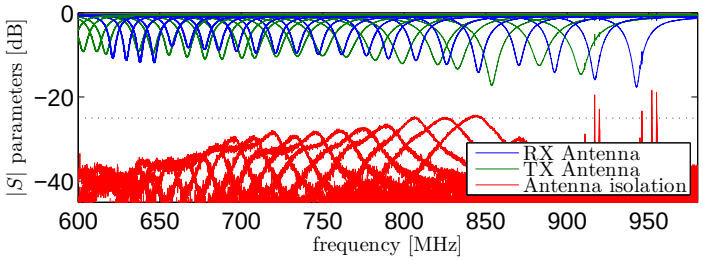

Fig. H.6: Measured | S | parameters of the LB antennas.

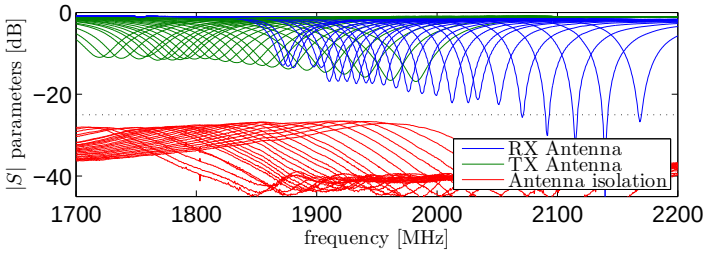

Fig. H.7: Measured | S | parameters of the HB antennas.

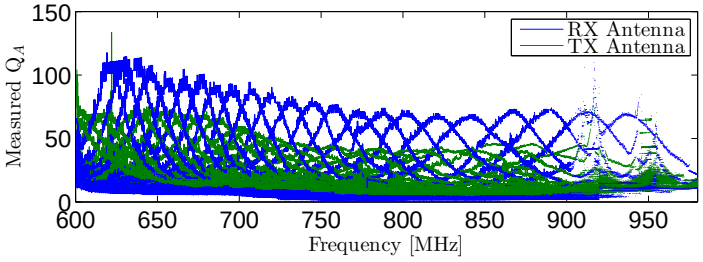

Fig. H.8: Measured Q_A of the LB antennas.

Table H.1: Measured η_T

f [MHz]	η_T [dB]	f [MHz]	η_T [dB]
960	-3	2170	-3
824	-4	1710	-4

5 Conclusion

Radio spectrum and PCB area are the two most precious entities in the mobile phone landscape nowadays. The user's demand for mobile data drives the RF FE content. However, the number of bands required worldwide lead to high component duplication and PCB space has become an issue. Moreover, antennas covering a large bandwidth are typically large and difficult to fit into thin and modern mobile phone designs. A novel architecture is proposed in this letter combining a new approach for the FE design and for the antenna design. The implementation of antenna tuning and antenna isolation will save space and power consumption, leading to an efficient design. A mock-up was built, as a proof-of-concept of the proposed architecture. Antenna duplex isolation above -25 dB was achieved. The total efficiency of the mock-up is a nominal value and can still be improved, mainly by improving the quality factor of the tuner.

References

[1] 3GPP TS 36.101, "LTE; Evolved Universal Terrestrial Radio Access (E-UTRA); User Equipment (UE) radio transmission and reception," p. V11.3.0 Realease 11, 2013.

[2] D. Vye, "The Economics of Handset RF Front-end Integration," pp. 1–13, 2010. [Online]. Available: www.microwavejournal.com/articles/print/9983-the-economics-of-handset-rf-front-end-integration

[3] R. F. Harrington, "Effect of Antenna Size on Gain, Bandwidth, and Efficiency," *Journal of Research of the National Bureau of Standards- D. Radio Propagation*, vol. 64D, no. 1, pp. 1–12, 1960. [Online]. Available: http://archive.org/details/jresv64Dn1p1

[4] D. Manteuffel and M. Arnold, "Considerations for Reconfigurable Multi-Standard Antennas for Mobile Terminals total efficiency :," in *Antenna Technology: Small Antennas and Novel Metamaterials, 2008. iWAT 2008. International Workshop on*, 2008, pp. 231–234.

[5] L. Huang and P. Russer, "Electrically Tunable Antenna Design Procedure for Mobile Applications," *IEEE Transactions on Microwave Theory and Techniques*, vol. 56, no. 12, pp. 2789–2797, Dec. 2008.

[6] R. Valkonen, J. Ilvonen, P. Vainikainen, and A. Radiating, "Naturally Non-Selective Handset Antennas with Good Robustness Against Impedance Mistuning," in *European Conference on Antennas and Propagation (EuCAP)*, 2011, pp. 796–800.

[7] R. Valkonen, M. Kaltiokallio, S. Member, and C. Icheln, "Capacitive Coupling Element Antennas for Multi-Standard Mobile Handsets," *IEEE Transactions on Antennas and Propagation*, vol. 61, no. 5, pp. 2783–2791, 2013.

[8] R. Valkonen, C. Luxey, J. Holopainen, C. Icheln, and P. Vainikainen, "Frequency-reconfigurable mobile terminal antenna with MEMS switches," in *Antennas and Propagation (EuCAP), 2010 Proceedings of the Fourth European Conference on*, 2010, pp. 1–5.

[9] M. G. S. Hossain and T. Yamagajo, "Reconfigurable Printed Antenna for a Wide-band Tuning," in *European Conference on Antennas and Propagation (EuCAP)*, vol. 1, 2010, pp. 1– 4.

[10] H. Li, J. Xiong, Y. Yu, and S. He, "A Simple Compact Reconfigurable Slot Antenna With a Very Wide Tuning Range," *IEEE Transactions on Antennas and Propagation*, vol. 58, no. 11, pp. 3725–3728, 2010.

[11] Y. Tsutsumi, M. Nishio, S. Obayashi, H. Shoki, T. Ikehashi, H. Yamazaki, E. Ogawa, T. Saito, T. Ohguro, and T. Morooka, "Low Profile Double Resonance Frequency Tunable Antenna Using RF MEMS Variable Capacitor for Digital Terrestrial Broadcasting Reception," in *IEEE Asian Solid-State Circuits Conference*, 2009, pp. 125–128.

[12] S.-k. Oh, H.-s. Yoon, and S.-o. Park, "A PIFA-Type Varactor-Tunable Slim Antenna With a PIL Patch Feed for Multiband Applications," *Antennas and Wireless Propagation Letters*, vol. 6, no. 11, pp. 103–105, 2007.

[13] J. R. De Luis, A. Morris, Q. Gu, and F. de Flaviis, "Tunable Duplexing Antenna System for Wireless Transceivers," *IEEE Transactions on Antennas and Propagation*, vol. 60, no. 11, pp. 5484–5487, Nov. 2012.

[14] "600 MHz Auction Speculation," 2013. [Online]. Available: http://www.dailywireless.org/2013/05/06/600-mhz-auction-speculation/

[15] A. James, "Reconfigurable Antennas for Portable Wireless Devices," *IEEE Antennas and Propagation Magazine*, vol. 45, no. 6, pp. 148–154, 2003.

[16] T. Nesimoglu, "A Review of Software Defined Radio Enabling Technologies," 2010, pp. 87–90.

[17] I. Dufek, "Concept of the Tunable Filter Unit for Agile Mobile Handsets," in *Loughborough Antennas and Propagation Conference (LAPC)*, no. November, 2012, pp. 5–8.

[18] H. Okazaki, T. Furuta, K. Kawai, Y. Takagi, A. Fukuda, and S. Narahashi, "Reconfigurable RF Circuits for Future Multi-Mode Multi-Band Mobile Terminals," in *2013 International Symposium on Electromagnetic Theory*, 2013, pp. 432–435.

[19] P. Carson and S. Brown, "White paper: Less is More - The New Mobile RF Front-End," pp. 1–7, 2013.

[20] B. D. Pilgrim, "White paper: Simplifying RF front-end design in multiband handsets," pp. 30–33, 2008.

[21] M. B. Knudsen, P. Bundgaard, J.-E. Mueller, G. F. Pedersen, and M. Pelosi, "Impedance Tuning of Transmitting and Receiving Antennas," 2012.

[22] M. B. Knudsen, B. Adler, P. Bundgaard, J.-E. Mueller, G. F. Pedersen, and M. Pelosi, "Wireless Communication Device Antenna with Tuning Elements," 2013.

[23] WiSpry Tunable Digital Capacitor Arrays (TDCA), "http://www.wispry.com/products-capacitors.php."